UNIVERSITY OF BIRMINGHAM

CYBER-PHYSICAL INTERACTIVE IMPACTS ON SMART GRIDS WITH RENEWABLE ENERGY RESOURCES

by

ADEPEJU ABIODUN ADESINA OYEWOLE

A thesis submitted to the University of Birmingham for the degree of

DOCTOR OF PHILOSOPHY

Department of Electronic, Electrical and Systems Engineering

College of Engineering and Physical Sciences

The University of Birmingham

July 2021

Abstract

Cyber systems infrastructure is extensively integrated in smart grids to improve system control, monitoring, protection, and data processing. Effective operation of a smart grids with significant integration of cyber systems infrastructure depends on the availability of cyber network enabled functions. Smart grid's dependency on cyber enabled functions exposes the whole system operation to cyber failures, cyber-attacks and causes changes in the system functionalities. However, the failures of cyber elements could affect power system security. Incorporating cyber failures and cyber presence is inevitable in security assessment process.

This thesis proposes a multi-state smart component model and a unified system level ternary Markovian cyber-physical components interaction model to operate in Monte Carlo simulation. The multi-state smart component model is based on differential time dependent Markovian framework to capture and simulate component operational behaviour of a smart grid environment. The framework quantitatively evaluates the impacts of smart components failure conditions in the presence of intermittent power outputs.

The unified ternary Markovian cyber-physical components interaction model is based on interactions and characteristics of three subsystem functional layers of the cyber physical power system operation with the presence of random and unforeseen contingencies. The framework also evaluates interdependency impacts on physical power system security. Investigations find that the ternary Markovian model at system level effectively captures the dynamics of subsystem layers' interactions in a cyber-physical power system operation.

Further, presence of cyber-attacks in a cyber-physical power system components operation could lead to severe insecurities. The thesis contributes in four folds: (1) an innovative multi-state smart component model, (2) a new mathematical state probability algorithm and an innovative performance assessment algorithm, (3) an advanced unified

ternary Markovian model and (4) an embedded innovative cyber-physical performance assessment algorithm. The thesis provides bases for a holistic assessment of interactions in the decision-making layer, information, communication and coupling layer and power system layer in a cyber-physical power system.

Acknowledgements

I am grateful to God Almighty, who has given me life and grace throughout this research work.

I would like to express my sincere gratitude and appreciation to my supervisor, Dr Dilan Jayaweera for his noble supervision, valuable guidance and continuous support throughout my PhD research. I really appreciate his helpful comments, feedbacks and discussions which have contributed a lot to this achievement. His supervision and dedication have motivated my technical research excellence and he has been instrumental to my professional practice development.

I would like to thank my colleagues in the Power and Control Group for their help and support. I greatly benefited from their suggestions, discussions, and inspiration. It was very enjoyable working with them.

Finally, I would also like to express my sincere gratitude to my family, husband and loved ones, especially my daughters. Thank you, my angels, for your support, encouragement and understanding throughout my PhD study.

Table of Contents

List of Figures

List of Tables

List of Abbreviations

AC	Alternating Current
CCSFL	Communication and Coupling Subsystem Functional Layer
CPPS	Cyber-Physical Power System
CPS	Cyber-Physical Systems
DISFL	Decision-making intelligent subsystem functional layer
EENS	Expected Energy not Supplied
ENS	Energy not Supplied
ESs	Ethernet Switches
FAN	Field Area Network
FL	Functional Layers
FR	Failure Rate
HAN	Home Area Network
ICT	Information Communication Technologies
IEDs	Intelligent Electronic Devices
LoLE	Loss of Load Expectation
LPP	Line Protection Panel

MCS	Monte Carlo Simulation
MTTF	Mean Time to Failure
MTTR	Mean Time to Repair
MUs	Merging Units
PV	Photovoltaic
p.u.	Per Unit
PPSFL	Physical power subsystem layer
RER	Renewable Energy Resources
RN	Random Number
RTS	Reliability Test System
RTU	Remote Terminal Units
SC	Smart Component
SCADA	Supervisory Control and Data Acquisition
SG	Smart Grids
TMM	Ternary Markovian Model
TSP	Time Series Profiles
VoLL	Value of Lost Load

WAN	Wide Area Network
WPI	Wind Power Integration

Publications

- P. A. Oyewole and D. Jayaweera, "Power System Security With Cyber-Physical Power System Operation," in IEEE Access, vol. 8, pp. 179970-179982, 2020, doi: 10.1109/ACCESS.2020.3028222.

- Oyewole, Peju A; Jayaweera, Dilan: 'RELIABILITY OF SMART GRIDS WITH SMART ASSETS AND LARGE WIND FARMS', IET Conference Proceedings, , p. 59-64, DOI: 10.1049/icp.2021.1405 IET Digital Library, https://digital-library.theiet.org/content/conferences/10.1049/icp.2021.1405

- P. Oyewole and D. Jayaweera, **"Smart Grid Reliability Assessment with Large Wind Farms and Differential Time Dependent Smart Asset Model,"** in *Electric Power Systems Research journal*, (Submitted Feb.2021, under review).

Chapter 1: Introduction

1.1 Background

The concept of smart grids is motivated by demand for reliable, secure, flexible, effective, and sustainable management of a power system [1]. Smart grid (SG) concept has also emerged to mitigate the impacts of climate change, to meet the growing global energy demand and to meet fossil-fuel dependency shift. Its aim is to smartly integrate activities of all participants in the energy supply chain to effectively deliver environmentally sustainable, secure, and economic energy. The expectation of a smart grid is to operate, control, and support all existing and modern power system technologies to enable bidirectional power flows [2][3][4].

Smart grid is a sophisticated electric power system that incorporates the state-of-the-art computers, communication, information, and power electronics technologies to support energy generation, transmission, distribution and consumption for sustainability, flexibility, and effectiveness. It is a modernized power system that enhances the operation of its interconnected components through automatic control; modern information communications technologies; measurement technologies and advanced sensing; modern energy management techniques and analytical and decision making technologies in order to deliver efficient and flexible electricity to end-users [5]. SG is an intelligent power system with advanced sensors, higher computational functions, additional communication technologies, and more control hierarchies [6][7].

Smart grids integrate information communication technologies (ICT), advanced sensing and measurement technologies, analytical and decision-making technologies and automatic control to deliver electricity to end-users for a better reliability. SG integrates renewable energy resources and energy storage systems such as pumped storage, battery,

flywheel, etc. [1][2]. Smart grids allow dynamic flow of power and information to support new and current technologies in an optimized and reliable way from generation to end-users [3][4][5]. SG allows bi-directional communication between end-users and utilities; grid to vehicle(G2V) and vehicle to grid (V2G) operations; demand response and dynamic pricing [6][7]. The structure of SG is illustrated in Figure 1.1, the highly networked SG include many stakeholders.

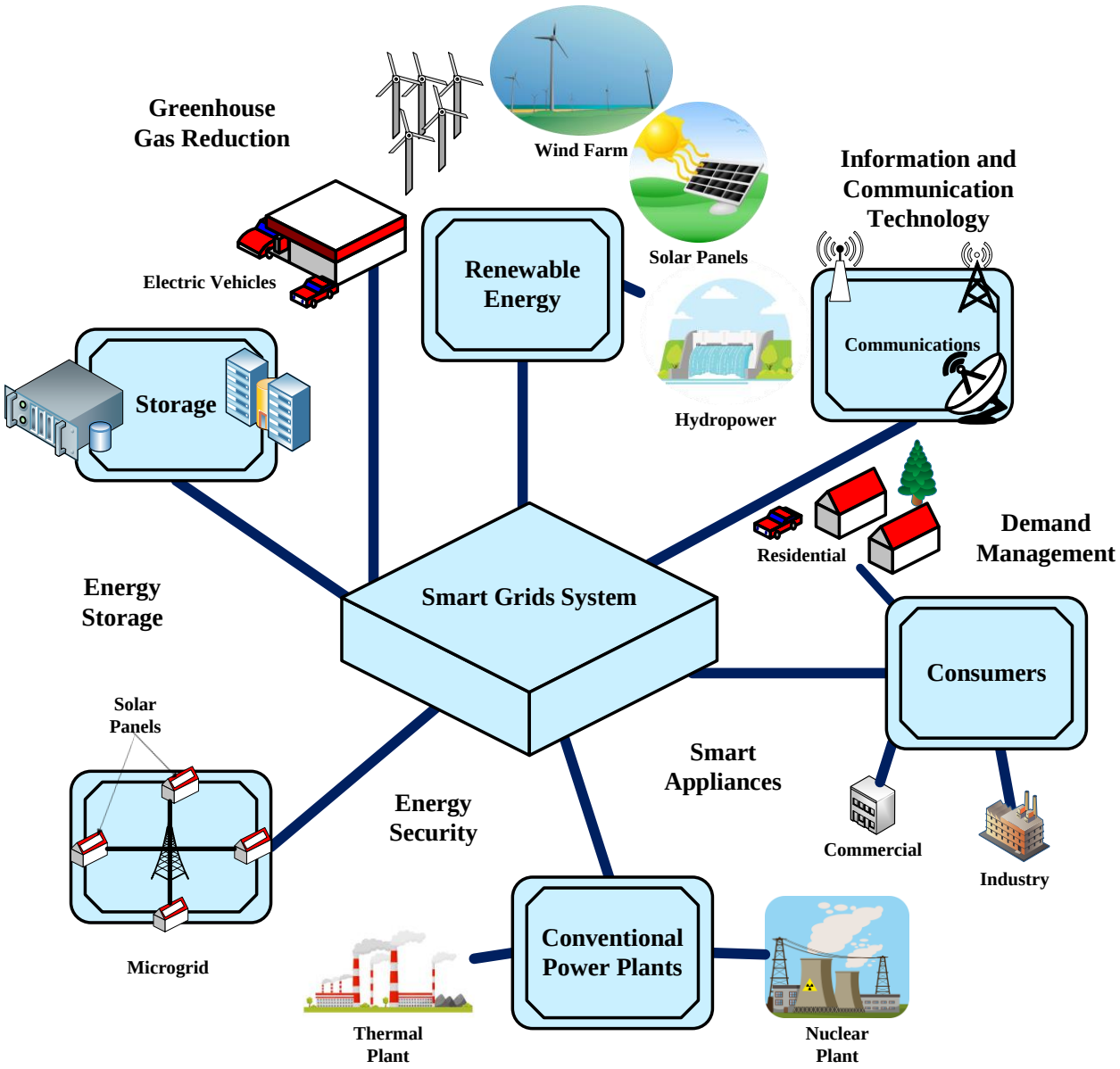

Figure 1. 1 Smart grids structure

1.1.1 Traditional Power System and Smart Grids

Traditional power grids have less or lack infrastructure that enhances communication technologies while the SG infrastructure enhances sensing and measurement technologies, advanced ICT and computing functionalities [8]. Generation in traditional power systems is centralised that is, from generating plant to transmission to distribution networks to end-users while in the SG generation is decentralised [5].

- Traditional power system infrastructure is mostly electro-mechanical in nature while SG infrastructure is digital in nature. Electro-mechanical devices have delays in their operation. SG infrastructure employs advanced intelligent technologies, advance measurement technologies, advanced sensing, and modern energy management techniques and near real-time decision-making technologies.

- Traditional power system uses one-way communication while SG uses two-way communication. The one-way communication is one directional flow of information from generation to end-users. Two-way communication is a real-time communication between consumer and utility to facilitate each end user's active participation in order to modify individual energy consumption based on individual preferences.

- In traditional power system sensors for measurement are often few while sensors are extensively used in SG.

- In traditional power system monitoring is mostly manual while monitoring in SG is mostly automatic control. That is, traditional power system has conventional monitoring devices which alert operator in the event of abnormal situations while SG has intelligent monitoring that is self-control and self-healing.

- No robust intelligent control technology in traditional power system while SG has robust intelligent control technology such as microgrid control, wide-area monitoring

and control, end-user energy management systems, renewable power generation control, energy and demand management system, analytical tools and operational applications.

- End-users have less or no scope to modify uses in traditional power system while there are modification capabilities in SG by end-users [5][9].

1.1.2 Smart Grids: Cyber-Physical Systems Perception

Cyber-physical system is a multidisciplinary complex system that incorporates embedded ICT and advance computing technologies into physical world [10][11]. The cyber-physical systems (CPS) demonstrate the following typical characters [12]:

- Seamless integration and interaction of physical systems infrastructure and communication technologies, control, information sensing, intelligence, and processing infrastructure. The physical systems situations are intelligently delivered to control centres as input and modify the simulation models to influence the future performance the physical systems as demonstrated in control algorithms such as microgrid control, wide-area monitoring and control, etc.
- Self-healing and self-restoration capability that support response to emergencies, faults, attacks and takes the corrective actions immediately to enable secure and safe system as demonstrated in autonomous outage detection and restoration.
- Distributed information data processing and real-time computation that support system timely decisions-making as demonstrated in intelligent load balancing and feeder reconfiguration.

- Interactions between physical components and cyber components systems through communication and coupling systems for timely responses, as demonstrated in real-time rating of distribution and transmission line flows.

Power system infrastructure is the physical systems that integrates with the cyber systems (which is the control, information sensing, intelligence, processing, ICT and advanced technologies). SG is multidimensional and multidisciplinary cyber-physical power system in which the advance computers and communication technologies intelligently control and monitor all physical power system infrastructure processes for a reliable energy delivery [13][14][15]. Thus, intelligent operation in a SG system is when the higher computational functions and decision-making technologies (control algorithms) perform decisions and generate control signals (expected to influence and modify the system state) based on information given by the measurement technologies and advanced sensors through the communication infrastructure. Therefore, core functionalities of smart grids are as a result of extensive deployment of cyber systems in the generation, transmission, and distribution systems for system data processing, protection, control, and monitoring.

1.1.3 Smart Grids with Renewable Energy

Authors in [16][17][18][19][20] state that substantial portion of global energy demand can be achieved with a renewable energy system. Authors in [21] state that with suitable storage and transmission facilities in place, the whole of the world energy needs can be supported by renewables. Currently, US Energy Information Administration 2019 data states that USA renewable energy resources deliver 11% of the total energy demand and 17% of all electricity generation [22]. Interestingly, this is more than the share quantity of nuclear generation of 8% of electrical energy. Thus, USA is confident of all-renewable grid by 2050[21]. In 2017, China accounted for additional 94GW solar PV, this is greater than half of all global solar PV capacity [23]. Denmark is aspiring a no-fossil energy by 2050 and only-

renewable heating and electricity by 2035[24][25]. In 2014, Denmark reported that solar, wind and biomass power plants delivered 60% electricity generation; 29% renewable energy generation in Spain; non-hydropower renewable provided about 30% of electricity demand in Portugal [26][27]. The world has accomplished a new track record of newly installed 167 GW renewable power capacity in 2017 with renewables delivering greater than 60% of all the new electricity capacity [23]. There is globally increased installed capacity of photovoltaic (PV) as part of the fossil-fuel dependency shift from fossil-fuel based power generations towards environmentally sustainable clean fuel power generations [28]. Renewable energy is one of the key technologies for SG and provide great opportunities for de-carbonization [29].

1.2 Research Motivation

High dependence of the smart grids on the cyber systems infrastructure exposes the whole cyber-physical power system operation to malicious attacks, cyber intrusion, information and data failures. Also, extensive integration of renewable energy resources causes new vulnerabilities in SG due to intermittent nature as compared to traditional power generation [30][31][32]. These failures could cause failure propagation that could affect interdependencies within the cyber-physical power system operation of the SG, adversely, impacting power system security. Failure can transmit or spread more rapidly and extensively thus, the SG security could be risked [33].

Loss of monitoring and control of the physical power systems infrastructure may impact the real-time cyber-physical power systems operation of the SG [34]. Failure of communication and coupling technologies may cause lack of control of the physical power systems infrastructure which may result in succession of failures in the SG [35]. For instance, accidental shutdown of a power station in Italy (2003 blackout) led to failures of the communication network nodes and the supervisory control and data acquisition (SCADA) system of the power

grid. This incident led to more failures in the power grid and subsequently led to a sequence of tragic cascading failure in the system [36][37]. The combination of power components failures, lack of real-time information and diagnostic support, local decision-making without regard to interconnectivity, computer and human errors that resulted in cascading failures eventually led to the huge blackout in the Northeast of United States in 2003 [38]. The Northeast blackout affected almost 50 million customers in seven US states and Ontario, Canada. The blackout caused a sudden shutdown of over 100 power plants at a localized generating plant [39][40].

Smart grids is susceptible to failures or mal-functioning such as components failure, cyber network failures, software failures, human errors and operational uncertainty [41]. The likelihood of cyber failure, failure propagations and interdependency failure in the SG could affect effective operation of the cyber physical power system therefore, jeopardizing the power system security. In the traditional power system reliability assessment, focus is entirely on physical power components, the approach assumes cyber components effective since cyber network enabled functions are limited in the traditional power systems. The approach does not consider cyber presence and cyber interaction in its assessment. Thus, cyber failures need to be considered in the SG performance assessment because effective operation of a SG with significant integration of cyber systems infrastructure depends on the availability of cyber network enabled functions.

Changes in the measurement technologies, computing functionalities, communication, monitoring and control due to the increasing integration of cyber systems infrastructure in the smart grids need to be considered in the performance assessment. Therefore, an approach that effectively incorporates cyber intelligent operation, and cyber interactions in smart grids operation is necessary.

This thesis presents investigation of smart grid operation at component level and their impacts at system level. The investigation of the SG operation at component level models smart component that simulates component operational behaviour of a smart grid environment. The system level models a unified cyber-physical components interaction and quantifies the interdependency impacts on physical power system security.

1.3 Research Aim and Objectives

The aim of the research is to capture cyber intelligent characteristic and cyber physical interdependency operation of a smart grids to quantitatively assess cyber-physical interactive impacts with the presence of renewable power generation penetration. The objectives of this research are as follows:

- To model and investigate smart component model to capture smart component's intelligent operational behaviour.
- To develop smart component state probability algorithm in order to compute the smart component states probabilities.
- To develop Monte Carlo simulation based performance assessment algorithm to investigate the performance of the smart component model and to assess impacts with the presence of renewable power generation penetration.
- To model and investigate a unified cyber-physical components interaction model to capture three function subsystem layers' interactions and interdependency of the cyber-physical power system.

- To develop Monte Carlo simulation based performance assessment algorithm to investigate the unified cyber-physical components interaction model and to assess the interdependency impacts on physical power system security.

1.4 Research Contributions

The main contributions of the research are summarized as follows:

- An innovative multi-state smart component model that captures cyber enabled functions influence on physical power components for a realistic intelligent characteristic evaluation is proposed.
- A new mathematical state probability algorithm of the multi-state smart component based on Markovian differential time dependent approach is proposed.
- An innovative and feasible performance assessment algorithm to assess realistic impacts of smart grids that justifies the value of smart operation of its components is proposed.
- An advanced unified ternary Markovian model of cyber-physical power system operation based on dynamic operation of subsystem functional layers' interactions of communication and coupling layer, decision-making layer and power layer is proposed.
- An embedded innovative cyber-physical performance assessment algorithm that quantitatively assesses realistic impacts of subsystem layers' interactions on power system security is proposed.

These contributions will significantly advance the existing knowledge of smart component operation and cyber-physical interactive operation in a smart grid, and then enables an

innovative way of assessing the extended impacts on the security of the physical power system.

1.5 Thesis Structure

This thesis consists of seven chapters including this introductory chapter. The chapters are outlined below:

Chapter 2

Chapter 2 presents literature review to provide an overview of related research work in a smart grid reliability assessment. The chapter explores various approaches of smart grids reliability assessment. It outlines smart grids component reliability, cyber-physical power system reliability and cyber-physical power system interdependency.

Chapter 3

Chapter 3 presents reliability concepts applied in the performance assessment of this research and smart component behaviour modelling. The chapter presents probabilistic approach in steady state security assessment framework with a focus on stochastic techniques. The chapter outlines multi-state smart component modelling approach; mathematical framework to compute the differential time dependent Markovian state probabilities and wind farm integration model. This is followed by Monte Carlo simulation based performance assessment algorithm and case studies to investigate and assess the multi-state smart component model with the presence of large wind.

Chapter 4

Chapter 4 presents smart grids system level modelling. The chapter describes SG as a cyber physical power system operation. The chapter outlines three main subsystem functional layers:

decision-making layer, communication and coupling layer and physical power layer. It outlines failure and interdependency in cyber-physical power system operation. This is followed by an innovative ternary Markovian modelling approach and mathematical computations. Table of various states the ternary Markovian model can exist is highlighted.

Chapter 5

Chapter 5 presents system level performance assessment of the cyber-physical power system operation. The chapter reflects the operational dynamics of the ternary Markovian model presented in chapter 5 in order to investigate the unified cyber-physical power system operation interactions and interdependency impacts on power system security. The chapter outlines ternary Markovian model Monte Carlo simulation based performance assessment algorithm and case studies.

Chapter 6

This chapter presents the research conclusions and future work.

Chapter 2: Literature Review

Comprehensive literature review is conducted in this chapter to provide an overview of related research. Literature on various approach of smart grids reliability is reviewed to shape the conducted project within this thesis, with a focus on smart grids component reliability, cyber-physical power system reliability and cyber-physical power system interdependency in order to investigate detailed reliability performance of the entire smart grids. Also, this chapter highlights power system performance assessment.

2.1 Introduction

Smart grids system is a computerized and technologically modernized concept of delivering electricity to protect, monitor, communicate and automatically enhance the operation of its interconnected components [30][42][16]. Smart grids system allows the integration of different kinds of renewable energy resources and deliver electricity to end-users with information and communication technologies (ICT) for better control and monitoring [43][44]. Although, there is no unique definition of a smart grids in the published domain other than reflecting facts that being better monitoring, better performance, better security, better economic value, and more flexible with the support of internet of things and information technologies through interactive operation of cyber and physical power system operation.

The extensive integration of renewable energy resources in smart grids system could potentially lead to new vulnerabilities such as voltage fluctuations, variability, and instability. Heavy dependence of the smart grid on the ICT exposes the whole smart grids to malicious attacks, cyber intrusion, information and data failures [30][31][32]. Also, smart grids system is susceptible to failures or mal-functioning such as components failure, cyber network failures, software failures, human errors and operational uncertainty [41]. Considering the integration

of renewable energy resources and high dependence of the smart grids on the ICT, failure is likely because each individual component has potential to fail [33]. Likewise, unreliability of a system is a function of the individual irregularity of its components. Thus, system operational awareness and plan remedy are very important for a realistic reliability assessment.

2.2 Smart Grids Component Reliability

Components in the traditional power system is assessed from a two-state approach: working state and failed state. Although two-state approach offers a reduced computational and design complexity, it does not always consider component operational behaviour before getting to a complete failure state [45][46]. Two-state approach most cases fail to characterize the actual component operational behaviour [47][48]. Two-state approach is insufficient to describe all states component can exist [49]. Representing all component behaviour model as a two-state approach can be unrealistic because some components can have some intermediate states that are unaccounted for in the reliability process [50][51]. Components in a smart grid system operate at different operational levels due to its complex functionalities. That is, a smart component can be in either operational state, pre-defect state, preventive state, correction state, derated state or failed state. Therefore, assessing smart component operation using a two-state approach is unrealistic.

Figure 2.1 illustrates a two-state model of a single repairable component in a traditional reliability assessment [52]. There are two states: working state(S_W) and failed state(S_F). Where $\boldsymbol{\lambda}$ and μ are transition rate. The traditional two-state approach assumes that systems or components can be either completely working or completely failed. Multi-state approach is a multiple states concept that sufficiently capture different levels of operational behaviour.

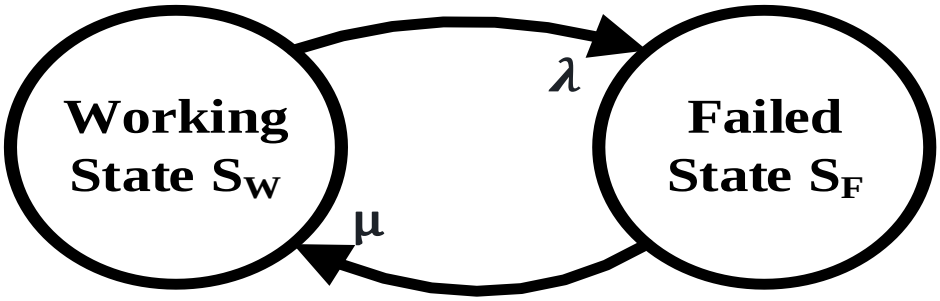

Figure 2. 1 Two states of a single component

Smart grids component is an intelligent component that operate at various levels of operational behaviour due to its complex functionalities as opposed to the traditional components. Smart grids component demonstrates different and distinct performance levels which differ from complete functioning to total failure as in the case of conventional components [46][53]. Therefore, an appropriate model is very important for a realistic and robust evaluation.

Various frameworks have been established in smart grids system reliability assessment to analyse smart grid components operation for a detailed reliability assessment. The frameworks are reliability block diagrams and fault tree; analytical based graph theory approach; Monte Carlo simulation approach and Markov approach. Reference [54] proposes a smart component model based on mathematical concept of absorbing state to represent functional states of smart components and to quantify component reliability with smart monitoring operation. The analysis shows great significant improvement with the component reliability with smart monitoring system. In this framework, absorbing state concept is used to investigate impact of events on component failure with smart monitoring.

Some frameworks conceptualised smart grids reliability assessment based on reliability block diagrams and fault tree. Authors in [55] propose a combinational approach model based

on reliability block diagrams and Markov model with the purpose of capturing the structure and the dynamic behaviour of the system. A smart grids reliability assessment based on reliability block diagram is proposed in [56] to assess the reliability of isolated grids integrated with wind and PV generators.

Several studies investigate smart grids' reliability assessment using analytical based graph theory approach. An analytical approach based on state matrix using the segmentation concepts and graph theory is proposed in [57] to evaluate the reliability of smart grids system. Reference [58] proposes an analytical approach based on the complex network theory to evaluate risk of communication network malfunction with associated latency and ICT network within a smart grids. The methodology shows a way of reliable quantification of cyber system's risks. Authors in [59] propose a stochastic Petri net based on analytical approach with the purpose of analysing the reliability of smart grids system in order to capture topology attacks during intrusion detection systems and malfunction recovery.

Several conceptualisations of smart grids reliability assessment are based on Monte Carlo simulation approach. A futuristic smart distribution network reliability assessment based on a pseudo-sequential Monte Carlo simulation to enable a stochastic approach for the reliability evaluation is proposed in [60]. Reference [61] proposes an hierarchical Monte Carlo simulation technique based on a layered fault tree model for a smart grid reliability considering consumers' perspective.

A mathematical model based on a Markov chain model is proposed in [62] to assess the impact of smart monitoring on reliability of power systems. The results show that loss of load expectation (LoLE) and expected energy not supplied (EENS) decrease with smart monitoring significantly. Reference [63] proposes an approach to capture vulnerabilities in critical infrastructure systems based on Markov imbedded systems model. The results show a reduction in costs due to intelligent control. Also, [33] proposes a Markov model based on the

reliability metric of system components, details of availability and unavailability system states with and without an intelligent control devices. The results demonstrate that the intelligent control enhances the reliability of physical infrastructure. Likewise, authors in [64] propose a probabilistic PRISM model checker to analyse the reliability of smart grid components based on Markovian models. The results show substantial improvements in accuracy and completeness. Similarly, a mathematical approach based on the variable weather Boolean logic Markov process driven is proposed in [65] to assess the reliability of smart grid considering weather variability.

None of the above mentioned frameworks focused on evaluating smart components reliability based on differential time dependent Markovian approach which is one of the emphases of this thesis. The approach demonstrates a flexible and clear representation of possible states a smart component can exist during operation. The differential time dependent Markovian approach [52] innovatively captures smart component's operational behaviour as a multi-state model. The differential time dependent Markovian approach has capacity to capture distinct performance levels of smart components. The approach has capacity to characterize the actual component operational behaviour. The approach incorporates intelligent characteristic of the smart component to characterize the actual component operational behaviour. The approach sufficiently represents all states component can exist and all intermediate states can be accounted for in the reliability computation. Thus, the approach demonstrates a realistic and robust evaluation.

2.3 Reliability in Cyber-Physical Power Systems

Cyber-physical power system (CPPS) is a smart system with series of components connected by power infrastructure, information and communication infrastructure and decision-making infrastructure. It is a modern-day intelligent power system with various systems and component

interactions. In a CPPS, the normal operation of one subsystem depends on the interactive functions of other components or subsystems of the CPPS.

Communication and decision-making infrastructures are to ensure that a better reliability of CPPS is achieved [66]. Authors in [35][41] state that communication and decision-making infrastructures support the transfer of power from generation to end-users in a reliable and secure manner. Also, authors in [39][34] argue that use of real-time communications support dynamic flow of power and information data to ensure a reliable power supply.

Growing interactions of cyber systems makes CPPS more susceptible to component failure, cyber network failure, software failure and human errors. References [30][32] state that extensive reliance of the power system on cyber systems may leads to new threats and makes the CPPS more vulnerable to malicious attacks, information and data failure. Reference [35] indicates that communication system failures may cause lack of controllability and observability of a power system which may result in succession of failures in the system. Authors in [33] state that any failure can transmit or spread more rapidly and extensively, and as a result the system reliability could be reduced. Failures could cause failure propagation that could affect interdependencies of the CPPS, adversely, impacting power system security.

Considering the likelihood of failure propagations and failure due to uncertainties and unpredictability in a CPPS, system modelling is important in order to assess true impacts. Thus, different frameworks have been proposed in CPPS modelling to analysis CPPS operation. Authors in [67] analyse electrical cyber-physical systems operation by modelling communication network associated in a power transmission grid using a mesh topology to characterize the networks interdependency based on various types of information channels. The model investigates vulnerability of electrical cyber-physical systems under various cyber-

attacks. Reference [68] proposes a CPPS equivalent model to quantitatively evaluate effect of improper control commands due to cyber contingencies on the power system of a CPPSs. Hierarchical control systems of cyber networks were designed as directed branches and directed graph with data nodes. The model effectively evaluates the impact of cyber contingencies without entire system simulations. An hierarchical CPP model based on flocking theory considering transient stability associated problems is proposed in [69] to maintain a transient stability during severe disturbances. The model facilitates identification of distributed control approaches that improve resiliency in power grid operation. An hybrid simulation model of CPPS considering time delay in predictive control model with low frequency oscillation damping controller is proposed in [70] to simulate CPPS operation. The model demonstrates good performance with improved cyber control systems. Lastly, a dynamic transmission model and a static connection model are proposed in [71] to evaluate effect of cyber components failure and quality of information transmission on distribution system of CPPS. These two models are developed to create CPPS model based on service restoration, fault location and isolation of the distribution system operation. The results show significant failure rates of the cyber components causing considerable impact on the distribution system reliability.

Most CPPS modelling focuses on a single dynamic characteristic of the CPPS operation. The CPPS model proposed in [72] is based on delay, dynamic routing and communication error. The approach in [68] is an hierarchical control system of a cyber network based on directed branches and directed graph with data nodes. Reference [73] models a unified electrical cyber physical system framework considering information flows and routers. These studies implement dynamic of the communication network in the CPPS modelling, the dynamic characteristics of the decision-making layer and power network are missing.

Reference [71] explores the CPPS modelling as separate models. CPPS operation in [71] is modelled as two separate models: the static connection model and the dynamic transmission model based on service restoration, fault location isolation and of the CPP distribution system operation. This study does not reflect a single unified framework modelling.

Several frameworks in CPPS modelling focus on cyber physical coupling mechanisms characteristic operation of the CPPS. Framework proposed in [67] models cyber-physical electrical power systems with integration of both power grids and communication networks, based on power transmission grid characteristics: high-voltage levels, long transmission distances and node importance in transmission grids. This approach models the communication network as a meshed topological network with each node linked to a physical node within the power transmission grid. Framework proposed in [74] models CPPS based on community theory to assess the vulnerability of CPPS. The CPPS model is characterized with the cyber network, power grid, and their interaction. The approach in [75][76] models CPPS based on correlation characteristic matrix using information and energy flows interactions of the CPPS. The approach in [77] models CPPS based on communication network and power flow dynamics. The framework proposed in [13] models CPPS as a two layer Markov model based on information flow performances and physical power characteristics. These studies implement the coupling mechanisms in the CPPS modelling, the dynamic characteristic of the decision-making layer is missing. The hierarchical CPPS model in [69] is based on flocking theory considering transient stability associated problems.

Each of the above mentioned studies does not reflect the characteristics of the three subsystem functional layers' interactions of the CPPS which is one of the emphases of this thesis. Also, as stated in [78] that it is very important in power system planning and operations of CPPS modelling to be established as a single unified model. Thus, the CPPS operation model

presented in this research work is a single unified model that combine series of consequences of events from the decision-making subsystem layer, the communication and coupling subsystem layer to the power subsystem layer. A non-unified model does not combine consequences of events from each of the main subsystem functional layers.? Non-unified model does not demonstrate combined reliability modelling and assessment.

2.4 Interdependency Impacts in Cyber Physical Power System

The states of a component or a subsystem in a CPPS can potentially influence the performance of other subsystems due to various interdependencies. The successful operation of a power system with a significant integration of cyber infrastructure depends on the cyber network security. Interdependency of cyber and power system is extremely important [78], because loss of interdependency in a CPPS due to uncertainty, unpredictability and failure could affect effective operation of the power system thus, the power system security could be jeopardized. Reference [34] states that loss of monitoring and control of power system components may influence the real-time operation of the whole power system. For instance, accidental shutdown of a power station in Italy (2003 blackout) led to failures of the communication network nodes and the supervisory control and data acquisition (SCADA) system of the power grid. This incident led to more failures in the power grid and subsequently led to a sequence of tragic cascading failure in the system [37]. The combination of power components failures, lack of real-time information and diagnostic support, local decision-making without regard to interconnectivity, computer and human errors that resulted in cascading failures eventually led to the huge blackout in the Northeast of United States in 2003 [38]. The Northeast blackout affected almost 50 million customers in seven US states and Ontario, Canada. The blackout caused a sudden shutdown of over 100 power plants at a localized generating plant [39][40].

In view of likelihood of failure propagations and interdependency failure due to uncertainties and unpredictability in a CPPS, interdependency assessment is important to assess its true impacts. Thus, relevant studies have been established on interdependencies in a CPPS in order to analyse its impact on CPPS operation. Reference [79] develops a mathematical model to evaluate the impacts of interdependencies in a cyber-physical system quantitatively. It concludes that the intelligent devices of the cyber-physical network could experience failures in two ways: direct and indirect interdependencies that might have effects on the reliability of a power system. An interdependency Markov-chain framework is proposed in [39] to investigate and forecast resilience to cascading failures and to study interdependency impacts on system reliability. It concludes that interdependencies among systems with reliable systems may lead to an unreliable system. A mathematical model to assess interdependency in power and communication systems of smart grid components is proposed in [77] for system vulnerability analysis. The model reveals interdependency between components and system vulnerabilities induced by system dynamics. Reference [80] proposes an analytical reliability model to capture effects of cyber-physical interdependencies and effects of failures from both physical and cyber components in a smart grids. The results argue that cyber infrastructure can have less reliability than a conventional power grid. An analytical reliability assessment considering both power and cyber component failures is proposed in [81] to investigate impact of direct cyber network failures on a power network. The results show that is very important to consider cyber negative impacts on power grid for reliability assessment. Though impacts of interdependency in a CPPS reliability have been explored, a unified framework that reflect characteristics of three subsystem functional layers' interactions of the CPPS is missing.

Other frameworks have been explored in interdependency of the CPPS. Reference [82] proposed a vulnerability analysis considering interdependence of CPPS based on bilevel optimization model of the system. Approach in [83] models CPPS as two interdependent

complex networks: physical resource and computational resource networks based on percolation theory to evaluate interdependency failure propagation of the system. The approach in [84] models interdependencies of the CPP critical infrastructures using analytic network process based on failure sequences and components functional dependencies graph. Approach in [85] models interdependencies between network SCADA (Supervisory Control And Data Acquisition) system and power transmission system using Boolean based approach to analyse systems' cascading failures. Approach in [86] is based on a decision diagram to assess the reliability of interdependent networks. In [87] the approach uses realistic network operational settings based on networks critical nodes to assess interdependent cascading failures of power grids. Reference [88] utilize multi-objective optimization based on undominated sorting genetic algorithm to assess power system robustness against cascading failure. A Q-learning approach based on power flow cascading failure model is developed in [89] to identify optimal sequential restorations of large scale smart grids after cascading failures. In a vulnerability analysis [90] the approach is based on AC power flow model utilising centrality theory of complex network to find important nodes in power grids. Reference [91] proposes one to multiple interdependencies model in order to analyse cascading failure of the CPPS based on dependent links and control threshold. Approach in [92] is based on three dimensional complex network theory to analyse interdependency, vulnerable and critical components of the CPPSs.

The above mentioned frameworks do not explore the CPPS modelling as a unified framework. Thus, the research presented in this thesis is a unified ternary Markovian model. The unified ternary Markovian model reflects characteristics of three subsystem functional layers' interactions of the CPPS. The model reflects dynamic operation of subsystem layers' interactions of communication and coupling layer and decision-making layer to power layer. The model combines consequences of events from each of the main subsystem functional layers. The model framework demonstrates combined reliability modelling and assessment. It

captures dynamics of subsystem layers' interactions for assessment of interdependency impacts.

2.5 Power System Reliability

Power system is a complex system designed for the generation, transmission and distribution of electricity to customers. It consists of lots subsystems, components and complex interactions spread over a wide geographical area. Power systems have evolved with growing global energy demand, significant integration of renewables and increasingly use of interconnected ICT infrastructures [38]. Over decades, measures in power system design and operation have been established to incorporate existing and new technologies to enhance an economically reliable system. However, continuous increasing loads, different generation types and changes in some operating parameters (such as rate of change of frequency) make the power system operation and protection extremely complex thus, causing further vulnerabilities, threats or operational uncertainties [41]. In recent years, the frequency of uncertainties continues to increase, due to the complexity in modern power systems and the demand for a high-quality power supply. Although, mitigation of the increased uncertainties has been demonstrated over the years to reduce severity of system disturbances and to maintain reliable power system. Methodologies in reliability assessment were well developed for generation system, transmission system and distribution system in the past decades [93][52]. However, power systems reliability assessment approach that captures the ICTs integration in its reliability assessment process is limited.

2.5.1 Power System Reliability Assessment

Reliability is generally termed as the ability of a system or component to perform its function. Power systems reliability is the ability of the power system to satisfy all customers electricity demand in quality, quantity and at minimum cost. That is, all customers demand must be satisfied within the required quantity while maintaining minimum cost at all acceptable values such as frequency and voltages [94] [95]. Power systems reliability assessment is the analysis and evaluation of power systems to guarantee all customers electricity demand in quality, quantity and minimum cost are satisfied. This includes generation, transmission and distribution contingencies analysis, operating policies, modelling needed for generating units dispatch, power flows assessment on transmission system components, network violations alleviation and load-shedding, if necessary [96]. Power system reliability assessment is grouped into system adequacy and system security.

Security refers to system's ability to respond to transient or dynamic disruptions and voltage instability within the system. This includes local disruptions, widespread disruptions, sudden loss of main generation or transmission facilities that can cause voltage instability, dynamic disruptions, or transient disruptions [97]. Adequacy is sufficiency of system's facilities to satisfy load demand of all consumers or operational constraints of the system. These facilities include all systems required to produce adequate energy and combine transmission and distribution facilities necessary to deliver the energy to the load points. Adequacy relates to static conditions [97].

Adequacy assessment is classified into three functional zones: power generation, power transmission, and power distribution. Adequacy studies are performed in each functional zone. The functional zones are combined to form ranked levels as shown in Figure 3.1. Hierarchical-Level I includes the generation facilities only. Hierarchical-Level II comprises both generation

and transmission facilities and Hierarchical-Level III comprises all three functional area: the generation, transmission and distribution facilities [97].

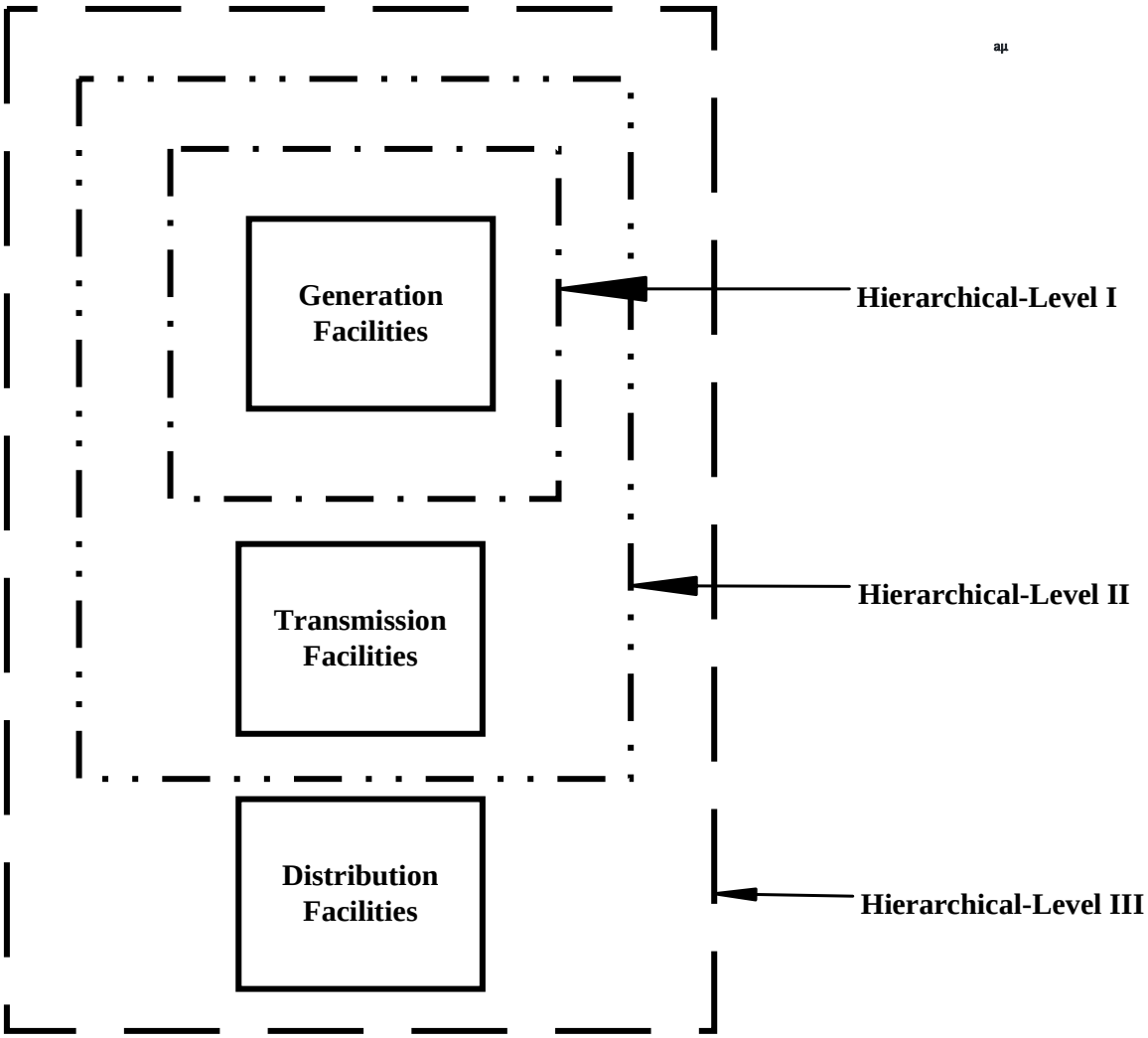

Figure 2. 2 Hierarchical-levels [97]

2.5.2 Power System Reliability Assessment Techniques

Reliability is the probability of a component or device or system performing its purpose satisfactorily for intending period of time and within an acceptable quality [98][99]. Reliability evaluation is used for: understanding how system operates; identifying how system fails; identifying causes of failures; identifying frequency of failures; deducing and monitoring

consequences of failures; deriving models to represent these factors and selecting reliability evaluation technique(s) [56][100][52]. Reliability evaluations enable operators to predetermine frequency and causes of failures, protection system fragile areas and areas of extreme amount of energy not supplied [101]. Technique in the reliability evaluation is broadly categorized into two approaches: deterministic approach and probabilistic approach [101][102].

The deterministic approach is conducted by choosing one or more operating base cases and then subjecting each of the operating base case to several incidents - out of service component(s) during the incidents is noted. Then the reliability of power system is evaluated. Examples of deterministic approach are percentage reserves in generation capacity planning and *N-1* contingency criteria in transmission system planning [97][103]. The deterministic approach does not respond to stochastic nature of component failures, system behaviour and customer demands. The approach considers all incidents and operating conditions as having the same likelihood of occurrence [97].

The probabilistic approach is performed by applying probabilistic control on the selection of incidents and operating cases. This is also known as risk assessment of a power system. The probabilistic approach involves two criteria, the first criterion is system states characterisation used to identify system states using probabilistic models. These probabilistic models are generally got from historical operating data and failures. The second criterion is quantification of consequences of each system state. These two criteria provide bases for probabilistic evaluation of power systems. There are two main techniques in probabilistic approach: analytical and simulation techniques [97][52].

Analytical techniques assess systems using mathematical models and evaluates indices from the models using mathematical methods. The analytical techniques are more effective with systems that exhibit less complex operating conditions and/or small number of

components failure probabilities. Some of these techniques do not consider the actual system behaviour. Some of the analytical techniques are block diagram technique, event tree technique, fault tree technique, Markov model technique, etc. Monte Carlo simulation technique estimates indices by simulating actual processes and random system behaviour. The technique is performed as a series of experiments. Monte Carlo techniques are often preferred when complex systems are involved [97][52].

Advantages and disadvantages with both analytical technique and simulation technique are detailed below [97][52]:

- In analytical technique, solution time is relatively short while the solution time for Monte Carlo simulation techniques is usually extensive.
- Analytical model gives the same numerical result(s) for the same set of input data, same model and same system while Monte Carlo simulation result(s) technique dependent on random number and number of simulations.
- Analytical approach model is generally a simplification of the system and at times becomes completely unrealistic. The Monte Carlo simulation approach can incorporate any recognized system characteristic and simulates accordingly.
- Analytical approach output is generally limited only to calculated values. The Monte Carlo simulation approach provides a wide range of estimated output parameters.

2.6 Summary

This chapter presents various research on smart grids component reliability, cyber-physical power system reliability, and cyber-physical power system interdependency. Several frameworks have been extensively researched on smart grids system to analyse smart grid components operation. Many mathematical concepts, reliability block diagrams, fault tree analysis, analytical based approach and simulation-based approach have been explored. However, no published study focuses on smart components reliability evaluation based on differential time dependent Markovian approach.

The differential time dependent Markovian approach is continuous Markov processes characterized by transition rate. The approach demonstrates a flexible and clear representation of possible states and transitions that stimulate random behaviour of systems which vary continuously with space and time. It innovatively captures smart component's operational behaviour as a multi-state model. The approach has capacity to capture distinct performance levels of smart components. The approach has capacity to characterize the actual component operational behaviour. It incorporates intelligent characteristic of the smart component to characterize the actual component operational behaviour. It sufficiently represents all states component can exist and all intermediate states can be accounted for in the reliability computation.

Different frameworks have been explored and researched on cyber-physical power system reliability approach to analyse cyber-physical power system operation. Most cyber physical power system modelling focuses on a single dynamic characteristic of the cyber physical power system operation. Some approaches explore the cyber-physical power system modelling as separate models. Some frameworks in cyber-physical power system assessment focus on cyber-physical coupling mechanisms characteristic operation of the cyber physical

power system. However, none of the published frameworks explores cyber-physical power system as a unified framework.

The cyber-physical power system model presented in this research work is a single unified ternary Markovian model. The unified ternary Markovian model reflects characteristics of events of three subsystem functional layers' interactions of the CPPS. The model reflects dynamic operation of subsystem layers' interactions from communication and coupling layer, and decision-making layer to power layer. The modelling framework demonstrates combined reliability modelling and assessment. It captures dynamics of subsystem layers' interactions for the assessment of interdependency impacts.

Chapter 3: Smart Component Modelling and Performance assessment with Wind Farm Integration

The aim of this chapter is to highlight concepts applied in accomplishing this research and smart component behaviour modelling. This research work presented in this thesis applies probabilistic approach in steady state security assessment framework with a focus on stochastic techniques: Markov modelling and Monte Carlo simulation. This research explores both Markov modelling technique and Monte Carlo simulation technique to establish an effective impact assessment process and the context is extended to smart grid level.

Also, this chapter models smart component behaviour with smart intelligent characteristic and quantitatively assess performance of the entire smart grids with the presence of large wind farms. This chapter presents an innovative multi-state smart component model, a mathematical framework embedded in Monte Carlo simulation and case studies. The state-of-the-art multi-state smart component model presented in this chapter is based on Markovian differential time dependent state probability concept to capture dynamic and intelligent operational behaviour of a smart grid component. Viability of the model is assessed through a Monte Carlo simulation based algorithm with the presence of large wind farms. Further, some parts of this chapter have already been published in [104]. The multi-state smart component model presented in this chapter have also been published in [104].

3.1 Markov Modelling

Markov modelling is a flexible and clear representation of possible states and transitions technique to stimulate random behaviour of processes or systems that vary continuously or discretely considering space and time [105][106][52]. The continuously or discretely varied random behaviour of processes or systems is called stochastic process. Markov modelling is utilized in the analysis of systems' reliability, maintainability and availability [107][108][109][110]. Markov modelling offers better insight into dynamic behaviour of a system or component [52][111][112]. In Markov modelling, model is conceptualized having sets of identifiable states, set of transitions between the states, component in one of the states always, component in only one state at a time, and component makes a transition from state to state at time to time. In order to present a component or system as a Markov model, the component or system behaviour have to be characterized as homogeneous, memoryless and identified state [52][113]. Homogeneous is when system behaviour is the same at every point of time regardless of time being considered, that is, the probability of changing or transiting between two states is the same at every time. Memoryless is when system future random behaviour dependent on immediate prior state but independent of past previous states or how it got to its current position, that is, present state is used as an input to predict the future states [38][52][114]. Markov analysis can be described mathematically as a sequence of random variables $(F_1, F_2, F_3, \ldots)$ in which the future states $(F_{n+1}, F_{n+2}, \ldots)$ are not dependent of all previous states $(F_1, F_2, \ldots, F_{n-1})$ but only dependent upon the current state F_n.

3.1.1 Markov Chain

Markov chain is a method that represent stochastic processes where states change at discrete time steps. Markov chain contain finite states $(F_1, F_2, F_3 \ldots F_n)$ that make the process to occur at any given time. Markov chain is described in terms of its transition probabilities y_{ij} which

define the probability of moving from one state to another state. Transition probability y_{ij} is the probability of the process moving from state F_i to state F_j. Transition probability y_{ii} is the probability of the process remaining in the same state [52].

Markov chain has various applications such as: dynamic of system behaviour through different states [112]; cascading failures prediction in power grids [39]; energy usage prediction [115]; solar array systems fault analysis [116]; wind power prediction [117]; communication network control analysis [118] and so on.

Markov chain can be illustrated using a simple system as shown below in Figure 3.1. The system shows two identified states S_A and S_B, the system has probabilities to remain in a state or leave a state to another state in a finite time [52]. Remaining in a state or leaving a state is called transition. The probability of the system remaining in state S_A is p_{ii} and the probability of transiting from states S_W to state S_B is p_{ij}. The sum of these probabilities must be one as indicated in (3.2). This principle is applicable to all systems irrespective of their levels of complexity with the sum of the probabilities of transiting in or transiting out of a state maintain as unity [52] as shown in (3.2) below;

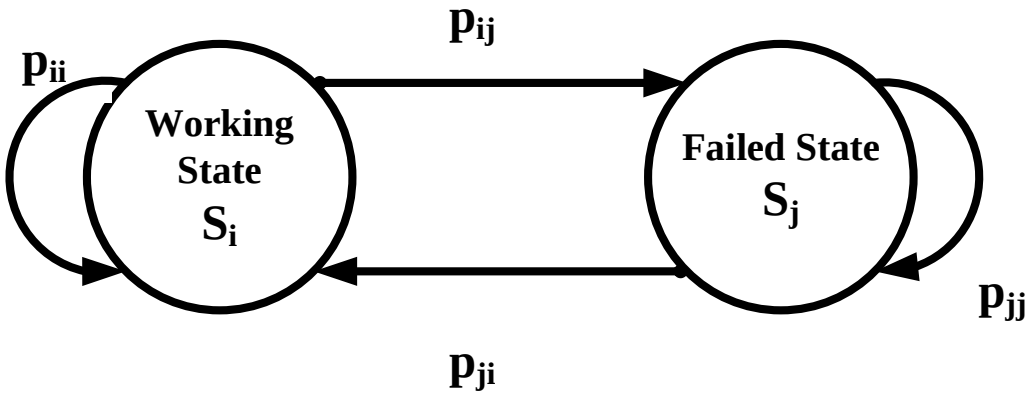

Figure 3. 1 Basic two states system

$$p_{ij} \forall i, j \in X = 1, 2, 3 \ldots . n \qquad (3.1)$$

$$\sum_{j \in X} p_{ij} = 1 \qquad (3.2)$$

Where, p_{ij}, p_{ji} and p_{ii} are the transition probabilities**,** X is the set of all possible states, n.

Generally, the most likely state begins with the system fully-functional, S_A. This is when the system is available and working as expected. However, operational uncertainty and unpredictability may cause the system to transit from its fully functional state to another state, S_B which might impact the whole system.

Markov chain has a *n-by-n* stochastic transition matrix *P*. The stochastic transitional probability matrix *P* consist of all the transition probability values for the system states as expressed in (3.3) below.

$$P_{k,\ k+1} = \begin{bmatrix} p_{11} & p_{12} & \cdots & p_{1n} \\ p_{21} & p_{22} & \cdots & p_{2n} \\ \vdots & \vdots & \vdots & \vdots \\ p_{n1} & p_{n2} & \cdots & p_{nn} \end{bmatrix} \qquad (3.3)$$

where: $P_{k,\ k+1}$ is state transition probability matrix, *k* and *k+1* is the current and next state respectively, *n* is number of states and p_{ij} is the transition probability that depict the probability of transiting from state *i* to state *j* during a given time interval. Within the transition probability matrix, the rows are the current state of the system while the columns are the next state, the sum of each row in the transition probability matrix must be unity [52][111].

3.1.2 Markov Processes

Markov processes is a method that represent components having a constant conditional probability of failure/repair during any given time interval. Markov processes is illustrated using transition rates and finite set of states [52].

Considering a repairable component with constant failure rate and repair rate, that is, the failure rate and repair rate are characterized by an exponential distribution, Figure 3.2 illustrates the state transition of the repairable component.

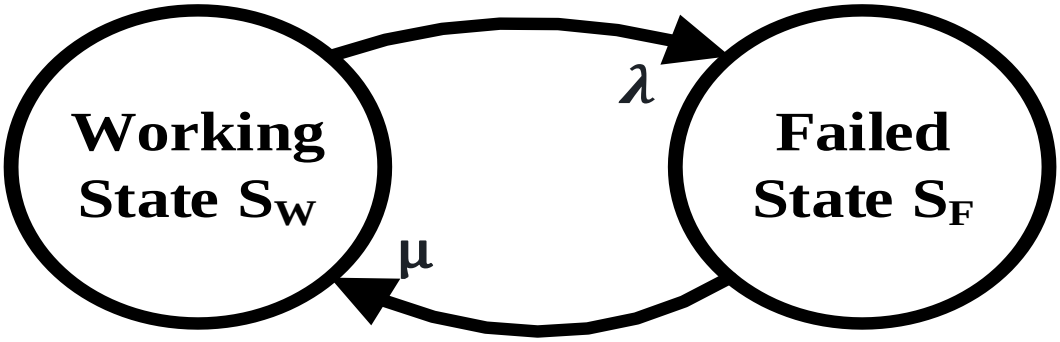

Figure 3. 2 State space diagram of a repairable component

The parameters **μ** (repair rate) and $\boldsymbol{\lambda}$ (failure rate) are state transition rates, they characterize the component rate of transition from one state to another. S_W and S_F are working state and failed state respectively.

An increased interval of time *dt* is assumed, *dt* is made very small so that during the incremental time, probability of two or more events happening is negligible. With standard assumptions that a component with failure rate of $\boldsymbol{\lambda}$, the probability of a failure transition in time *dt* is $\boldsymbol{\lambda}$dt, then the probability of not failing in time dt is 1-$\boldsymbol{\lambda}$dt. Thus, the probability of the component residing in a state after the time interval $t + dt$ is $P_{i\ldots n}(t + dt)$ [52].

From Figure 3.2, the component probability of residing in working state S_W at (t+dt) is equal to probability of residing in state S_W at *t* and not transiting out at *dt* + probability of residing in state S_F at t and transits to state S_W in *dt* [52]. This can be expressed as:

$$P_W(t+dt) = P_W(t)(1-\lambda dt) + P_F(t)(\mu dt) \quad (3.4)$$

Similarly, the component probability of residing in failed state S_F at (t+dt) is expressed as:

$$P_F(t+dt) = P_F(t)(1-\mu dt) + P_W(t)(\lambda dt) \quad (3.5)$$

From (3.1)

$$\frac{P_W(t+dt) - P_W(t)}{dt} = -\lambda P_W(t) + \mu P_F(t)$$

As $dt \to 0$, then,

$$\frac{P_W(t+dt) - P_W(t)}{dt} = \frac{dP_W(t)}{dt} = P'_W(t)$$

Therefore,

$$P'_W(t) = -\lambda P_W(t) + \mu P_F(t) \quad (3.6)$$

Also, from (3.2) applying the same method.

$$P'_F(t) = \lambda P_W(t) - \mu P_F(t) \quad (3.7)$$

Equation (3.3) and (3.4) is solved with Laplace transforms.

Where, $P_{i\ldots n}(s) = P_{i\ldots n}(t)$ in Laplace transformation. Therefore, each (3.3) and (3.4) is expressed in s-domain as:

$$sP_W(s) - P_W(0) = -\lambda P_W(s) + \mu P_F(s) \quad (3.8)$$

$$sP_F(s) - P_F(0) = \lambda P_W(s) - \mu P_F(s) \quad (3.9)$$

Where, $P_i(0) =$ Probabilities of residing in *i* state at *t = 0.*

Practically, the most likely start state of a component or system is working state, that is, the system is in a working condition at time zero. Hence, assuming the component starts in state S_W:

$P_W(0) = 1 \; and \; P_F(0) \; = 0.$

From (3.5)

$$(s + \lambda)P_W(s) - \mu P_F(s) = \; 1 \qquad (3.10)$$

From (3.6)

$$-\lambda P_W(s) + (s + \mu)P_F(s) = \; 0 \qquad (3.11)$$

Equation (3.7) and (3.8) is expressed in matrix form in s-domain as:

$$\begin{bmatrix} s + \lambda & -\mu \\ -\lambda & s + \mu \end{bmatrix} \begin{bmatrix} P_W(s) \\ P_F(s) \end{bmatrix} = \begin{bmatrix} 1 \\ 0 \end{bmatrix} \qquad (3.12)$$

To obtain each state probability in time domain: $P_W(t)$ and $P_F(t)$. Equation (3.9) is transformed back into the time domain:

$$\mathrm{P_W(t)} = \frac{\mu}{\lambda + \mu} + \frac{\lambda e^{-t(\lambda+\mu)}}{\lambda + \mu} \qquad (3.13)$$

$$\mathrm{P_F(t)} = \frac{\lambda}{\lambda + \mu} - \frac{\lambda e^{-t(\lambda+\mu)}}{\lambda + \mu} \qquad (3.14)$$

$P_W(t)$ and $P_F(t)$ are the probabilities of being in the working state and failed state respectively in time domain given that the component started at time t = 0 in the working state.

3.2 State Space Diagrams

State space is a set of all possible components or systems states, it is described as state space diagram. State space diagram includes all relevant states in which components or systems can reside. State space diagram facilitates solution of continuous or discrete Markov modelling. It translates operation of component or system into mathematical modelling that can be computed or solved by applying Markov techniques. Figure 3.2 is an example of state space diagram for a single repairable component.

3.3 Monte Carlo simulation

Monte Carlo simulation (MCS) is a stochastic simulation method with the use of random numbers. MCS is a simulation method that simulates events with sampling techniques at each trial. Process is repeated for a large number of trials and then estimate the parameters that was aimed at the convergence [119]. MCS estimates probability and other indicators by counting frequency of occurrence of an event. It examines and predicts system actual behaviour patterns in a simulated time. It estimates reliability/security indicators by modelling real process and random behaviour of system[52][103]. MCS utilizes state space sampling approach in order to include most situations and configurations easily. MCS uses mathematical concepts and probabilistic methods to model real time systems and then anticipate future systems values. Results accuracy in MCS depends on number of iterations (trials), the more the number of iterations the better accuracy. Thus, MCS is computationally expensive due to numerous numbers of iterations of the sampling process [101][120].

MCS can be categorised into two techniques: sequential MCS and Non-sequential MCS. Sequential MCS simulates system behaviour chronologically by sampling sequences of system states for numerous periods of time. In sequential MCS, sequence of events is created

by using probability distributions of random variables representing durations of component state and random numbers. Non-sequential MCS simulates system behaviour randomly by sampling sequences of system states for numerous periods of time. In non-sequential MCS, states are sampled based on random numbers and probability distributions of component states. This technique is simple, easy and offers less computational time and effort than sequential MCS [101][121].

3.4 Basic Probability Concept

Random event is an occurrence that may or may not occur in a given trial, time, or space. Assume an experiment is done repeatedly G times applying the same conditions, assume F is number of occurrences of event X. Ratio F/G reaches a defined value as G becomes very large. This value is defined as the probability of event X happening, that is:

$$P(X) = \lim_{G \to \infty} \left(\frac{F}{G} \right) \qquad (3.15)$$

Probability is measure of likelihood occurrence of a random event, probability is numerical and its value is between 0.0 and 1.0 [97].

3.5 Reliability Perspectives in a Smart Grid

Smart grids reliability is the ability of each of the cyber part and the physical part to perform its function at all acceptable values. That is, the physical part (known as primary side) is capable of sustaining high currents and satisfying duties of power generation and delivery. The cyber part (known as secondary side) is capable of transmitting communication signals, measurement, control functions, data acquisition, monitoring, and protection. The physical and cyber parts are very essential for proper functioning of a futuristic smart system.

In the traditional reliability evaluation process cyber failures are considered negligible or cyber functionalities is assumed reliable. This assumption is acceptable for traditional power grids reliability evaluation process because of limited cyber functionalities activities in the traditional power system. Also, components and systems in the traditional power system are assessed from a two-state approach: functional state and failed state. Considering the complexity and dimensionality of smart grids system due to the increasing deployment of cyber technologies and extensive dependent on cyber enabled functions, it is necessary to include cyber functionalities in reliability evaluation process of the smart grids system to achieve more realistic results [122][93][78]. In assessing smart grids system or smart component, two-state approach is inappropriate because two-state approach is insufficient to describe all component's states [49] and this approach most cases fail to characterize actual component or system performance behaviour [47][48]. In addition, authors in [51][50] state that multi-state approaches are appropriate for systems with complex functionalities and different levels of performance behaviour. Therefore, to achieve a robust and realistic performance assessment approach, research presented in this thesis proposed a multi-state approach in its smart grids performance assessment approach to captured cyber functionalities.

3.6 Smart Component Modelling

Smart grids component is typically an intelligent component and operates at various levels of operational behaviour due to the added functionalities, flexibility, and efficiency as opposed to the traditional component functionalities. Due to added functionalities and different levels of performances of a smart component, multi-state system reliability techniques are more appropriate for modelling the component operational behaviour in order to incorporate into smart grid reliability assessment [104]. The work presented in this chapter considers smart components as physical power components overlaid with ICT network enabled functions and control logic The smart components are the physical power components that are intelligently managed.

3.6.1 Multi-State Smart Component Modelling Approach

Multi-state is mathematical model that represents system with more than two performance levels. Multi-state allows analysable system to be described in more detail than traditional two-state approach [123]. Multi-state has also been utilized in reliability analysis of systems in oil/gas production, transportation networks, supply chain networks, manufacturing networks, and water distribution [50][124][125][126]. For such systems it could be inadequate to utilise a two-state performance level assessment. Multi-state modelling has received considerable attention over the years. Multi-state approach has capability to characterize the actual component operational behaviour [50]. In multi-state approach, component behaviour model demonstrates a finite number of functioning levels, from working condition to complete failure thus, it is a better representation with higher accuracy and flexible way to compare with the two-state approach [127].

The study presented in this chapter modelled smart grid component as a multi-state model to capture the dynamic intelligent operational behaviour. In this approach, the smart component (SC) model is conceptualized as having sets of identifiable states, set of transitions between the states, component in only one state at a time and component makes a transition from state to state at time to time. The multi-state Markovian model of a single SC illustrated in Figure 3.3, which reflects the dynamic intelligent operational behaviour of a smart component in a smart grid. State S_W, S_P, S_V, S_D and S_F present the component identifiable states during operation: working state, pre-defect state, preventive state, derated state and failed state respectively [104].

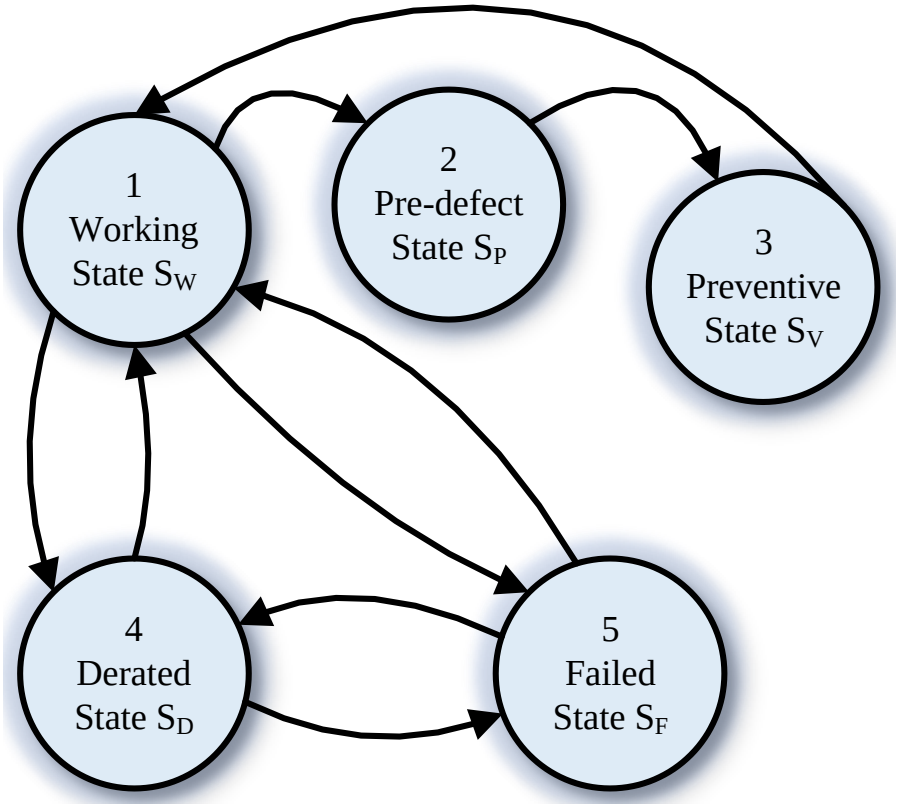

Figure 3. 3 Multi-state Markov model of a single smart component.

.

State S_W is state 1, formed as an operational state that indicate the component is working as expected. State S_W might transit to state S_P, state S_D or state S_F during any operational condition including threats [104].

State S_P is state 2, formed as a pre-defect state. In this state the SC detects any form of operational abnormality during operational conditions including threats. State S_P transits to state S_V [104].

State S_V is state 3, formed as a preventive state and correction state. In this state preventive actions are applied without any interruption and make the SC return back to its operational state (state 1). State S_V transits to S_W [104].

State S_D is state 4, formed as a derated state or a partial output state when component's partial output is expected (such as generating unit operating at reduced capacity). State S_D might transit to S_W or S_F.

State S_F is state 5, formed as a failed state when the component is not operating. State S_F might transit to S_W or S_D.

The five states in Figure 3.3 are reduced to four states as shown in Figure 3.4 to reduce computational complexity and to ensure effective implementation. State S_P and state S_V are merged to form intelligent state S_I [104].

Parameters μ_i and λ_i are state transition rates, they characterize the component rate of transition from one state to another[52][113].

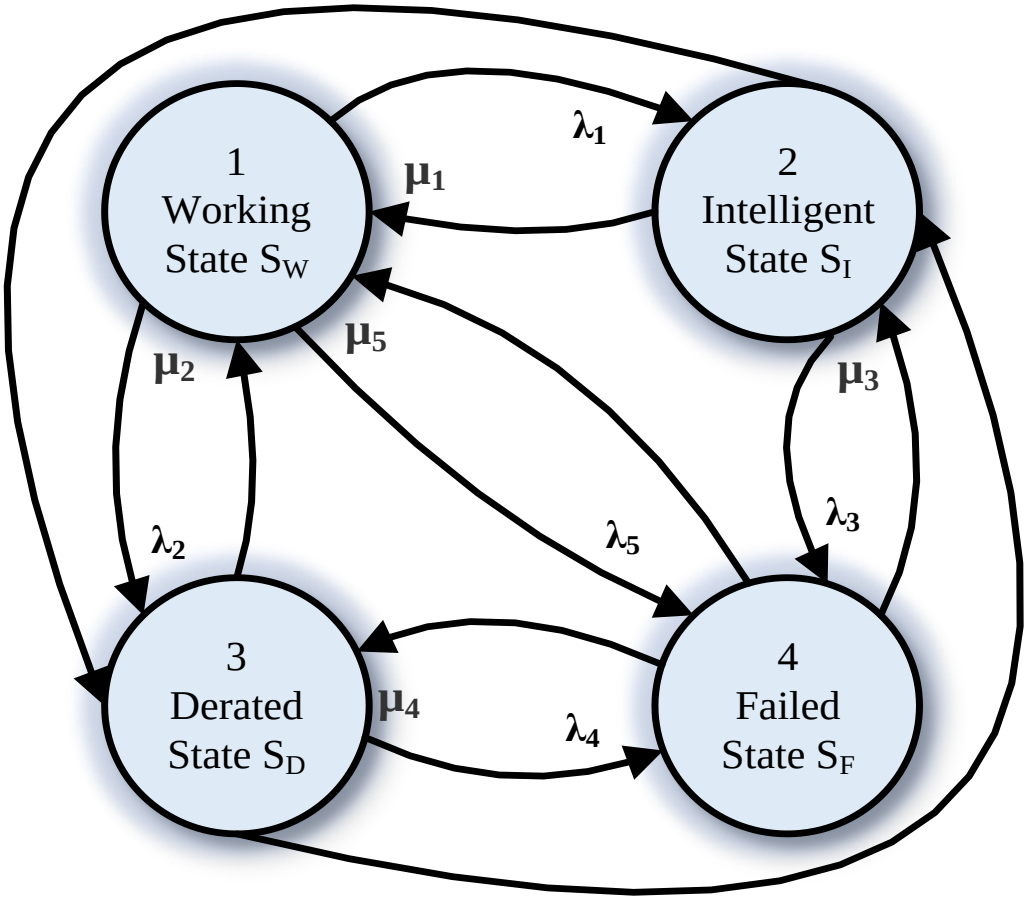

Figure 3. 4 Reduced Multi-state Markov model of a smart component [104]

In Figure 3.4 State 1 is formed to transit to state S_I, state S_D or state S_F during any operational uncertainties or threats. State 2 is formed as an intelligent state that detect any form of operational abnormality and carry out preventive actions without any interruption. State S_I transits to state S_W state S_D or state S_F. State 3 and state 4 are formed as stated above.

Practically, some transitions are allowed in the model to avoid component going into failed state or when a planned partial output is required for components maintainability purposes. Such as transition of state 2 to state 3 [104].

The Figure 3.4 is truncated to Figure 3.5 to reduce complexity in the state probabilities expressions and to ensure effective implementation of the model. The transition from state 4 to state 2 and transition from state 3 to state 2 are neglected due to low probability of occurrence. The SC is modelled to transit from a failed state S_F to S_W or S_D [104].

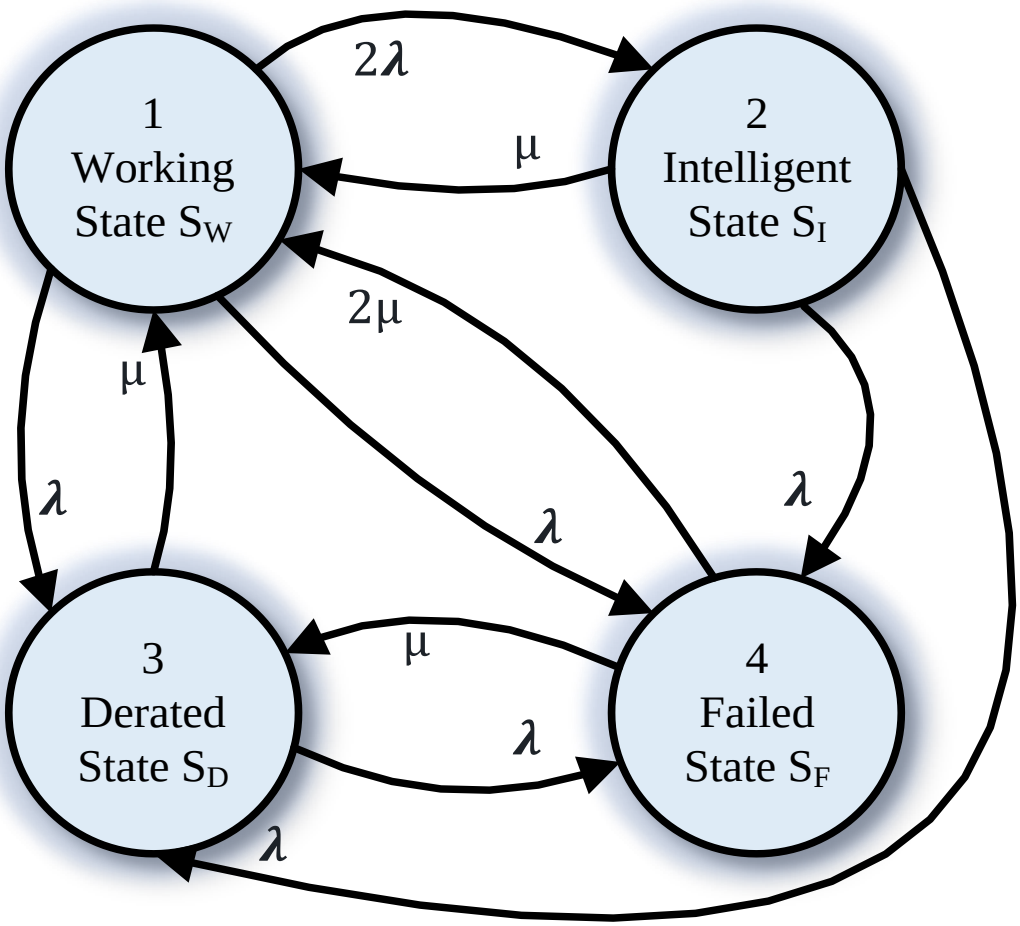

Figure 3. 5 Reduced transition rates Multi-state Markov model of a single smart component

In components or systems modelling, inaccuracy or error that may occurs because of the state reduction, transition reduction or any simplification is normally negligible and mostly within the associated tolerance of components reliability data.

3.6.2 Model Benefits

- The mode has capacity to capture distinct performance levels of smart components.
- The model has capacity to characterize the actual component operational behaviour.
- The mode incorporates intelligent characteristic of the smart component to characterize the actual component operational behaviour.
- The mode represents all states smart component can exist and all intermediate states can be accounted for in the reliability computation.
- The model identifies and demonstrates actions of the component level reliability.
- The mode is more effective in capturing impacts than two-state models**.**
- The model achieved a new mathematical state probability algorithm of the multi-state smart component.

3.7 Differential Time Dependent Markovian State Probabilities

Figure 3.5 shows a state space diagram of the SC dynamic intelligent operational behaviour. The model has identifiable states, state transitions and values of the transition rates in order to analyse the model using Markov differential methods to establish time dependent states probabilities.

An increased interval of time *dt* is considered, *dt* is made very small so that during the incremental time the probability of two or more events happening is negligible [52]. A component with failure rate of λ, the probability of a failure transition in time dt is λdt, then the probability of not failing in time *dt* is $1-\lambda dt$ [52]. Thus, the probability of the SC residing in a state after the time interval $t + dt$ is $P_{i\ldots n}(t + dt)$ [104].

From Figure 3.5 the SC probability of residing in working state S_W at (t+dt) is equal to probability of residing in state S_W at *t* and not transiting out at *dt* + probability of residing in state S_I at *t and* transits to state S_W in *dt* + probability of residing in state S_D at *t* and transits to state S_W in *dt*. + probability of residing in state S_F at t and transits to state S_W in *dt*. This can be expressed as [104]:

$$P_W(t+dt) = P_W(t)[1-(4\lambda)dt] + P_I(t)\mu dt + P_D(t)\mu dt + P_F(t)2\mu dt \quad (3.16)$$

The component probability of residing in intelligent state S_I at (t+dt) is equal to probability of residing in intelligent state S_I at t and not transiting out at dt + probability of residing in operative state S_W at t and transiting to state S_S at dt + probability of residing in derated state S_D at t and transiting to intelligent state S_I at dt + probability of residing in failed state S_F at t and transiting to intelligent state S_I at dt. This can be expressed as [104]:

$$P_I(t+dt) = P_I(t)\ x\ [1-(\mu dt + 2\lambda)dt)] + P_W(t)2\lambda dt \quad (3.17)$$

With the same conceptual consistency as demonstrated with the operative state, the component probability of residing in derated state S_D at (t+dt) is expressed as:

$$P_D(t+dt) = P_D(t)[1-(\mu+\lambda)dt] + P_W(t)\lambda dt + P_I(t)\lambda dt + P_F(t)\mu dt \quad (3.18)$$

Similarly, the component probability of residing in failed state S_F at (t+dt) is expressed as:

$$P_F(t+dt) = P_F(t)[1-(3\mu)dt] + P_W(t)\lambda dt + P_I(t)\lambda dt + P_D(t)\lambda dt \quad (3.19)$$

From (3.16)

$$\frac{P_W(t+dt)-P_W(t)}{dt} = -(4\lambda)P_W(t) + P_I(t)\mu + P_D(t)\mu + P_F(t)2\mu$$

As $dt \to 0$, then,

$$\frac{P_W(t+dt) - P_W(t)}{dt} = \frac{dP_W(t)}{dt} = P'_W(t)$$

Therefore,

$$P'_W(t) = -(4\lambda)P_W(t) + P_I(t)\mu + P_D(t)\mu + P_F(t)2\mu \quad (3.20)$$

Also, from (3.17), (3.18) and (3.19) respectively applying the same method.

$$P'_I(t) = 2\lambda P_W(t) - (\mu + 2\lambda)P_I(t) \quad (3.21)$$

$$P'_D(t) = \lambda P_W(t) + \lambda P_I(t) - (\lambda + \mu)P_D(t) + \mu P_F(t) \quad (3.22)$$

$$P'_F(t) = \lambda P_W(t) + \lambda P_I(t) + \lambda P_D(t) - (3\mu)P_F(t) \quad (3.23)$$

Equations (3.20), (3.21), (3.22) and (3.23) is solved with Laplace transforms.

Where, $P_{i\ldots n}(s) = P_{i\ldots n}(t)$ in Laplace transformation. Therefore, each (3.20) to (3.23) is expressed in s-domain as:

$$sP_W(s) - P_W(0) = -4\lambda P_W(s) + \mu P_I(s) + \mu P_D(s) + 2\mu P_F(s) \quad (3.24)$$

$$sP_I(s) - P_I(0) = a\lambda P_W(s) - (\mu + 2\lambda)P_I(s) \quad (3.25)$$

$$sP_D(s) - P_D(0) = \lambda P_W(s) + \lambda P_I(s) - (\mu + \lambda)P_D(s) + \mu P_F(s) \quad (3.26)$$

$$sP_F(s) - P_F(0) = \lambda P_W(s) + \lambda P_I(s) + \lambda P_D(s) - (3\mu)P_F(s) \quad (3.27)$$

Where, $P_i(0) =$ Probabilities of residing in *i* state at *t = 0.*

Practically, the most likely start state of a component or system is working state, that is, the system is in a working condition at time *0*. Hence, assuming the SC starts in state S_W:

$P_W(0) = 1, P_I(0) = 0, P_D(0) = 0 \; and \; P_F(0) = 0.$

From (3.24)

$$(s + 4\lambda)P_W(s) - \mu P_I(s) - \mu P_D(s) - 2\mu P_F(s) = 1 \quad (3.28)$$

From (3.25)

$$-2\lambda P_W(s) + [s + (\mu + 2\lambda)]P_I(s) = 0 \qquad (3.29)$$

From (3.26)

$$-\lambda P_W(s) - \lambda P_I(s) + [s + (\lambda + \mu)]P_D(s) - \mu P_F(s) = 0 \qquad (3.30)$$

From (3.27)

$$-\lambda P_W(s) - \lambda P_I(s) - \lambda P_D(s) + [s + (3\mu)]P_F(s) = 0 \qquad (3.31)$$

Equation (3.28) to (3.31) is expressed in matrix form in s-domain as:

$$\begin{bmatrix} s+4\lambda & -\mu & -\mu & -2u \\ -2\lambda & s+B & 0 & 0 \\ -\lambda & -\lambda & s+C & -\mu \\ -\lambda & -\lambda & -\lambda & s+3\mu \end{bmatrix} \begin{bmatrix} P_W(s) \\ P_I(s) \\ P_D(s) \\ P_F(s) \end{bmatrix} = \begin{bmatrix} 1 \\ 0 \\ 0 \\ 0 \end{bmatrix} \qquad (3.32)$$

Where, B=2λ+μ, C=λ+μ

To obtain each state probability in t: $P_W(t)$, $P_I(t)$, $P_D(t)$ and $P_F(t)$. Equation (3.32) is transformed back into the time domain as [104]:

$$P_W(t) = \frac{3\mu^2 + 2\lambda\mu}{(\lambda + 3\mu)(4\lambda + \mu)} - \frac{\exp\big(-t(4\lambda + \mu)\big)(-12\lambda^2 + 7\lambda\mu)}{(4\lambda + \mu)(3\lambda - 2\mu)}$$

$$- \frac{\lambda\mu \exp\big(-t(\lambda + 3\mu)\big)}{(\lambda + 3\mu)(3\lambda - 2\mu)} \qquad (3.33)$$

$$P_I(t) = \frac{\exp\left(-t(4\lambda+\mu)\right)(-12\lambda^2+7\lambda\mu)}{(4\lambda+\mu)(3\lambda-2\mu)} - \frac{\exp\left(-t(2\lambda+\mu)\right)(-2\lambda^2+3\lambda\mu)}{(\lambda-2\mu)(2\lambda+\mu)} + \frac{4\lambda^2\mu+6\lambda\mu^2}{(2\lambda+\mu)(\lambda+3\mu)(4\lambda+\mu)} - \frac{2\lambda^2\mu\exp\left(-t(\lambda+3\mu)\right)}{(\lambda-2\mu)(\lambda+3\mu)(3\lambda-2\mu)} \quad (3.34)$$

$$P_D(t) = \frac{\exp\left(-t(2\lambda+\mu)\right)(-2\lambda^2+3\lambda\mu)}{(\lambda-2\mu)(2\lambda+\mu)} - \frac{\exp\left(-t(\lambda+3\mu)\right)(-\lambda^2+\lambda\mu)}{(\lambda-2\mu)(\lambda+3\mu)} + \frac{4\lambda\mu}{(2\lambda+\mu)(\lambda+3\mu)} \quad (3.35)$$

$$P_F(t) = \frac{1}{(\lambda+3\mu)} - \frac{\lambda\exp\left(-t(\lambda+3\mu)\right)}{(\lambda+3\mu)} \quad (3.36)$$

$P_W(t)$, $P_I(t)$, $P_D(t)$ and $P_F(t)$ are the state probability of working state, intelligent state, derated state and failed state respectively of the SC.

3.8 Multi-State Smart Component Model in Monte Carlo Simulation

Monte Carlo simulation trials are conducted to determine the SC's status and to predict real behaviour in simulated time in order to obtain the frequency of some reliability parameters and to estimate the expected value of each of the parameters. Figure 3.6 shows the basic steps of the SC model through MCS. In this approach, the MCS examines and predicts various SC states status in simulated time to obtain energy not supplied (ENS) and to estimate expected value of the ENS.

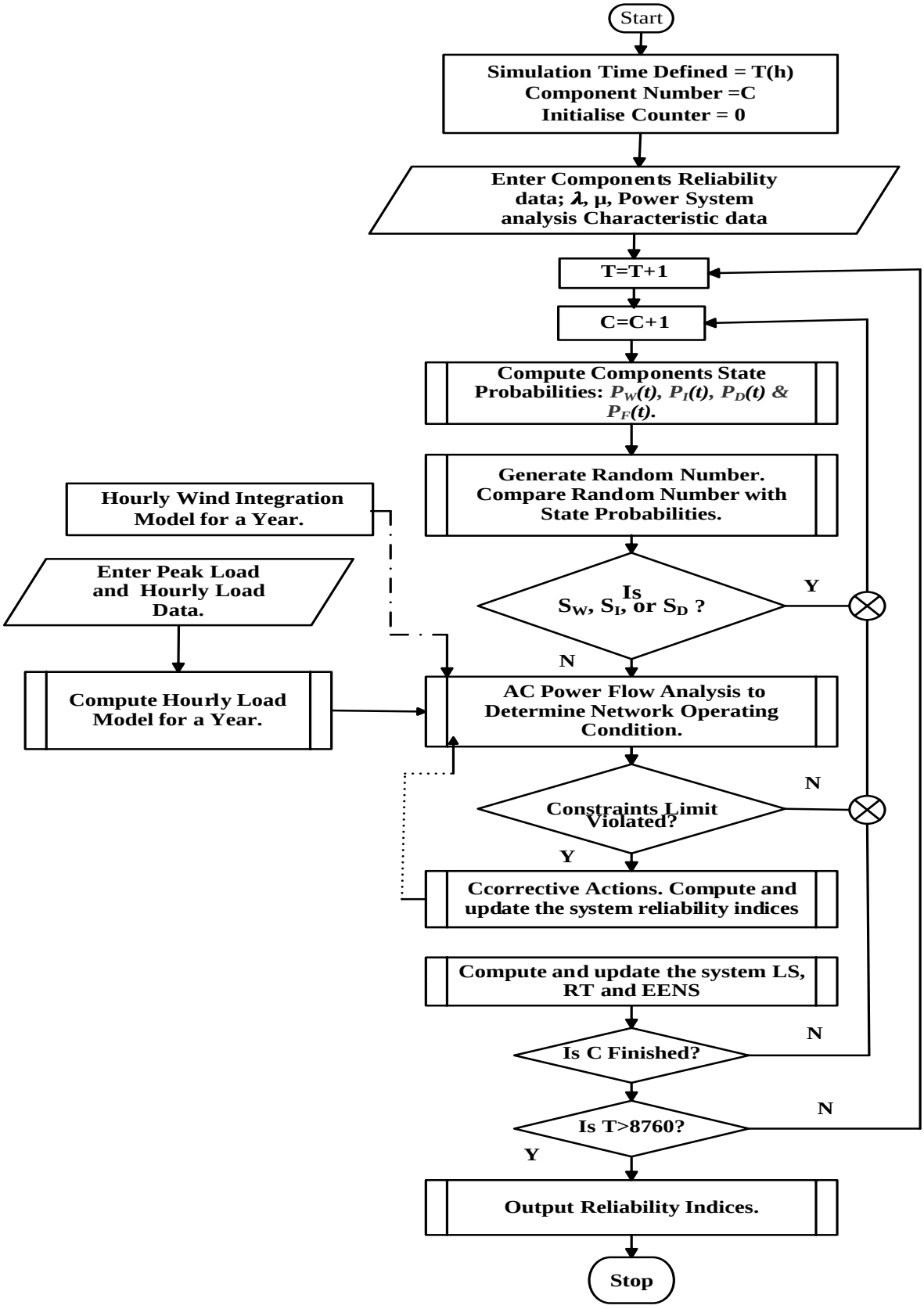

Figure 3. 6 Basic flow chart of multi-state smart component model in Monte Carlo Simulation with wind power integration.

Component state is determined by sampling the probability that the component exists in that state [97]. In simple random sampling, component status is determined by comparing generated random numbers (RN) with the state probability of the component state. The SC status is determined by sampling the probability that the SC exists in that state considering each state of the SC: $P_W(t)$, $P_I(t)$, $P_D(t)$ and $P_F(t)$. This is achieved by using generated random numbers (RN) and the SC states probabilities: $P_W(t)$, $P_I(t)$, $P_D(t)$ and $P_F(t)$. RN consists of a uniform distribution over a specified range of values [103][121][101]. This study assumes a uniform distribution of random number within [0,1]. With different states probabilities of the multi-state SC model stated above, MCS steps are programmed and simulated in MATLAB to determine the SC performance.

The multi-state SC through MCS Steps for system performance assessment includes the following basic steps.

Step 1: Select SC state.

Step 2: If the state is a working state, intelligent state or derated state go back to Step 1 to select a new SC state. If the state is a failed state, go to Step 3.

Step 3: Perform a Newton-Raphson A/C power flow to check the network operating condition. If constraints limits are not violated, then go back to Step 1 to select a new SC state. Otherwise, go to step 4.

Step 4: Perform remedial actions. Remedial actions is corrective actions to prevent network collapse or to alleviate sustained violations. The incorporated corrective actions in this study are reactive power compensation, on-load-tap changing, generation re-dispatch and shedding of loads.

Step 5: Compute and update the system reliability indices. If component is finished, then go back to step 6. Otherwise, go to Step 1 to select a new SC state.

Step 6: Steps 1–5 are repeated until 876000 iterations are met.

In this investigation, the performance of SC is estimated by EENS and VoLL indices. EENS index is the expected energy not supplied and VoLL [128][129][130] is value of lost load.

At each sample trial: if the smart component is in working state S_W, intelligent state S_I or derated state S_D a new SC state is selected; if the SC state is in failed state, then a Newton-Raphson A/C power flow is performed to check the network operating condition. if any constraint is violated, it is rectified through corrective actions to prevent network collapse or to alleviate sustained violations, then corresponding reliability indices is computed and updated.

At the end of each sample trial: mean value of the curtailed load and corresponding cost of lost load of all the processed samples are calculated with maximum number of samples trials, the EENS is estimated as [122]:

$$\mathrm{EENS} = \frac{1}{y}\sum_{i}^{y} K_i \text{ x } T_i \qquad (3.37)$$

where, y is the processed samples, K_i is the magnitude of curtailed (shed load) at the sample *i* and T_i is the restoring time of K_i.

This chapter is aimed at component level assessment. The performance of the smart component operation with and without wind power integration has been quantified through the application of MCS. In a power system context, the MCS requires running a significantly large number of sample trials beyond 10,000 in many cases. MCS is a probabilistic approach that apply probabilistic distribution on the selection of incidents and operating cases in order to achieve a nearer adherence to reality. MCS examine and predict various component states in simulated time.

3.9 Smart Component Performance Assessment with Large Wind Farms

3.9.1 Wind farm Model

Wind power integration characteristic is captured in this study by applying time series profiles(TSP) of wind power generation outputs of wind farms. This is an hourly output data of wind power generation. The output data are normalized through their installed capacities to ensure the output profiles spans from 0 to 1.0 against time. The wind power integration characteristic synthesizes the TSP to match the individual sample trial duration of MCS and they are sequentially applied to the network operating condition as the trials progress. Annual wind power time series profile for Birmingham, United Kingdom (UK) wind site in 2018 [131] used in this study is shown in Figure 3.7.

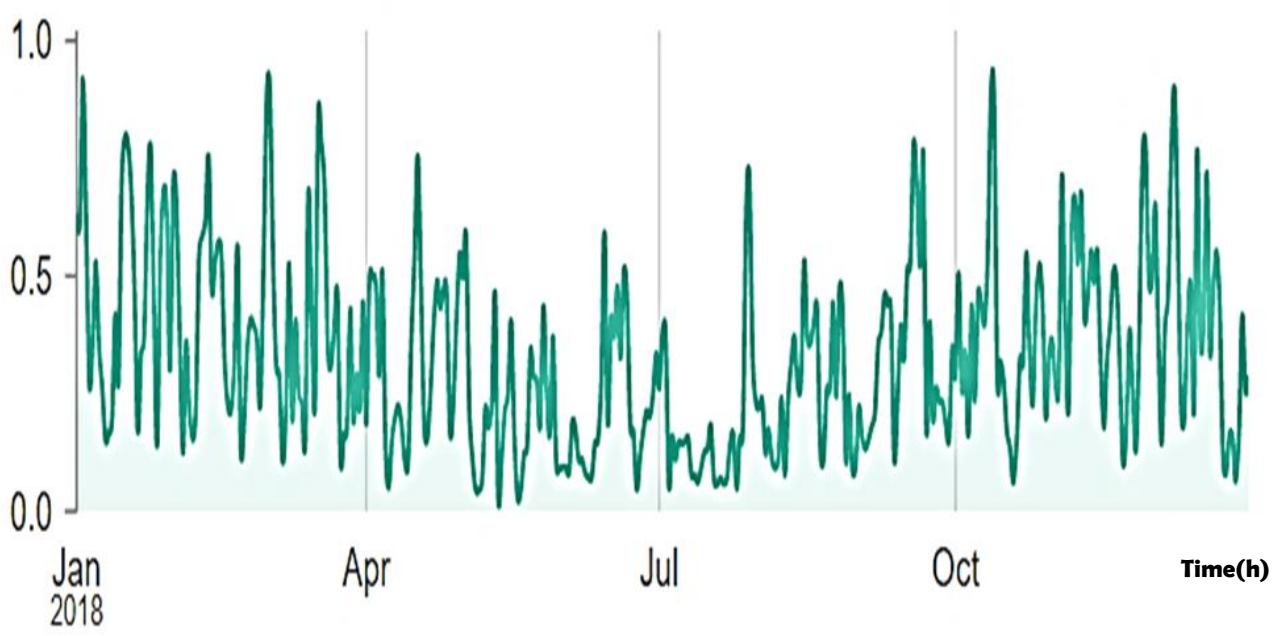

Figure 3. 7 Annual wind power time series profile for Birmingham wind site in 2018 [131].

3.10 Case Studies

Case studies are presented to investigate the smart component model performance and to assess detailed reliability performance of a smart grids with the presence of large wind farms. This section presents IEEE 24-Bus Reliability Test System (RTS) and some case studies scenarios in order to investigate and evaluate the impacts of the smart components' operation in a smart grid environment in the presence of wind farms.

3.10.1 Test System

The 24-Bus RTS [132] is used for the case studies scenarios and its details are given in appendix A. The test system network as shown in Figure A.1, is used for different scenarios simulations presented in this chapter. The transmission system consists of 24 buses, 33 lines and 5 transformers as shown in Table A.1and Table A.2 respectively. The transmission lines are at two voltage levels, 230 kV and 138 kV. The 138 kV system is in the lower part of the power system. The buses 11, 12, and 24 represent the 230/138 kV tie-stations. There are 10 generator buses connecting 32 generating units and 17 load buses in the system as shown in Table A.3, Table A.4 and Table A.5 respectively. All the generating units are modelled as multi-state smart component. Bus 14 and bus 6 have a synchronous condenser and a reactor connected respectively as voltage corrective devices. The data of the system components are given in [132] with annual peak active power load of 2850 MW and reactive power load is 580 MVAr. Peak hourly load model for three seasons are given in Table A.6 [132].

Different values of wind power at various substations (buses) are used to demonstrate the potential scenarios of wind farms, this is applied to the network operating condition as the MCS trials progress [52][129]. With the integration of the wind power, the network maximum capacity, as in shown in Table A.4 is maintained.

3.10.2 Scenarios

Various scenarios are implemented to investigate the multi-state smart component(SC) model performance and to assess the impacts on a smart grid environment in the presence of large wind farms. Various scenarios with and without wind power integration (WPI) were investigated in this chapter in order to explore smart component operation for any system abnormalities. Having such leverage can ensure extra planning in the events of unforeseen contingencies in the smart grid system.

3.10.2.1 Scenario 1

This scenario incorporates the proposed multi-state SC model. This scenario has two sub-scenarios: Scenario 1A and Scenario 1B. Scenario 1A is the base case (BC) designed by incorporating the operating condition given in Section 3.10.1 without wind power integration. Scenario 1B is designed by incorporating the BC operating condition given in Section 3.10.1 with 142.5MW WPI at load bus 3. The wind power integration is implemented at load bus because load buses typically have no prior generation activities.

3.10.2.2 Scenario 2

The aim of scenarios 2 is to investigate the contrast between the BC scenario and scenario 2. Scenario 2 has two sub-scenarios: Scenario 2A and Scenario 2B. Scenario 2A is the traditional power system security assessment (two-state approach). Scenario 2B is the traditional power system security assessment (two-state approach) with 142.5MW wind power integration at load bus 3.

3.10.2.3 Results and Analysis of Scenario 1 and Scenario 2

Table 3.1 shows the annual EENS, load shed and restoration time values for scenarios 1A, 1B, 2A and 2B. Figure 3.8, Figure 3.9 and Figure 3.10 show annual load shed, EENS and restoration time respectively for scenarios 1A, 1B, 2A and 2B. In Fig. 7, the load shed level is significantly reduced in scenario 1A compared to scenario 2A. Also load shed level is significantly reduced in scenario 1B compared to scenario 2B. These indicate less components failure rate and less disturbance in the smart grids of the scenarios 1A and 1B. These impose reduced rate of system disturbance and stress thus, making the system to be less unbalanced which subsequently enhanced the system performance which is demonstrated in reduced level of the load shed. This depicts the intelligent preventive and correction capability response of component in smart grids system to sudden failures or attacks without any interruption. These results suggest that the SC is more reliable and effective than the traditional components. The load shed level is significantly reduced in scenario 1A compared to scenario 2AAlso load shed level is significantly reduced in scenario 1B compared to scenario 2B.

Table 3. 1 Scenario 1 and Scenario 2

Scenarios	EENS (MWh/y)	Load Shed (MW/y)	Restoration Time (h)
1A	6.E+03	9.E+03	12
1B	3.E+04	4.E+04	49
2A	4.E+04	5.E+04	46
2B	7.E+04	1.E+05	127

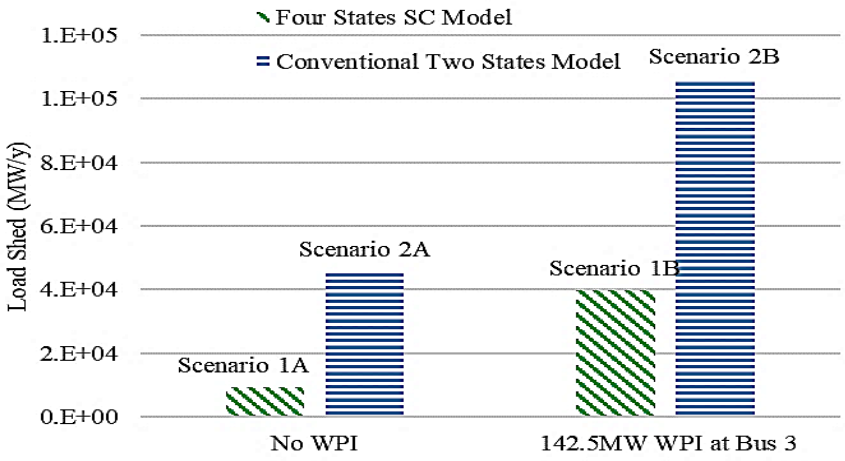

Figure 3. 8 Annual load shed for scenarios 1A, 1B, 2A and 2B

In Figure 3.9 and Figure 3.10, the EENS and restoration time respectively are significantly reduced in scenario 1A compared to scenario 2A. Also, both the EENS and restoration time is significantly reduced in scenario 1B compared to scenario 2B. They maintain a consistent argument as before. These indicate less components failure rate and fewer disturbances in the smart grids of the scenarios 1A and 1B. These impose reduced rate of system disturbance and stress thus, making the system to be less unbalanced and subsequently enhanced the system performance which is demonstrated in reduced level of the load shed, the EENS and the restoration time.

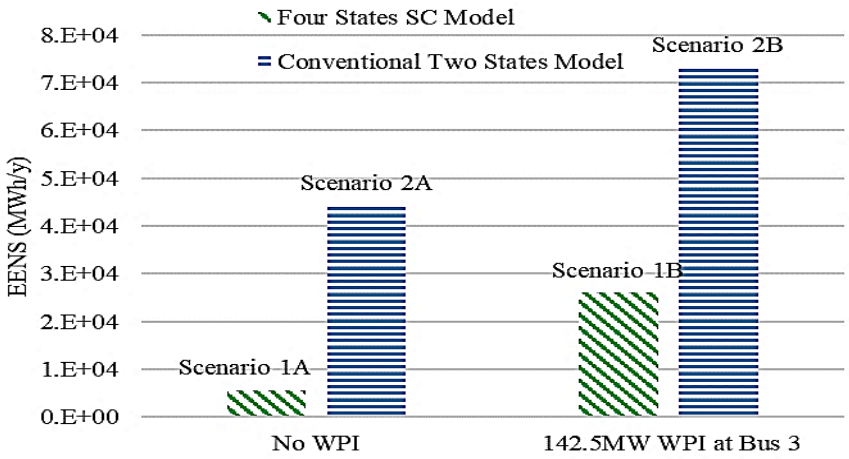

Figure 3. 9 System annual EENS for scenarios 1A, 1B, 2A and 2B

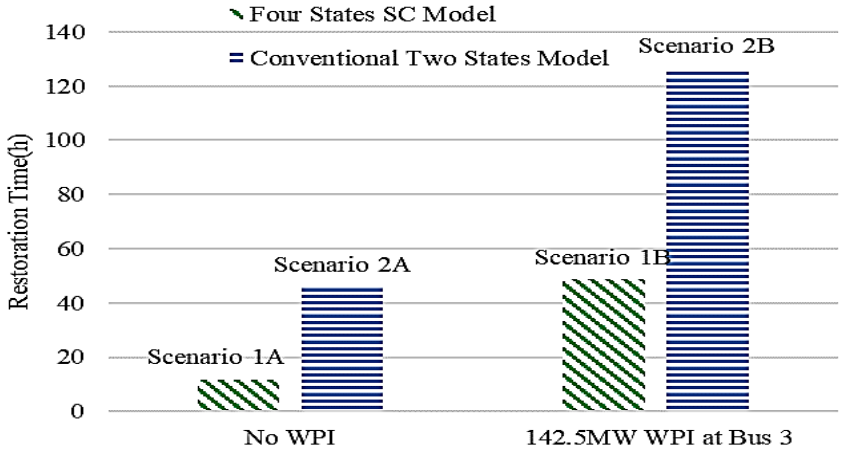

Figure 3. 10 System annual restoration time for scenarios 1A, 1B, 2A and 2B.

3.10.2.4 Scenario 3

The aim scenarios 3 is to investigate sensitivities in the eventualities of increase in the WPI and any significant impacts for extreme situations awareness and plan remedial actions accordingly. Scenario 3 has four sub-scenarios: Scenario 3A, Scenario 3B, Scenario 3C and Scenario 3D.

Scenario 3A is designed by incorporating the BC operating condition given in Section 3.10.1 with 142.5MW WPI at load bus 3, bus 4, bus 5, bus 6, bus 8, bus 9, bus 10, bus 11, bus 12, bus 17, bus 19, bus 20 and bus 24.

Scenario 3B is designed by incorporating the BC operating condition given in Section 3.10.1 with 285MW WPI at load bus 3, bus 4, bus 5, bus 6, bus 8, bus 9, bus 10, bus 11, bus 12, bus 17, bus 19, bus 20 and bus 24.

Scenario 3C is designed by incorporating the BC operating condition given in Section 3.10.1 with 427.5MW wind power integration at load bus 3, bus 4, bus 5, bus 6, bus 8, bus 9, bus 10, bus 11, bus 12, bus 17, bus 19, bus 20 and bus 24.

Scenario 3D is designed by incorporating the BC operating condition given in section 3.10.1 with 570MW WPI at load bus 3, bus 4, bus 5, bus 6, bus 8, bus 9, bus 10, bus 11, bus 12, bus 17, bus 19, bus 20 and bus 24.

3.10.2.5 Results and Analysis of Scenario 3

Figure 3.11 is the estimated results of the network load shed for scenario 3A. This figure shows different increased levels of load shed with respect to the BC. Buses 5, 6, 8, 10, 11, 12 and 17 experience substantial level of load shed compared to the rest of the buses. Buses 3, 4 and 9 experience less substantial level of load shed compared to the buses 5, 6, 8, 10, 11, 12 and 17. Buses 19, 20 and 24 experience insignificant level load shed compared to the buses 5, 6, 8, 10, 11, 12 and 17. These indicate that the WPI causes various increase levels of load shed due to sustained constraint violations with the purpose of maintaining power balance and avoiding system breakdown of the smart grids. However, rate of increase of the load shed of each bus varies. This variation depicts that geographical location of wind farm connected buses and the network topology varies with the level of system stress.

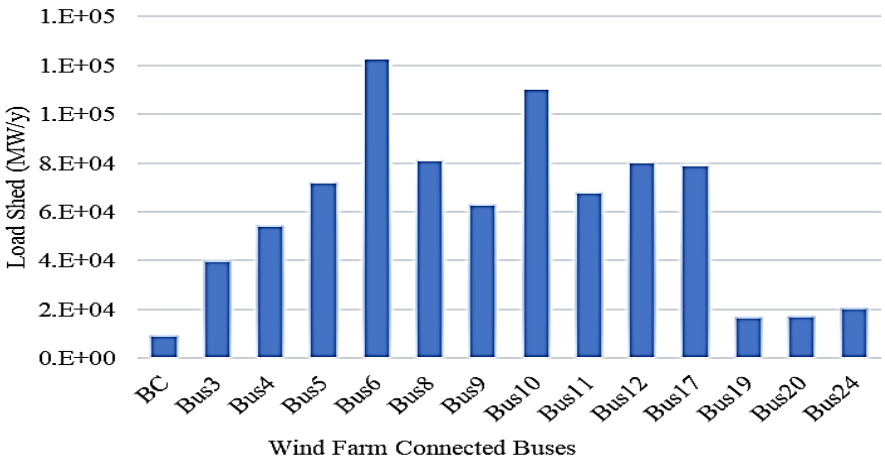

Figure 3. 11 Annual load shed with 142.5 MW of wind power installed at some specific buses

Figure 3.12, Figure 3.13 and Figure 3.14 show load shed for the scenarios 3B, 3C and 3D respectively with respect to the base case. Each of these figures shows various increase level of load shed. The rate of increase of the load shed in scenarios 3B, 3C and 3D with respect to the base case depicts that load shed increases as the capacity of WPI increases; however, rate of increase in each bus location varies. Increased WPI in the smart grids impacts the system considerably however, value of impact varies with various geographical locations of wind farms connected buses.

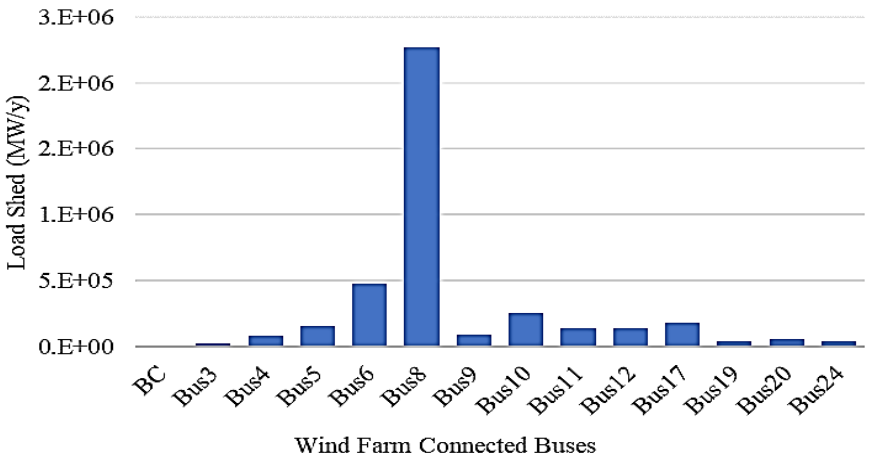

Figure 3. 12 System annual load shed with 285MW wind power installed at some specific buses

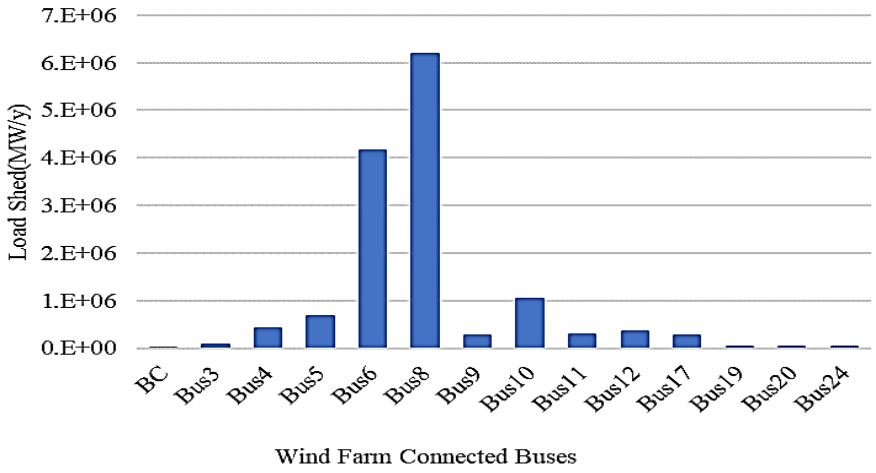

Figure 3. 13 Annual load shed with 427.5 MW wind power installed at some specific buses

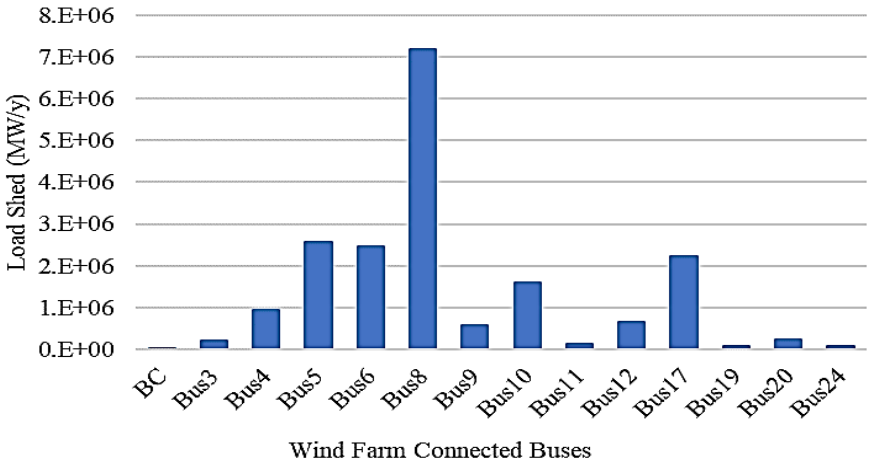

Figure 3. 14 Annual load shed with 570 MW wind power installed at some specific buses.

Figure 3.15 shows combined load shed for scenarios 3A, 3B, 3C and 3D. Figure 3.16 and Figure 3.17 show combined EENS and restoration time respectively for scenarios 3A, 3B, 3C and 3D. The results and illustrations depict that there is increase in the system load shed, EENS and restoration time with increase in installed capacity of WPI. As the rate of WPI increases, the system stress tends to increase, with increased system stress more load is shed in order to alleviate the stress due to sustained constraint violations, thus, EENS and restoration time increase.

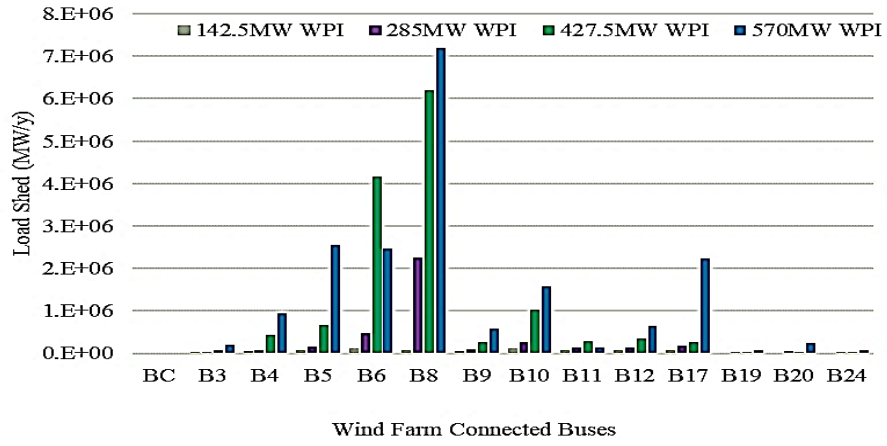

Figure 3. 15 Combined load shed of 142.5MW, 285MW, 427.5MW and 570MW wind power integration at some specific buses

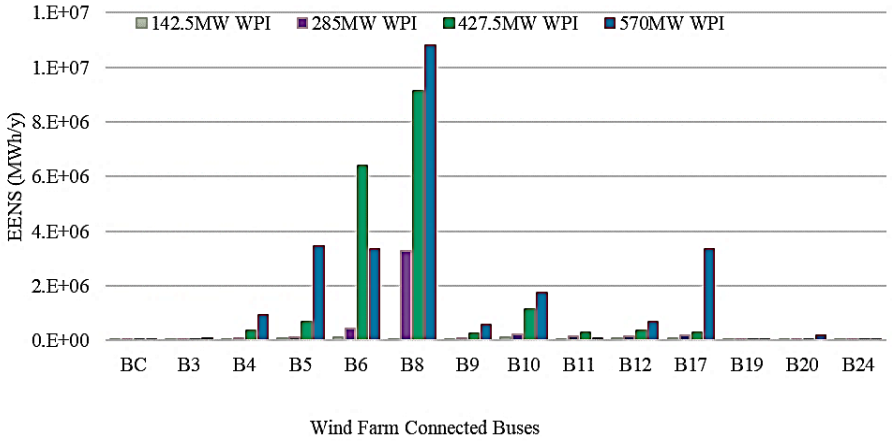

Figure 3. 16 Combined EENS of 142.5MW, 285MW, 427.5MW and 570MW wind power installed at some specific buses.

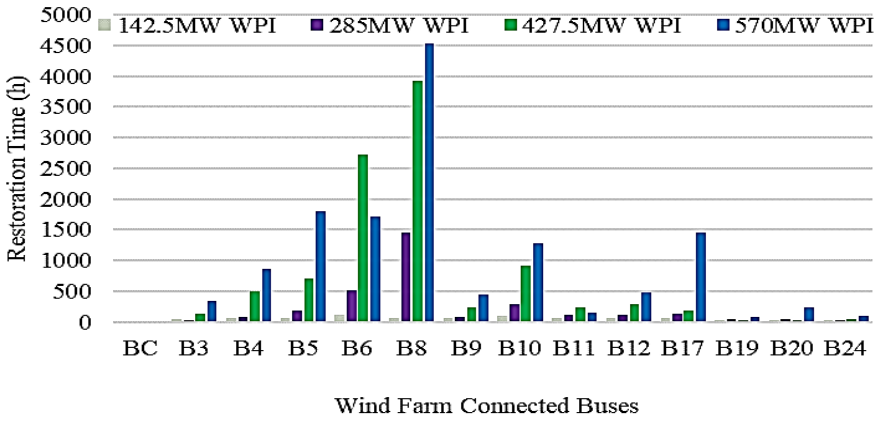

Figure 3. 17 Combined restoration time of 142.5 MW, 285 MW, 427.5 MW and 570 MW wind power installed at some specific buses.

3.11 Summary

This chapter considered smart component modelling of smart component operation for a smart grid performance assessment. The chapter presents an innovative multi-state smart component model based on Markovian differential time dependent state probability concept to capture the dynamic and intelligent operational behaviour. The framework in this chapter incorporates the multi-state smart component model, stochastic variation of wind power generation, and random load variations through Monte Carlo Simulation. The framework quantitatively evaluates impacts in a smart grid environment in the presence of large wind farms.

The multi-state smart component model effectively incorporates intelligent characteristic of the smart component that characterize actual component operational behaviour. The model presents states smart component can exist. The model demonstrates all intermediate states can be accounted for during reliability computation. The model captures cyber enabled functions influence on physical power components. The model is more effective in capturing impacts than conventional component models. The model achieved a new mathematical state probability algorithm of the multi-state smart component.

Various scenarios are implemented to investigate the multi-state smart component model performance and to assess the impacts on a smart grid environment in the presence of large wind farms. The case studies scenarios investigate contrast between the multi-state smart component model performance assessment and traditional power system security assessment; impacts and sensitivities with wind farms locations and network topology; and severity of impacts with wind power integration.

Results suggest that the multi-state smart components model is more effective in capturing impacts than two-state models. The results also justify that the smart components are more reliable and effective than the traditional components. Further investigations suggest that

the wind farm integration and their geographical locations can potentially impact the smart grids reliability considerably however, value of impact varies with various geographical locations of wind farms connected buses.

The framework provides an innovative pathway of modelling intelligence of smart grid component operation to effectively evaluate the performance of a smart grid. The framework can be an added means of assessing opportunities in expansion planning of smart grids.

Chapter 4: Cyber-Physical Power System Interactions Modelling

The aim of this chapter is to model a unified cyber-physical components interaction model in order to capture the subsystem functional layers' interactions of the cyber-physical power system. This chapter presents cyber-physical power system operation as a unified model embedded with three main subsystem functional layers: decision-making layer, communication and coupling layer and power layer. An innovative ternary Markovian model of the cyber-physical power system is presented to capture the subsystem functional layers' interactions of the cyber-physical power system. State space representation of the ternary Markovian model is presented to demonstrate various states that a cyber-physical power system can exists. The ternary Markovian model presented in this chapter have also been published in [122].

4.1 Introduction

Increasing ICT and advanced automation systems in power systems has created cyber-physical power (CPP) system paradigm. CPPS is a system with various intelligent systems and component interactions. In a CPPS, the normal operation of one subsystem depends on the interactive functions of other components or subsystems of the CPPS. Growing reliance on cyber systems makes CPPS more susceptible to component failure, cyber network failure, software failure and human errors. These failures could cause failure propagation that could affect interdependencies within the CPPS, adversely, impacting power system security. References [30][32] state that extensive reliance of the power system on cyber systems may leads to new threats and makes the CPPS more vulnerable to malicious attacks, information and data failure. Authors in [33] state that any failure can transmit or spread more rapidly and extensively, and as a result the system reliability could be reduced [122].

4.2 Cyber-Physical Power System

Smart grid is a cyber-physical power system in which advance computers and communication technologies intelligently control and monitor all physical power processes for a reliable energy delivery [44][92][93]. A cyber-physical power(CPP) system is an interconnected and complex cyber-physical system which form a multi-dimensional heterogeneous system [80]. CPPS is a sophisticated intelligent power system architecture that integrate advanced control, intelligent electronic devices(IEDs) and modern ICT to advance the performance of the composite system to achieve prime and other objectives.

CPPS is described as a series of components connected by power infrastructure, information and communication infrastructure and decision-making infrastructure. The information, communication and decision-making infrastructures execute the monitoring, control and decision-making processes. The communication and decision-making infrastructures are to ensure that a better reliability of CPPS is achieved [66]. Authors in [35][41] state that communication and decision-making infrastructures support the transfer of power from generation to end-users in a reliable and secure manner. Also, authors in [39][34] argue that use of real-time communications support dynamic flow of power and information data to ensure a reliable power supply.

Considering CPPS as a multidimensional intelligent power system with various complex interconnections and interactions, CPPS is divided into three main subsystem functional layers (FL) as shown in Figure 4. 1.

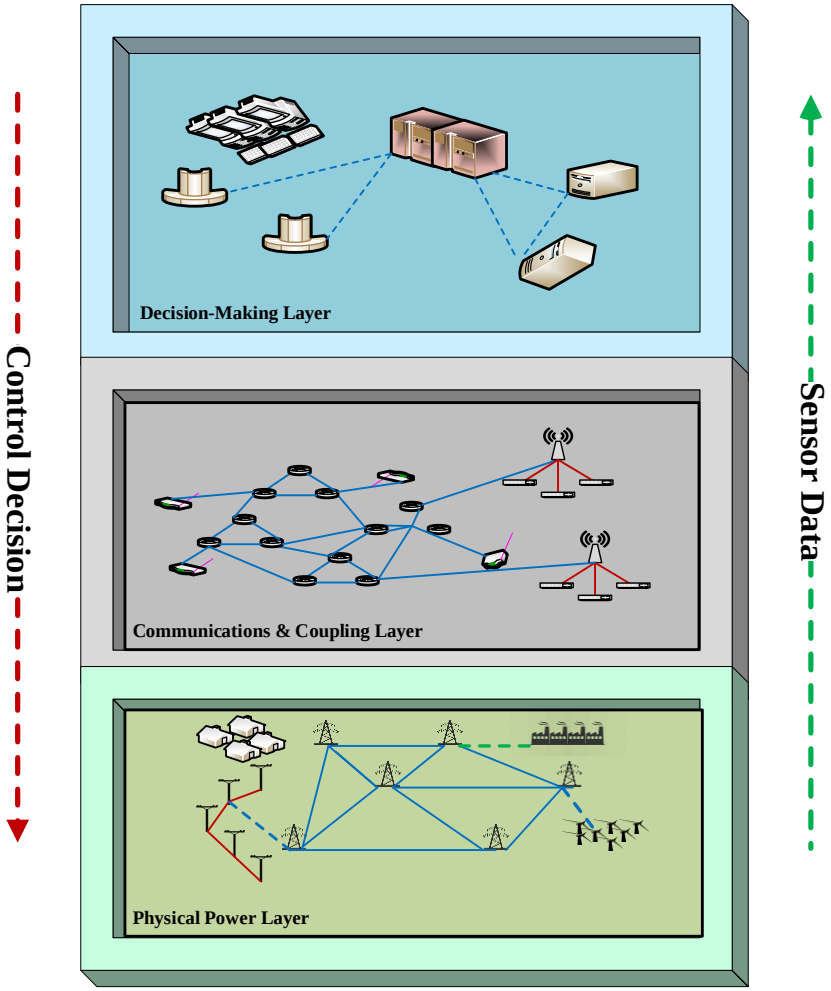

Figure 4. 1 Cyber-physical power system operation representation.

FLI is the decision-making intelligent subsystem layer, FLII is the information, communication and coupling subsystem layer and FLIII is the physical power subsystem layer. Both the decision-making intelligent layer and the information, communication and coupling layer make up the cyber layer.

4.2.1 Decision-Making Intelligent Subsystem Layer

Decision-making intelligent subsystem functional layer (DISFL) is the modern smart controlling supervisory technologies that control directives and support process decisions which is demonstrated within the physical power subsystem functional layer. Generally, the DISFL determines the smartness of a CPPS. It is made up of various programs or functions;

substation automation system, control center, control of renewable power generation, energy and demand management system of computer programs for relays, IEDs etc. These functions are for continuous operation of the power system [78]. They process information received from sensors or disseminate information from the communication infrastructure to others. Control directives or business process decisions exhibited in the physical layer is achieved in this layer [133][122].

Malfunctioning in the DISFL such as DISFL tools failure (including servers), incorrect decision-making and malicious intention might generate incorrect state estimation [96][97]. Various malicious intention could introduce cyber-attacks through sensor(s) hacking and measurement distortions [48][98]. This may lead to decision errors that could cause failures or lead to a blackout.

4.2.2 Communication and Coupling Subsystem Functional Layer

Communication and coupling subsystem functional layer (CCSFL) is an advance information exchange networks and interface technologies that deliver measurement and status information from and to the DISFL [133][32]. The CCSFL contain communication networks and interface devices such as remote terminal units (RTU). The communication networks are generally categorized into three: wide-area network (WAN), field area network(FAN) and home area network(HAN). They consist of various communication devices [63]. The interface devices convey control directives and decision programs from DISFL to the power layer and measurements from the power layer to the DISFL, the communication networks connect the interface devices and the links between them [133].

Communication networks and links are susceptible to wrong data injection attacks which may alter measurements during data transmission [134]. This might also cause wrong decisions from DISL and invariably could cause system malfunctions or lead to a blackout.

Any Malfunction or error in the communication networks or interface devices can affect the accuracy of the DISL functions [78][63] [122].

4.2.3 Physical Power Subsystem Functional Layer

Physical power subsystem layer (PPSFL) is simply the current-carrying components. PPSFL is the power network consisting of all physical devices generally, the power generation, power transmission and distribution assets including protection systems, power electronic interface devices, and storage technologies, and traditional and smart grid loads. The power system is usually grouped into three functional zones of generation, transmission and distribution. Power devices are connected to the communication and coupling layers via state awareness sensors and program execution devices [66] [122].

4.3 Interdependency in Cyber-Physical Power System

Interdependency is dependence of components or subsystems on another components, subsystems, or operations within a system. Interdependency in a CPPS is a mutual reliance of components or subsystems within a CPPS. [135][136][137]. Interdependency in a CPPS is a mutual reliance of components or subsystems within a system. The states of a component or a subsystem in a system can potentially influence the performance of other subsystems. The successful operation of a power system with a significant integration of cyber infrastructure depends on the cyber network security. Consideration of interdependency of cyber and power system is extremely important [78]. Moreover, loss of interdependency due to uncertainty, unpredictability and failure in the CPPS could affect effective operation of the power system thus, the power system security could be jeopardized [122].

4.4 Failures in Cyber Physical Power System

In a CPPS operation either the cyber system or the power system could be the source of failure from failures of their components, software failures, human errors, etc. All these failures may be categorized into three: component failure, cyber unavailability, and cyber intrusion [66][122].

- Component Failure is the loss of functionality in component(s) of the decision-making and intelligent layer, information, communication and coupling layer or power layer such as routers, servers, generators, etc., may malfunction or fail. This might cause interruption in communication networks or incorrect decision-making which could affect the security of the whole system.
- Cyber Unavailability is the loss of functionality in information & communication networks as a result of interruption such as link unavailability, packet loss, packet delay, etc., which may affect the decision-making process thus, jeopardizing the power system security.
- Cyber intrusion is the loss of functionality due to malicious attacks, false data-injection attacks [138], etc. which may affect the decision-making process.

4.5 Modelling Approach

This section presents CPPS operation modelling and mathematical framework based on three subsystem functional layers: communication and coupling layer, decision-making layer and power layer for system level reliability computation. This study demonstrates an integrated model that consider interactions of CPPSs as single system model, to reflect dynamic of operation of subsystem layers; communication and coupling layer, decision-making layer and power layer. Markov chain is utilized in the modelling approach of this study.

Markov chain offers better insight into dynamic behaviour of a system or component [39][52][111][112]. It is a type of stochastic process where system behaviour varies with time and space randomly [52][113]. Markov chain is a form of Markov modelling with some finite states (V1, V2, V3…. V_n) which make the process to occur at any given time. Transition probability y_{ij} is the probability of the process moving from state V_i to state V_j. Transition probability y_{ii} is the probability of the process remaining in the same state. A typical system consists of *n* components with one or all the components operating effectively or ineffectively at any given time. The entire system successful operation depends on the availability or unavailability of its components [122].

4.5.1 Ternary Markovian Model

The proposed approach is established using a ternary Markovian model (TMM) to incorporate the influence and interoperability of subsystem functional layers within the CPPS to capture the dynamics of subsystems' interactions in the CPPS. Ternary means that each of the subsystem functional layer is modelled as three states and it can be in one of three states[139] as shown in Figure 4.2 below. The PPSFL is characterized to operate in three states: available state indicated as "A", partial operated state indicated as "P" or unavailable state indicated as "F". Each of the subsystem functional layer is modelled as three states because the modelled dynamics of interactions in the CPPS is captured as series of consequence of events from three main subsystem functional layers that is the communication and coupling layer, the decision-making layer, and the power layer.

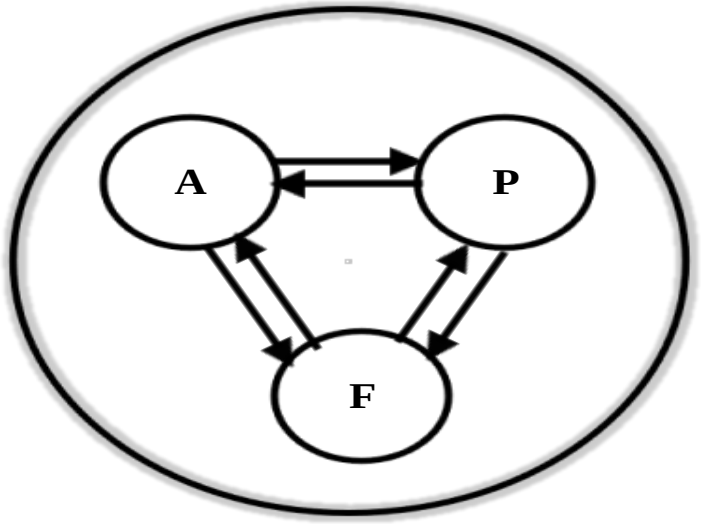

Figure 4. 2 Three states representation of the physical power subsystem functional layer

TMM is a single integrated probabilistic framework modelled as a unified system embedded with three subsystem functional layer interactions. Each subsystem functional layer(SFL) is characterized with three states to capture time varying behaviour under various cyber-attacks or unforeseen contingencies. The interactive operation and sequence of events in each of DISFL, CCSFL and PPSFL of the CPPS is modelled as a subsystem which exist in three states within a system as shown in Figure 4.3 below.

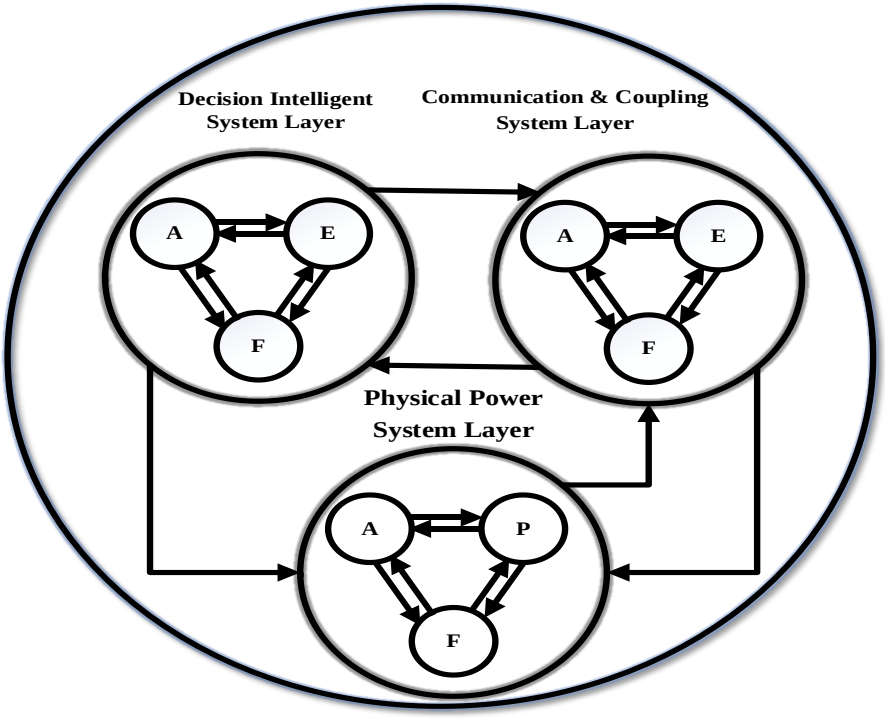

Figure 4. 3 Ternary Markovian model of a cyber-physical power system

The TMM is formed as an embedded three SFL interactions: the DISFL, the CCSFL and the PPSFL. Each of the SFL is formed to interact with each other. The DISFL is formed as a SFL with various procedures and functions including substation automation system, control of renewable power generation, operation of IEDs etc. for continuous operation of the physical power system. To capture time varying behaviour under various cyber-attacks and unforeseen contingencies the DISFL is further characterized to operate in three states: available without error state indicated as “A”, available with error state indicated as “E" or unavailable state indicated as “F.”

The CCSFL is formed as an interface and coupling SFL with various interface devices (such as RTU) and communication network to convey control directives and decision programs from the DISFL to the PPSFL and measurements from the PPSFL to the DISFL. To capture time varying behaviour under various cyber-attacks and unforeseen contingencies the CCSFL is

further characterized to operate in three states: available without error state indicated as “A”, available with error state indicated as “E" or unavailable state indicated as “F”.

The PPSL is formed as physical power system with of all physical devices generally. To capture time varying behaviour under various cyber-attacks and unforeseen contingencies the PPSL is further characterized to operate in *three* states: available state indicated as “A”, partial operated state indicated as “P” or unavailable state indicated as “F”.

Figure 4.3 shows that the DISFL and CCSFL can either exist as available without error state indicated as “A”, available with error state indicated as “E" or unavailable state indicated as “F”. PPSFL can either exist as available state indicated as “A”, partial operated state indicated as “P” or unavailable state indicated as “F”. Available without error state “A” is when each subsystem (DISFL CCSFL or PPSFL) is working as expected. Available with error state “E” is presence of error or incorrect data as a result of cyber intrusion, malicious attack, false data injection, etc., in the system that may affect the functionality of each/both DISFL and CCSFL which might impact the power system layer and whole system functionality. Unavailable state “F” is a failed state of the subsystem layer as a result of component failure, packet loss, packet delay, etc. which might impact the system security. Partial operated state “P” state is when the subsystem is operating partially or operating at a reduced-capacity [122].

4.5.2 Mathematical framework for TMM States

The TMM is conceptualized as varying with respect to time and space with state transition probabilities[112] as expressed in (4.1):

$$p_{ij} \forall i, j \in X = 1, 2, 3 \ldots . n \qquad (4.1)$$

where: X is set of possible states, n and p_{ij} is state transition probability from state i to state j. The state transition probabilities represent all the transitions from one state to another. Stochastic transitional probability matrix *P* consist of all the transition probability values for the system states as expressed in (4.2):

$$P_{k,\ k+1} = \begin{bmatrix} p_{11} & p_{12} & \cdots & p_{1n} \\ p_{21} & p_{22} & \cdots & p_{2n} \\ \vdots & \vdots & \vdots & \vdots \\ p_{n1} & p_{n2} & \cdots & p_{nn} \end{bmatrix} \qquad (4.2)$$

where: $P_{k,\ k+1}$ is state transition probability matrix, *k* and *k+1* is the current and next state respectively, *n* is number of states and p_{ij} is the transition probability that depict the probability of transiting from state *i* to state *j* during a given time interval. Within the transition probability matrix, the rows are the current state of the system while the columns are the next state, the sum of each row in the transition probability matrix must be 1, that is, from a given state, the transition probabilities must equal to unity [52] as expressed in (4.3):

$$\sum_{j \in X} p_{ij} = 1 \qquad (4.3)$$

The TMM state space diagram (see Figure 4.4) collectively represents the possible states of the CPPS due to operational consequences of events in the DISFL, CCSFL and PPSFL. There are three state variables in each of the subsystem functional layer. “A”, “E” and “F” (see Figure 4.3) state variables indicate that each of the DISFL and CCSFL could either be in available-without-error state, available-with-error state or failed state respectively. “A”, “P” and “F” state variables indicate that the PPSFL could either be in available state, partial operation state or failed state respectively.

Each subsystem functional layer state is denoted by a ternary variable $x_i = 2, 1, or\ 0$ such that, subsystem functional layer *i* is either available, error/partial or failed, respectively.

Let consider C_i as set of states for subsystem functional layer, i with a cardinality of N_i. For a system with n subsystems functional layer, the system state can be represented as a vector W:

$$\mathrm{W} = (\mathrm{w_i}), \qquad \text{where } w_i \in C_i \qquad 1 \leq \mathrm{i} \leq \mathrm{n} \qquad (4.4)$$

Also, the states of all subsystems can be described by a ternary vector:

$$\mathrm{x} = (\mathrm{x_1}, \mathrm{x_2}, \ldots . \mathrm{x_n}) \qquad (4.5)$$

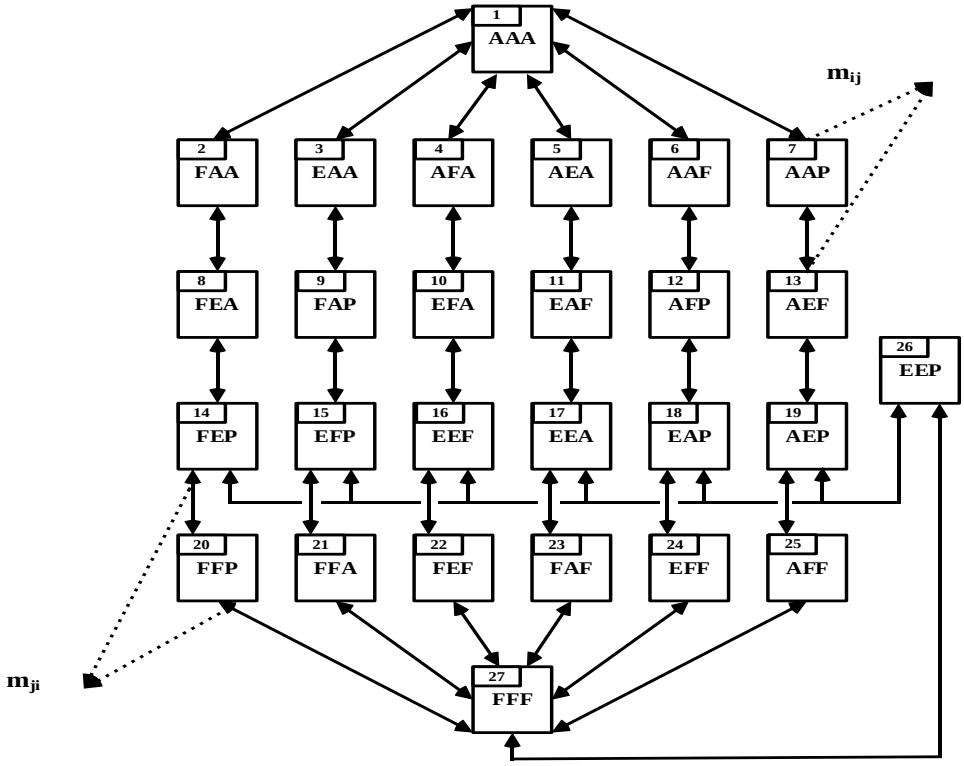

Figure 4. 4 TMM state space diagram representation of the CPPS operation

With standard assumptions, state of a system depends on combination of all components states [140][103], the ternary system state model is described by y and is subject to subsystems state vector x:

$$y = y(x) \tag{4.6}$$

The system can be in any different state since $w_i \in C_i$ therefore N is:

$$N = \prod_{i=1}^{n} N_i \tag{4.7}$$

The system state space is expressed as:

$$SS = \{ W_j \,|1 \leq j \leq N\}$$

Likewise, let Ω_i represent the state transition due to subsystem i operation and from 5.6, the system state transition can be expressed approximately as:

$$\Omega = \prod_{i=1}^{n} \Omega_i \tag{4.8}$$

Hence, as depicted in (4.2) the ternary Markovian CPPS stochastic transitional probability matrix is modelled as:

$$M_{k,\ k+1} = \begin{bmatrix} m_{11} & m_{12} & \cdots & m_{1n} \\ m_{21} & m_{22} & \cdots & m_{2n} \\ \vdots & \vdots & \vdots & \vdots \\ m_{n1} & m_{n2} & \cdots & m_{nn} \end{bmatrix} \tag{4.9}$$

where: $M_{k,\ k+1}$ is the state transition probability matrix, m_{ij}, m_{ji} and m_{ii} are the transition probabilities.

Considering subsystem functional layers' interactions and dynamics of one subsystem layer influence the dynamics of the other subsystem layer. The system may operate in either of any of the *N* possible states. Generally, the most likely state begins with the system fully-functional.

This is when each of the subsystem layers of the CPPS and the whole CPPS is available and working as expected. However, operational uncertainty and unpredictability may cause any of the subsystem layers to transit from its fully functional state to another state, which might impact the whole system. One or multiple transitions of subsystem layer(s) can cause one step transition of the whole CPPS. In Figure 4.4 state “AAA” of TMM can transit to state “AAP” as a result of the DISFL and CCSFL remaining fully functional and the PPSFL transits to partial operation state, individual subsystem functional layer transitions cause the TMM state transition as stated in (4.5) and (4.6).

To reduce design complexity and to ensure effective implementation, the state space representation in Figure 4.4 is reduced to smaller number of states by excluding states with very low probability of occurrences. Hence, the reduced number of state space transition representation of the CPPS is shown in Figure 4.5.

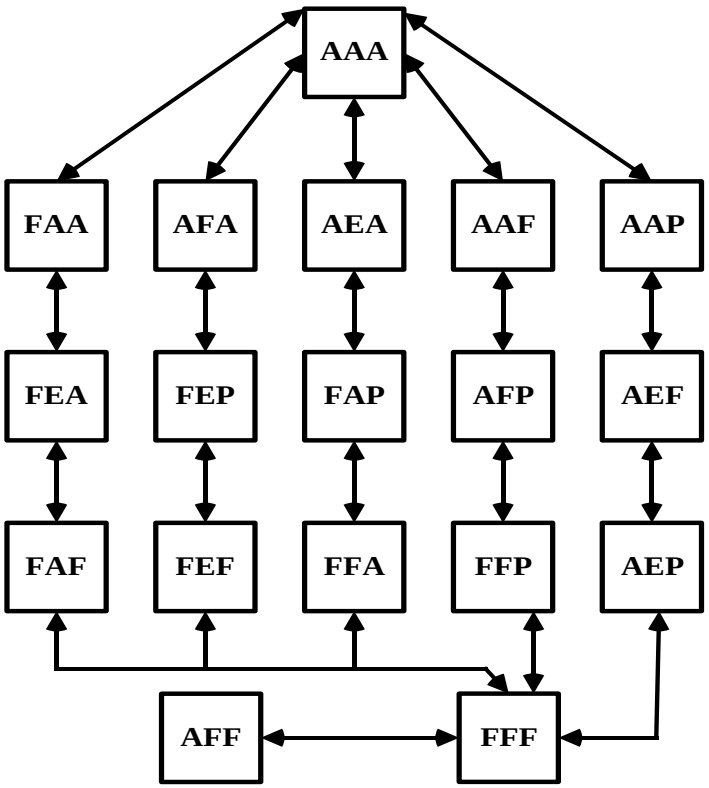

Figure 4. 5 Reduced TMM state space representation of the CPPS

Figure 4.5 shows the TMM reduced state space transition reflecting the subsystems layer interactions and their dynamics within a whole CPPS as result of one or more transitions of subsystem layer(s). All the possible N states of the TMM is categorized as fully functional, functional, fully blackout, blackout, conventional, conventional partial operation, conventional error partial operation and conventional error. Table 4.1 [122] shows the reduced states.

Table 4. 1 CPPS Reduced TMM States

States	States Names	Status
AAA	Fully Functional	CPPS Operation
AAP	Functional	
FFF	Fully Blackout	Non-Functional
AAF	Blackout	
AEF	Blackout	
AFF	Blackout	
FAF	Blackout	
FEF	Blackout	
FFP	Conventional Partial Operation	Conventional Operation
FAP	Conventional Partial Operation	
AFP	Conventional Partial Operation	
FFA	Conventional Operation	
FAA	Conventional Operation	
AFA	Conventional Operation	
FEP	Conventional Partial Operation	
AEP	Conventional Partial Operation	
FEA	Conventional Operation	
AEA	Conventional Operation	

The fully functional state refers when each subsystem (DISFL, CCSFL and PPSFL) of the system is fully available and in working state, functional state refers to when both subsystems DISFL and CCSFL of the system is fully available and in working state with subsystem PPSFL in partial operation state.

The fully blackout state is when each subsystem DISFL, CCSFL and PPSFL of the system failed, not in working condition, and not available. The blackout state is when subsystem PPSFL failed and either DISFL or CCSFL is available, error or failed state.

The conventional state refers to when the PPSFL is fully available and in working state with either subsystem DISFL or CCSFL in error state or failed state. The conventional partial state refers to when the PPSFL is not fully available but in partial operational state with either subsystem DISFL or CCSFL in the error state or failed state.

The conventional error state is when the PPSFL is fully available and is in working state with either subsystem DISFL in failed state or available state with CCSFL in error state. The conventional error partial operational state refers to when the PPSFL is in partial operated state with either subsystem DISFL in failed or available state with CCSFL in error state [122].

State-probability is set up for each of the state that the TMM exists by describing each state with a uniform distribution between 0 and 1 [97]. The state-probability of each state in the TMM state space representation diagram as shown in Figure 4.5 and Table 4.1 is achieved by severity/likelihood of each of the TMM's state.

Monte Carlo simulation tests are conducted in chapter 6 to determine the TMM's state status to predict real patterns of behaviour in simulated time in order to obtain the frequency of some reliability parameters and to estimate the expected value of each of the parameters.

4.6 Summary

This chapter considered system level modelling and mathematical formulations of cyber-physical power(CPP) system operation. The chapter presents an innovative modelling approach based on a ternary Markovian model(TMM) of cyber-physical components interactions. The cyber-physical power system model presented in this chapter is a single unified ternary Markovian model that reflects characteristics of three main subsystem functional layers' interactions of the CPPS. The model demonstrates dynamics of subsystem layers' interactions.

The TMM is multi-state model that represents various states that a cyber-physical power system operation can exists. The TMM reflects dynamic operation of subsystem layers' interactions of communication and coupling layer and decision-making layer to power layer. combines consequences of events from each of the main subsystem functional layers. The framework demonstrates combined reliability modelling and assessment. It captures dynamics of subsystem layers' interactions for assessment of interdependency impacts.

Existing frameworks are limited in combined reliability modelling and assessment of CPPS. Also, a non-unified CPPS model does not combine consequences of events from each of the three main subsystem functional layers of the CPPS that is from the decision-making subsystem functional layer, the communication and coupling subsystem functional layer to the power subsystem functional layer.

The CCPS operation modelling demonstrates that the TMM effectively captures the dynamics of subsystem layers' interactions in a CPPS operation.

Chapter 5: Power System Security Assessment with Ternary Markovian Model

The aim of this chapter is to reflect the operational dynamics of the ternary Markovian model presented in chapter 5 in order to investigate the integrated cyber-physical power system operation interactions and interdependency impacts on power system security. This chapter presents ternary Markovian model operation through Monte Carlo simulation, modified IEEE 24-Bus RTS. Case studies representing realistic physical power system operating conditions with the cyber network interactions are presented in order to justify the viability of the model. Further, some parts of this chapter and ternary Markovian model framework presented have already been published in [122].

5.1 Ternary Markovian Model in Monte Carlo Simulation

Monte Carlo simulation trials are conducted in this section to determine the TMM's state status and to predict real patterns of behaviour in simulated time in order to obtain the frequency of some reliability parameters and to estimate the expected value of each of the parameters. Figure 6.1 illustrates the basic steps of the TMM through MCS. In this approach, the MCS examines and predicts various TMM states status in simulated time to obtain energy not supplied (ENS) and to estimate expected value of the ENS.

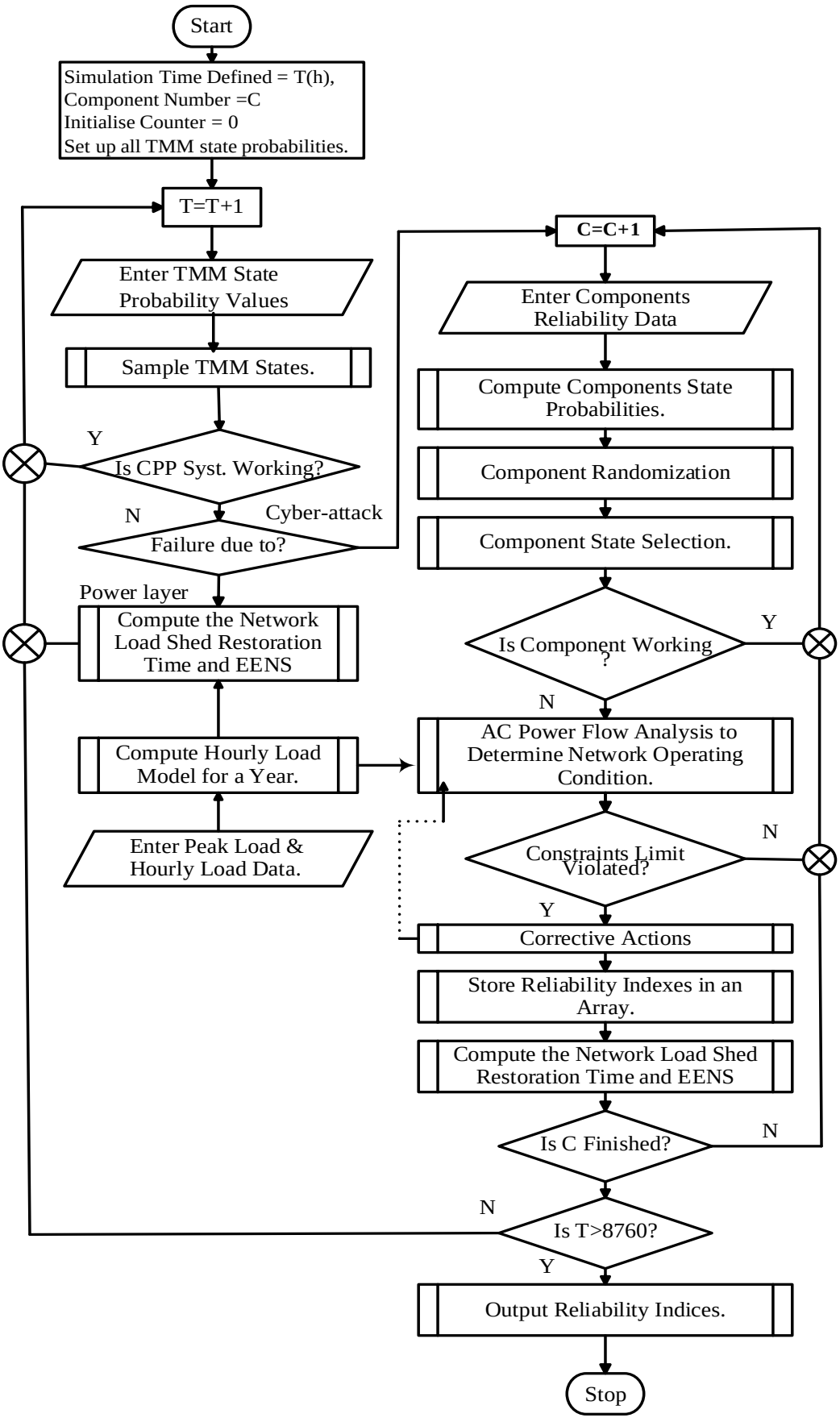

Figure 5. 1 Basic flow chart of TMM through Monte Carlo Simulation

System state is determined by sampling the probability that the system exists in that state [97]. TMM state status is determined by sampling the probability that the TMM exists in that state considering different states of the TMM as shown in chapter 4 Figure 4.5 and Table 4.1. This is achieved by using generated random numbers (RN) and TMM states probabilities. RN consists of a uniform distribution over a specified range of values [103][121][101]. This study assumes a uniform distribution of RN within [0,1]. The state probability of each state in the TMM state space representation diagram as shown in Figure 4.5 and Table 4.1 is achieved by severity/likelihood of each of the TMM's state.

Let *S* represents each state of the of TMM as shown in chapter 4 Table 4.1.

$$That\ is, \qquad S = \{\mathrm{AAA}, \mathrm{AAP}, \mathrm{FFF}, \mathrm{AAF}, \mathrm{AFP}, \ldots.\} \qquad (5.1)$$

Let generated random number for each *i* simulation sample trial = R_i.

At each *i* sample trial TMM can be any of the *S.*

TMM through MCS Steps for system performance assessment includes the following basic steps.

Step 1: Set up TMM state probabilities.

Step 2: TMM system state is sampled.

Step 3: If the state is a fully functional state or functional state, go back to Step 2 to select a new TMM state. If the state is a fully Blackout state or blackout state, go to Step 4. Otherwise, go to Step 5.

Step 4: Compute and update the system reliability indices. Then go back to Step 2 to select a new TMM state.

Step 5: Randomly sample the components in physical power layer to determine which component has been affected by the cyber failure (DISFL and/or CCSFL failure).

Step 5a: Select component state. If component is working, go back to Step 5 to select a new component. Otherwise go to step 6

Step 6: Perform a Newton-Raphson A/C power flow to check the network operating condition. If constraints limits are not violated, then go back to Step 5 to select a new component. Otherwise, go to step 7.

Step 7: Perform remedial actions. Remedial actions is corrective actions to prevent network collapse or to alleviate sustained violations. The incorporated corrective actions in this study are reactive power compensation, on-load-tap changing, generation re-dispatch and shedding of loads.

Step 8: Compute and update the system reliability indices. If component is finished, then go back to Step 2 to select a new TMM state. Otherwise, go to step 5.

Step 9: Steps 1–8 are repeated until 876000 iterations are met.

In this study the performance of TMM system is evaluated by EENS and VoLL indices. EENS index is the expected energy not supplied and VoLL [128][129][130] is value of lost load.

At each sample trial: if the TMM state is in fully functional state or functional state, then a new TMM system state is selected; if the TMM state is in fully blackout or blackout state as a result of PPSFL failure then corresponding reliability indices is computed and updated; if TMM system state is in conventional state as a result of DISFL and/or CCSFL failure then a Newton-Raphson AC power flow is performed to check the network operating condition. if any constraint is violated, it is rectified through corrective actions to prevent network collapse or

to alleviate sustained violations, then corresponding reliability indices is computed and updated.

At the end of each sample trial, mean value of the curtailed load and corresponding cost of lost load of all the processed samples are estimated, with maximum number of samples trials, the EENS is calculated as [122]:

$$\mathrm{EENS} = \frac{1}{y}\sum_{i}^{y} \mathrm{K_i\ x\ T_i} \qquad (5.2)$$

where, y is the processed samples, K_i is the magnitude of curtailed or shed load at the sample i and T_i is the restoring time of K_i. The VoLL is calculated as:

$$\mathrm{VoLL} = \frac{1}{y}\sum_{i}^{y} \mathrm{ENS_i\ x\ \ C_i(T_i)} \qquad (5.3)$$

where, C_i is sector customer damage function (SCDF) [130]for Residential, Commercial, Industrial and large user in £/MWh for the interruption duration T_i and ENS_i is energy not supplied for the sample i.

5.2 Case Studies

Case studies are presented to investigate the ternary Markovian model performance and to assess the interdependency in a CPPS operation in the event of power system failure or cyber system failure: components failure, cyber-attacks, malicious attacks and false data-injection attacks. This section presents modified IEEE 24-Bus Reliability Test System and several set of scenarios to investigate the viability of the ternary Markovian model. These scenarios represent realistic physical power system operating conditions with the cyber network interactions.

5.2.1 Test System

The IEEE 24-Bus Reliability Test System (RTS) [132] data used for the viability assessment of proposed approach is provided in appendix A. MATLAB programming codes were developed to stimulate the test system characteristics and other eventualities. The transmission system consists of 24 buses, 33 lines and 5 transformers as shown in Table A.1. and Table A.2 respectively. There are 10 generator buses of connecting 32 generating units and 17 load buses in the system as shown in Table A.3, Table A.4 and Table A.5 respectively.

Authors in [141] presented a benchmark CPP reliability test system to establish a reliability test system that incorporates ICT components into 24-Bus RTS. Therefore, in this study all generator buses of the 24-Bus RTS are incorporated with ICT components to achieve a comprehensive cyber-physical test system [141]. The 24-Bus RTS power network with selected buses (substations) of cyber part of the system (ICT configurations) is shown in Figure 5.2. Each of these selected buses is integrated with ICT features, such as Merging Units (MUs), Ethernet Switches (ESs) and line protection panel (LPP) with their connections, are shown in Figure 5.3 below. Mean time to failure (MTTF) and mean time to repair (MTTR) values of ICT components used in this study for reliability assessments are from [141][142][143] and are shown in Table 5.1 [122].

Table 5. 1 ICT Components' Reliability Data

ICT Components	MTTF (h)	MTTR (h)	Failure Rate (yr)
Protection Panels	438000	48	0.02
Merging Units	438000	48	0.02

Ethernet Switches	876000	48	0.01

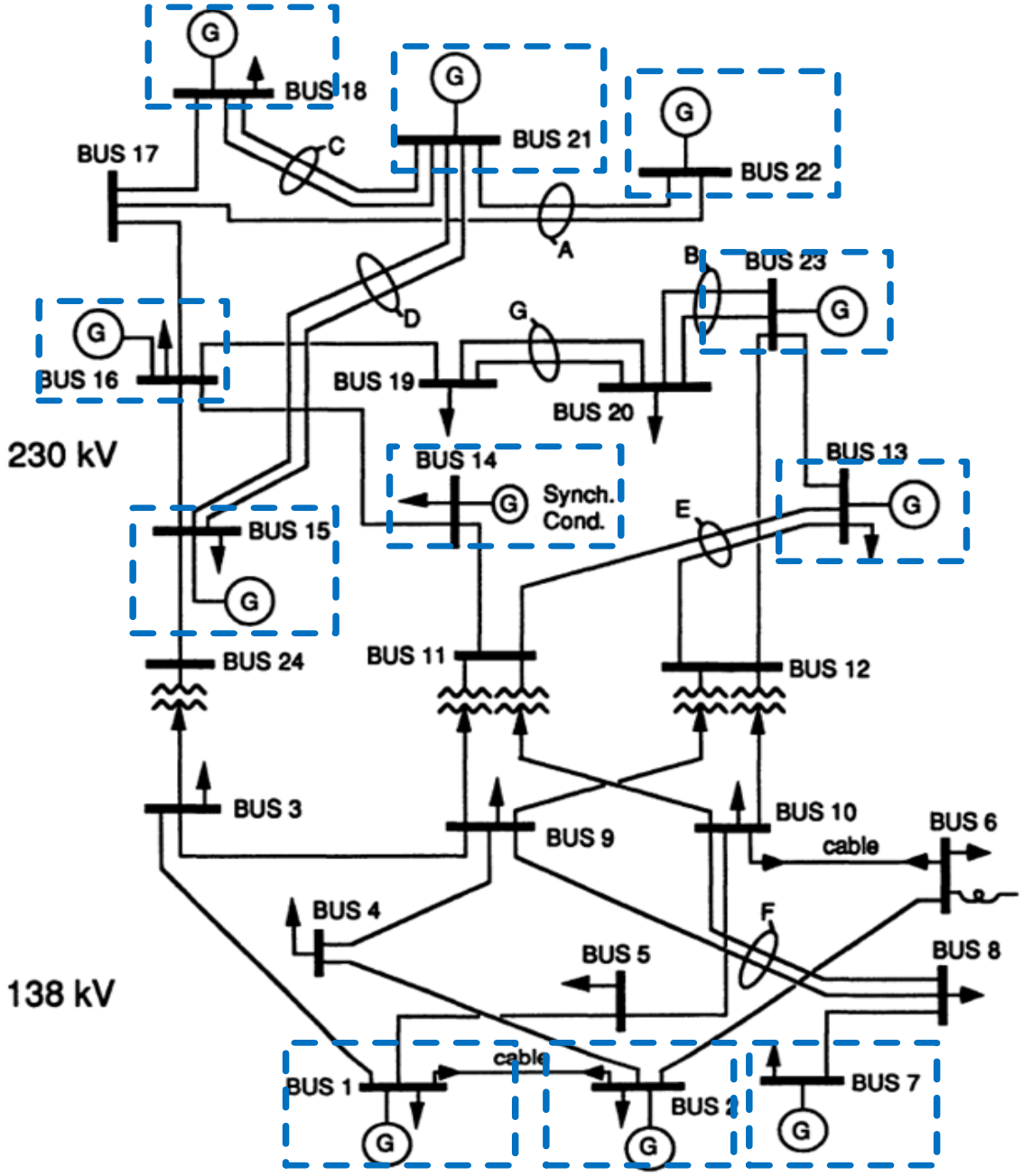

Figure 5. 2 EEE RTS physical network with selected buses indicating cyber system [122][132]

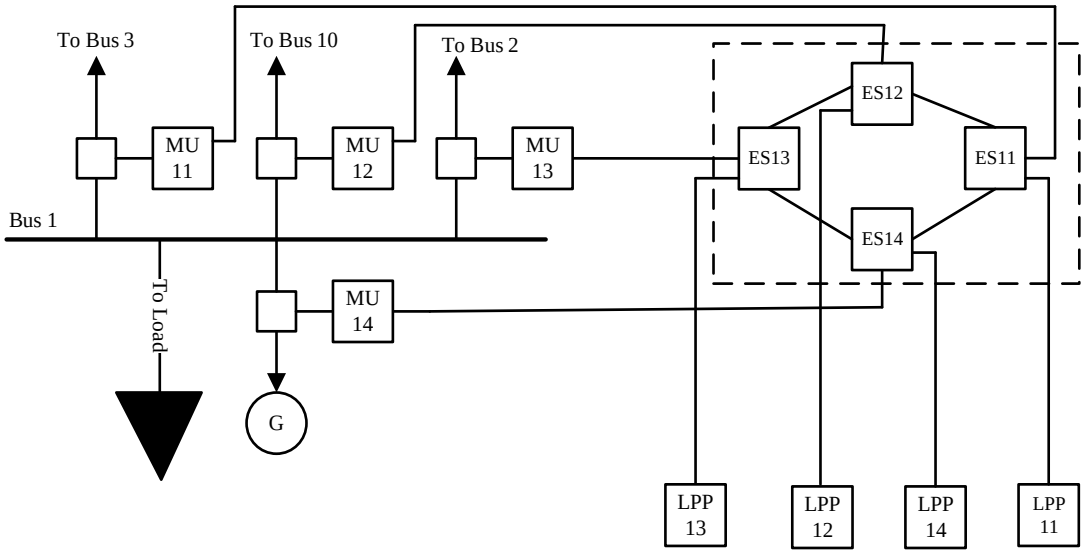

Figure 5. 1 Cyber configurations extension on bus 1 [122][141]

It is also to be noted that although the reliability is a combined reflection of adequacy and the security of the system, this study investigates the security part of the system and impacts on the physical power system from the cyber-physical interactive operation.

5.2.2 Scenarios

Several scenarios are performed to investigate the TMM performance and to assess the interdependency in a CPPS operation in the event of the power system failure or cyber system failure: components failure, cyber-attacks, malicious attacks and false data-injection attacks. Various failure rates(FR) of cyber-attacks are considered in this scenario in order to explore any abnormal transitions within the CPPS. Having such leverage can ensure extra planning in the events of unforeseen contingencies in the CPPS. However, such data may not be available in reality, but it is important to be aware of such transitions to mitigate unexpected contingencies. Thus, for every CPPS failure caused by cyber-attacks many scenarios were considered [122].

5.2.2.1 Scenario Set A

The aim of scenario set A is to investigate any significant transitions of impacts and sensitivities in the eventualities of significant increase in the failure rates due to cyber-attacks because it is vital to know the extreme situations and plan remedial actions accordingly.

Scenario set A investigates any significant transitions of impacts and sensitivities in the eventualities of significant increase in the failure rates of related components due to cyber-attacks on all generator substations and the generator associated transmission lines. Scenario set A contains five clusters scenarios: A1, A3, A5, A7 and A9. Each of the scenario in scenario Set A is designed by incorporating the base case (BC) operating condition given in Section 3.10.1 and then applying different failure rates of cyber-attacks on all generator substations and associated transmission lines for each failure due to cyber-attacks on the system. The probabilities of failure due to cyber-attacks on all the generators were increased in the scale 20% and simultaneously applying the failures rates of cyber-attacks at 10%, 30%, 50%, 70% and 90% on generator associated transmission lines for each failure due to cyber-attacks on the CPPS as [122]:

- The scenario cluster A1 is formed by simulating 10%, 30%, 50%, 70% and 90% failure rates (FR) of cyber-attack on all effective generator substations with FR of cyber-attack on all the generator associated transmission lines maintained at 10% each.
- The scenario cluster A3 is formed by simulating 10%, 30%, 50%, 70% and 90% FR of cyber-attack on all effective generator substations with FR of cyber-attack on all the generator associated transmission lines maintained at 30% each.
- The scenario cluster A5 is formed by simulating 10%, 30%, 50%, 70% and 90% FR of cyber-attack on all effective generator substations with FR of cyber-attack on all the generator associated transmission lines maintained at 50% each.

- The scenario cluster A7 is formed by simulating 10%, 30%, 50%, 70% and 90% FR of cyber-attack on all effective generator substations with FR of cyber-attack on all the generator associated transmission lines maintained at 70% each.
- The scenario cluster A9 is formed by simulating 10%, 30%, 50%, 70% and 90% FR of cyber-attack on all effective generator substations with FR of cyber-attack on all the generator associated transmission lines maintained at 90% each.

5.2.2.2 Results and Analysis for Scenario Set A

Figure 5.4, Figure 5.5 and Figure 5.6 show annual estimated results of system violations, load shed and EENS respectively for the scenario set A. In Figure 5.4, the levels of CPPS violations (undervoltage, overvoltage and line-overload) increased simultaneously with increase in failure rates of cyber-attack*s* on all generator substations and associated transmission lines with respect to the base case. Figure 5.4 indicates that the increase in failure rates of cyber-attacks on all generator substations and associated transmission lines imposed same increased rate of system disturbance and stress thus, making the system to be more unbalanced which subsequently affects the CPPS performance which is demonstrated in different increased levels of system violations.

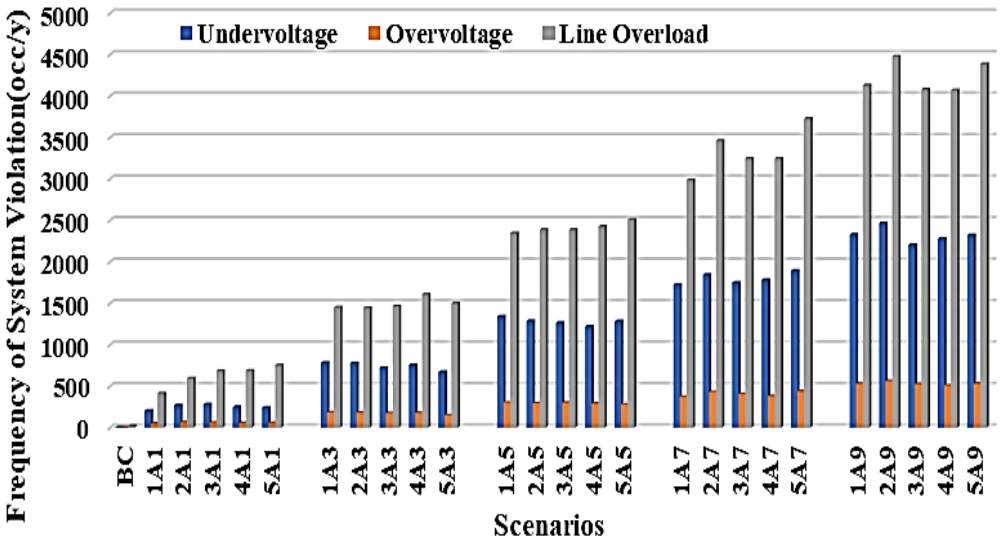

Figure 5. 2 System violations for scenario set A

Figure 5.5 shows different increased levels of load shed with respect to the base case. The increased load shed experienced at each of the scenario set A with respect to the base case indicates that the increase in failure rates of cyber-attack on all generator substations and associated transmission lines cause various degrees of load shed in order to maintain the sustained constraint violations and the power balance of the CPPS to avoid system breakdown.

Also, with respect to the increased failure rates of cyber-attack on all generator substations and associated transmission lines both Figure 5.5 and Figure 5.6 show a consistent increase in the load shed amount and EENS respectively from cluster scenario A1 through cluster scenario A5 but cluster scenario A7 and cluster scenario A9 show a decrease in the load shed and EENS. Cluster Scenario A9 in Figure 5.6 experiences a less total blackout thus, the level of load shed is reduced compared to scenario cluster A5 which experiences a more total blackout. This depicts nonlinearity behaviour of some power system components in response to system violations in order to maintain power balance of the system.

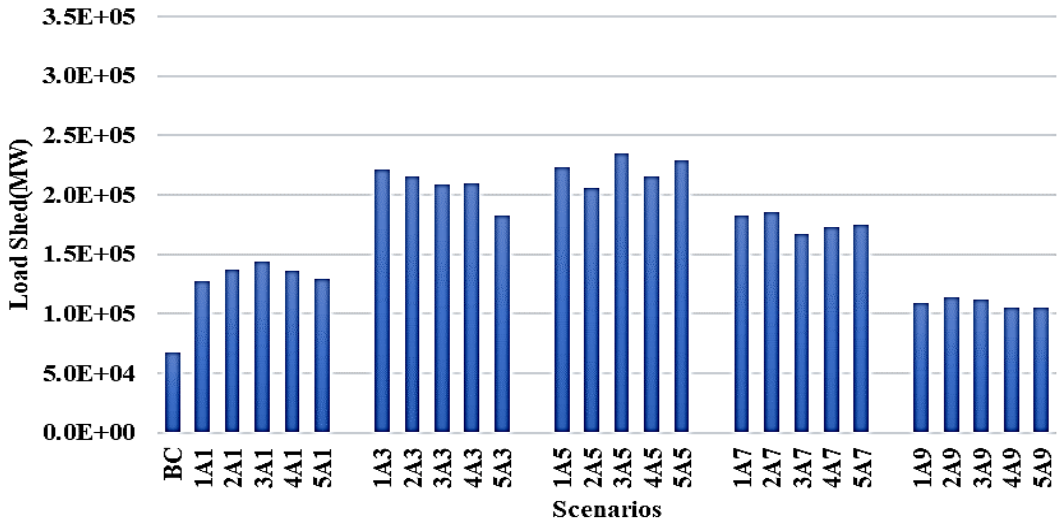

Figure 5. 3 Annual load shed for scenario set A

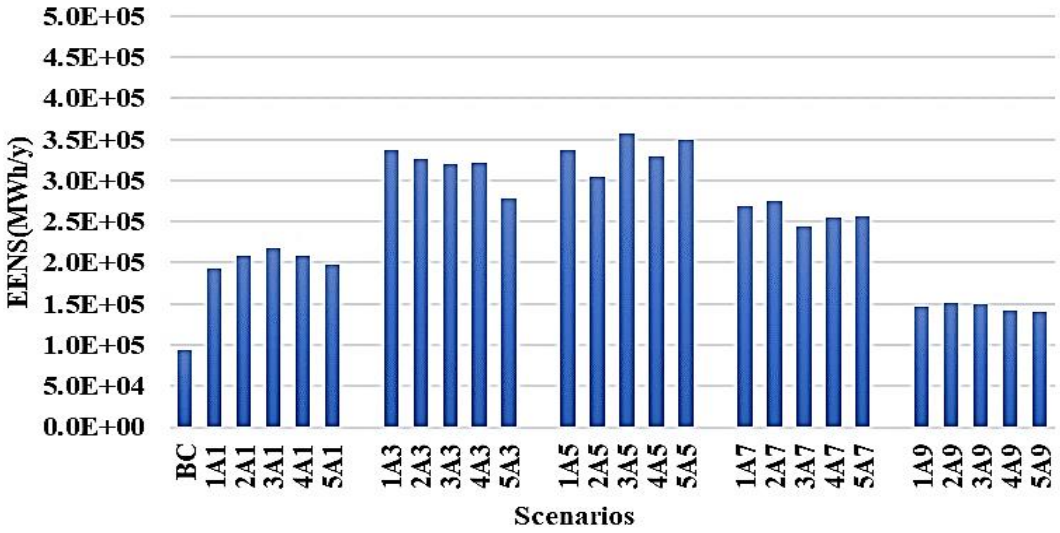

Figure 5. 4 Annual EENS for scenario set A

5.2.2.3 Scenario Set B

The aim of scenario set B is to investigate any significant transitions of impacts and sensitivities in the eventualities of significant increase in the failure rates due to cyber-attacks to know the extreme situations and plan remedial actions accordingly.

The scenario set B investigates any significant transitions of impacts and sensitivities in the eventualities of significant increase in the failure rates of related components due to cyber-attacks on all transformer substations and the transformer associated transmission lines.

Scenario set B contains five clusters scenarios: B1, B3, B5, B7 and B9. Scenario set B is designed by incorporating the base case operating condition given in section 5.2.1 and then applying different failure rates of cyber-attacks on all transformer substations and associated transmission lines for each failure is due to cyber-attacks on the system. The probabilities of failure due to cyber-attacks on all the transformer substations were increased in the scale of 20% and simultaneously applying the failures rates of cyber-attacks at 10%,30%, 50%, 70% and 90% on transformer associated transmission lines for each failure due to cyber-attacks on the CPPS.

- The scenario cluster B1 is formed by simulating 10%, 30%, 50%, 70% and 90% FR of cyber-attack on all effective transformer substations with FR of cyber-attack on all the transformer associated transmission lines maintained at 10% each.
- The scenario cluster B3 is formed by 10%, 30%, 50%, 70% and 90% FR of cyber-attack on all effective transformer substations with FR of cyber-attack on all the transformer associated transmission lines maintained at 30% each.
- The scenario cluster B5 is formed by 10%, 30%, 50%, 70% and 90% FR of cyber-attack on all effective transformer substations with FR of cyber-attack on all the transformer associated transmission lines maintained at 50% each.
- The scenario cluster B7 is formed by 10%, 30%, 50%, 70% and 90% FR of cyber-attack on all effective transformer substations with FR of cyber-attack on all the transformer associated transmission lines maintained at 70% each.

- The scenario cluster B9 is formed by 10%, 30%, 50%, 70% and 90% FR of cyber-attack on all effective transformer substations with FR of cyber-attack on all the transformer associated transmission lines maintained at 90% each.

5.2.2.4 Results and Analysis for Scenario Set B

Figure 5.7, Figure 5.8 and Figure 5.9 show annual estimated results of system violations, load shed and EENS respectively for the scenario set B. Figure 5.8 and Figure 5.9 shows different increased levels of load shed and EENS respectively with respect to the base case. This increased load shed and EENS experienced at each of the scenario set B with respect to the base case indicates that the increase in failure rates of cyber-attacks on all the transformer substations and associated transmission lines cause various increase levels of load shed and EENS in order to maintain the sustained constraint violations and the power balance of the CPPS to avoid system breakdown. However, rate of increase of the load shed and EENS is not consistent with the rate of increase of the cyber-attacks on all the transformer substations and associated transmission lines. This depicts nonlinearity behaviour of some power system components in response to system violations to maintain the power balance of the CPPS.

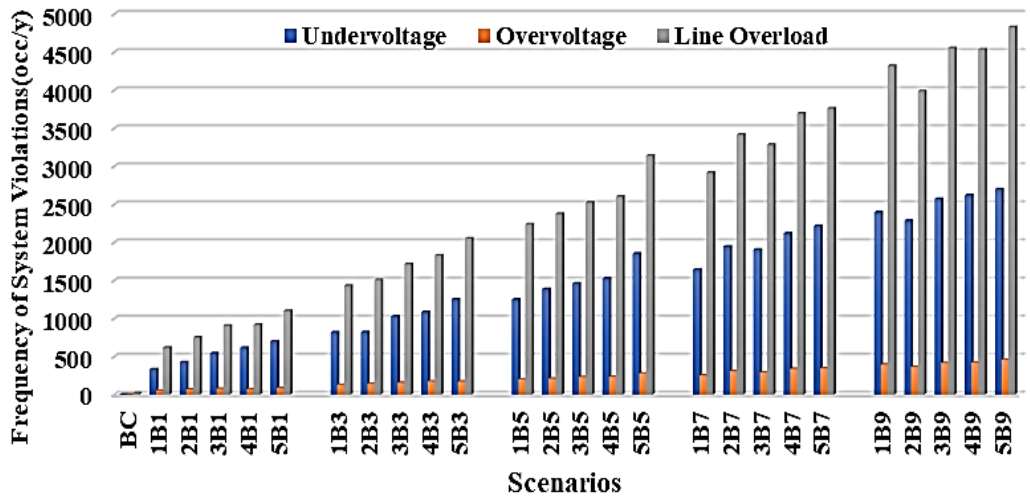

Figure 5. 5 Annual system violations for scenario set B

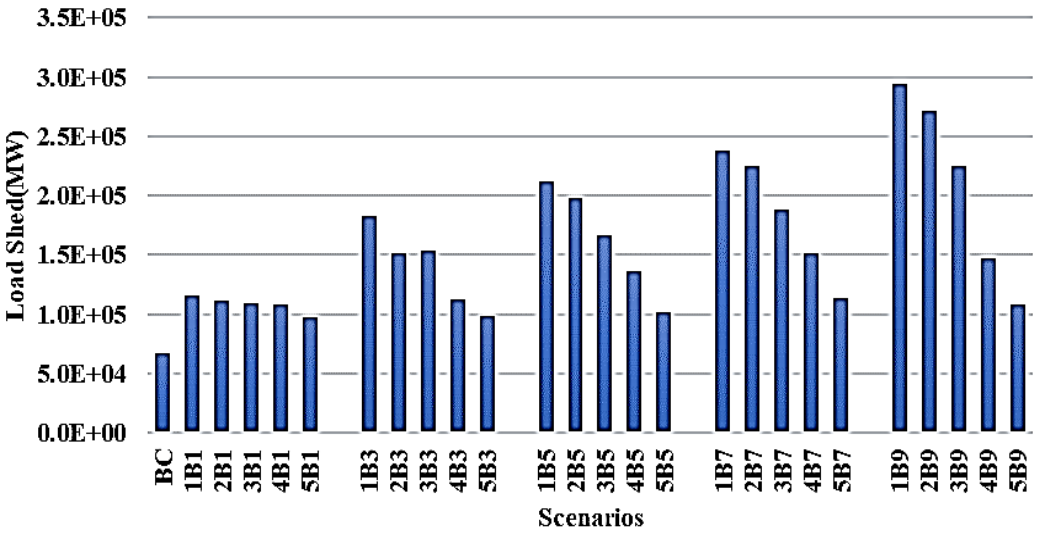

Figure 5. 6 Annual Load Shed for scenario set B

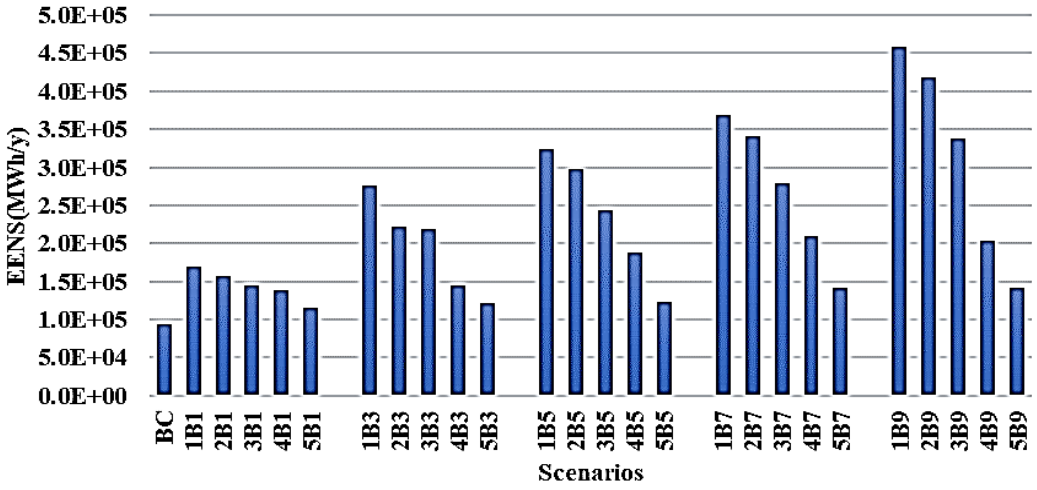

Figure 5. 7 Annual EENS for scenario set B

5.2.2.5 Scenario Set C

The aim of scenarios in set ‘C’ is to investigate sensitivities in the eventualities of significant increase in the failure rates of cyber-attacks with various power system components.

The scenario set C collectively groups the largest EENS value from each of the cluster scenario. Scenario set C contains ten scenarios: CA1 to CA9 and CB1 to CB9. Scenario set C collectively group largest EENS value from each of the cluster scenario [122].

- CA1 is the largest EENS of cluster scenario A1, CA3 is the largest EENS of cluster scenario A3, CA5 is the largest EENS of cluster scenario A5, CA7 is the largest EENS of cluster scenario A7 and CA9 is the largest EENS of cluster scenario A9.
- CB1 is the largest EENS of cluster scenario B1, CB3 is the largest EENS of cluster scenario B3, CB5 is the largest EENS of cluster scenario B5, CB7 is the largest EENS of cluster scenario B7 and CB9 is the largest EENS of cluster scenario B9.

5.2.2.6 Results and Analysis for Scenario Set C

Figure 5.10 and Figure 5.11 show the scenario set C load shed and EENS respectively with respect to the base case. In Figure 5.10 there is a considerably increase in the load shed. Increased effect level of 50% failure rates of cyber-attacks on all generator substations and associated transmission lines is 250% in scenario CA5. The increased effect level of 50% failure rates of cyber-attacks on all transformer buses and associated transmission lines is 117% in scenario CB5. The rate of increase of the load shed in scenario CA and scenario CB with respect to base case depicts that load shed increases regardless, of part or section of the network affected with cyber-attacks but rate of increase in different part of the network varies. Increased failure rate of a cyber-attack on the CPPS impacts the CPPS considerably however, value of impact varies with various power system components [122].

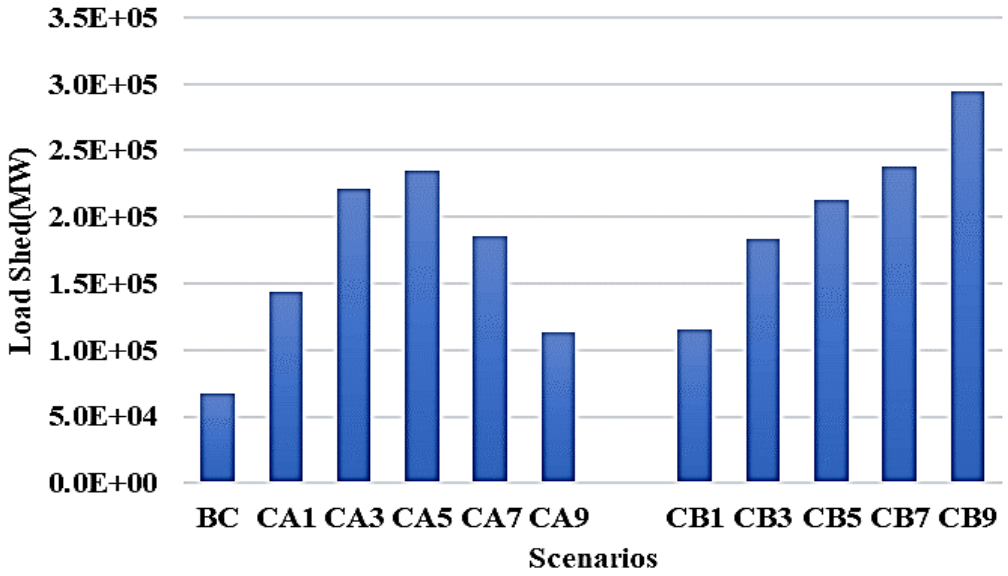

Figure 5. 8 Annual Load Shed for scenario set C

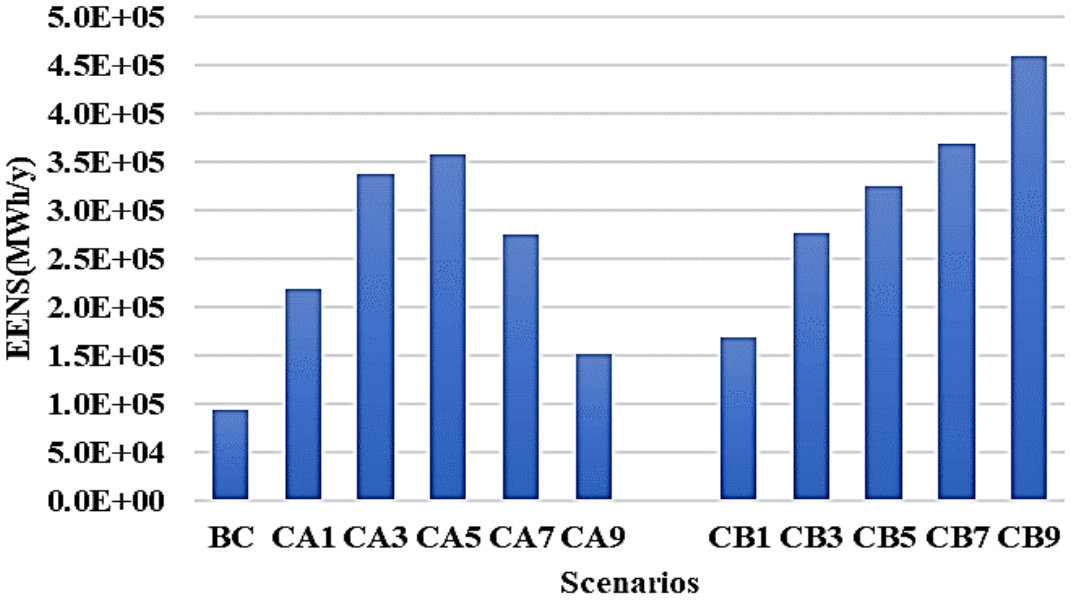

Figure 5. 9 Annual EENS for scenario set C

5.2.2.7 Scenario D

The aim of scenarios D is to investigate the contrast between traditional power system security assessment and the TMM base case system security assessment. Scenario D is power system

security assessment in the presence of component failure without considering cyber-attacks and subsystem layers' interactions of CPPS.

5.2.2.8 Results and Analysis for Scenario D

Figure 5.12 shows the load shed value of the base case, BC and scenario D. Figure 4.18 shows the EENS value of the base case, BC and scenario D. In Figure 5.12, the base case results show a significant increased level of load shed than the scenario D load shed. The results depict that there is a considerable increase in load shed due to interdependency operation in a CPPS caused by subsystem layers' interactions and dynamics of one subsystem layer influence the dynamics of the other subsystem layer. This makes CPPS more unreliable than the traditional power system [122].

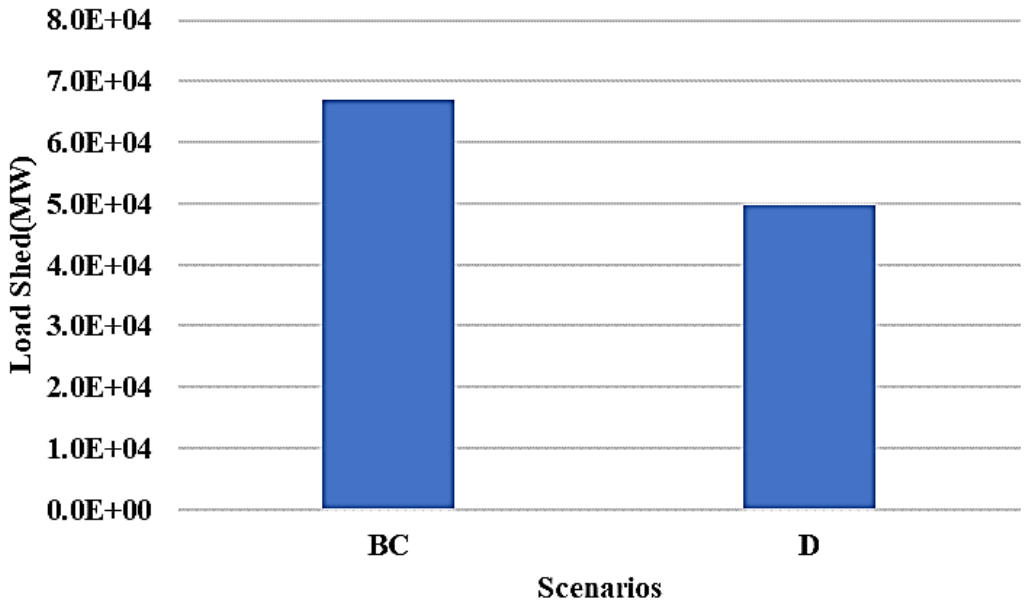

Figure 5. 10 Annual Load Shed for base case and scenario D

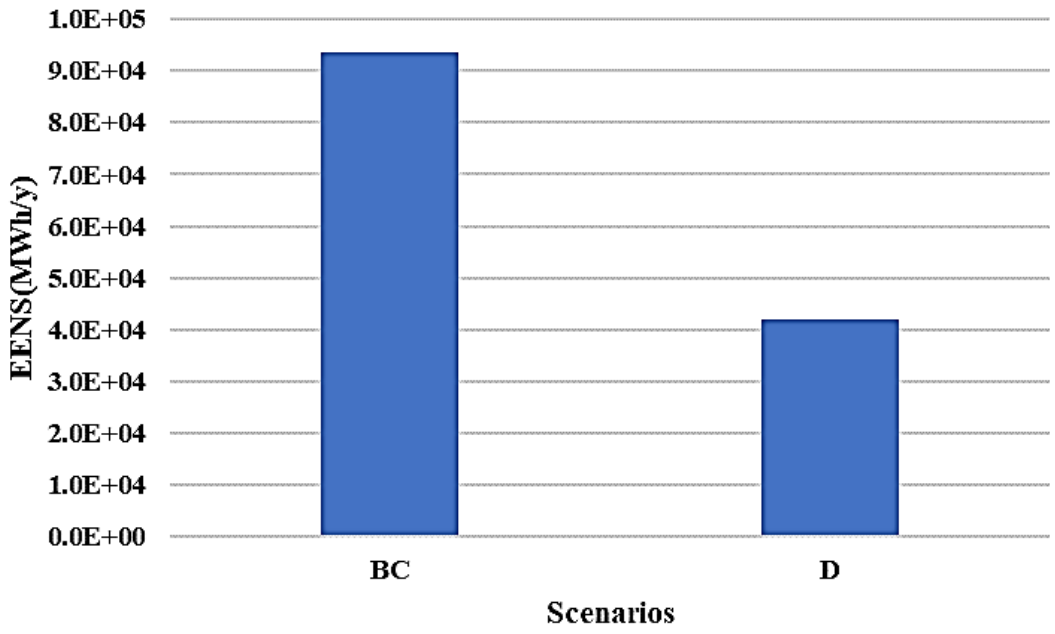

Figure 5. 11 Annual EENS for base case and scenario D.

5.3 Summary

This chapter considered system level performance assessment of the ternary Markovian model (TMM) to evaluate and quantify global impacts of the power system interacting with the cyber network processes.

In this chapter, the ternary Markovian model through Monte Carlo simulation is embedded into the security assessment algorithm and quantitatively assess realistic impacts of subsystem layers' interactions on power system security. The viability of the approach is investigated by simulating a set of scenarios, representing realistic physical power system operating conditions with the cyber network interactions. The case studies scenarios investigate any significant transitions of impacts and sensitivities with possibilities of significant increase in failure rates of cyber-attacks on all generator substations, transformer substations and the associated transmission lines. The scenarios also investigate contrast between the ternary Markovian model base case security assessment and the traditional power system security assessment.

Results justify that the presence of cyber-attacks in a cyber-physical power system components operation could lead to severe insecurities. Also, results suggest that increased failure rate of cyber-attacks on the cyber physical power system operation impacts the system considerably however, value of impact varies with various power system components. The findings from the TMM framework are:

- Cyber-attacks could cause various increase levels of load shed in a CPPS operation.
- Cyber-attacks could cause nonlinearity behaviour of some power system components in response to system violations.
- Cyber-attacks in a cyber-physical power system components operation could lead to severe insecurities.

- Cyber-physical power system operation could be less reliable than the traditional power system.
- The framework demonstrates various states that a cyber-physical power system operation can exists.
- The framework provides holistic assessment of interactions in decision-making layer; communication and coupling layer and power system layer in a CPPS operation. The framework offers innovative pathway to quantify the security impacts of interdependency of components in a CPPS.

Chapter 6: Conclusions and Future Work

6.1 Introduction

Smart Grids (SG) is an intelligent power system that incorporates the state-of-the-art computers, communication, information, and power electronics technologies to enable power generation, transmission, distribution and usage for sustainable, flexible, and effective energy flow. SG is a multidimensional and multidisciplinary cyber-physical power system that allows continuous integration and interaction of the information sensing, processing, intelligent operation, and control as cyber systems and the power system infrastructure as the physical power system. SG has many stakeholders from generator to distributor and consumer in an interconnected and advance technological environment to effectively deliver sustainable, secure, and economic energy.

Extensive integration of cyber systems' infrastructure in power system operation presents new challenges in the physical power system. It exposes the whole cyber-physical power system operation to malicious attacks, cyber intrusion, information and data failures. The changes in the measurement technologies, computing functionalities, communication, monitoring and control due to the increasing integration of cyber systems infrastructure need to be considered in the performance assessment of smart grids to achieve more realistic and robust results. The cyber vulnerabilities increase uncertainties thus, affect the security of the cyber physical power system operation. It is very important that cyber failures and cyber presence are considered in the SG performance assessment because effective operation of a SG with significant integration of cyber systems infrastructure depends on the availability of cyber network enabled function. Therefore, an approach that effectively incorporates cyber intelligent operation, and cyber interactions in smart grids operation are necessary.

Power system security assessment computes measures that can be used in the decision-making processes. The security assessment process in a traditional power system entirely focuses on physical power components and the approach does not consider presence of cyber components and their interaction in the assessment. Also, components and systems in a traditional power system are typically assessed from a two-state approach: functional state and failed state. Considering the complexity and dimensionality of smart grids system due to the increasing deployment of cyber technologies and extensive dependent on cyber enabled functions, it is necessary to include cyber functionalities in performance assessment process of the smart grids system to achieve more realistic results.

6.2 Smart Component Modelling and Performance Assessment with Large Wind Farms

This research achieved and established an innovative multi-state smart component model that captures distinct performance levels of smart components, a smart component state probability algorithm and a performance assessment algorithm framework that incorporates stochastic variation of wind power generation, and random load variations through Monte Carlo Simulation as demonstrated in chapter 3. The contributions in this research are:

I. A multi-state smart component model that captures cyber enabled functions influence on physical power components for a realistic intelligent characteristic evaluation is achieved.

- The model effectively incorporates intelligent characteristic of the smart component that characterize actual component operational behaviour.
- The model represents all states smart component can exist and all intermediate states can be accounted for in the reliability computation.

- The model captures cyber enabled functions influence on physical power components for a realistic intelligent characteristic evaluation.
- The model achieved a new mathematical state probability algorithm of the multi-state smart component.

II. A new mathematical state probability algorithm of the multi-state smart component based on Markovian differential time dependent approach is achieved.

III. An innovative and feasible performance assessment algorithm to assess realistic impacts of smart power grids that justifies the value of smart operation of its components is achieved.

Various scenarios are implemented to investigate the multi-state smart component model performance and to assess the impacts on a smart grid environment in the presence of large wind farms. Various scenarios with and without wind power integration (WPI) were also investigated.

- **Investigating impacts and sensitivities with wind farms locations and network topology.**
    - The results suggest that the wind power integration at different buses causes various increase levels of load shed however, rate of increase of the load shed of each bus varies.
    - This suggests that the geographical location of wind farm connected buses and the network topology varies with the level of system stress.
    - Therefore, the wind farm integration and their geographical locations can potentially impact the smart grids reliability considerably.
- **Investigating impacts with increased wind power integration**
    - The results suggest that the load shed increases as the capacity of WPI increases; however, rate of increase in each bus location varies.

- Increased wind power integration in the smart grids impacts the system considerably however, value of impact varies with various geographical locations of wind farms connected buses.

- **Investigating contrast between the multi-state smart component model performance assessment and traditional power system security assessment.**
  - The results suggest less components failure rate and less disturbance in a smart component operation.
  - This suggests that smart components operate at higher performance levels, more reliable and effective as opposed to traditional power system components.

The framework provides an innovative pathway of modelling intelligence of smart grid component operation to effectively evaluate the performance of a smart power grid. The framework is added means of assessing opportunities in expansion planning of smart power systems.

6.3 Physical power system security with interactions in the Cyber-Physical Power System

This research achieved and established a system level unified ternary Markovian model of the cyber-physical power system operation and a Monte Carlo simulation based performance assessment algorithm framework that quantitatively assesses realistic impacts of subsystem layers' interactions on power system security as demonstrated in Chapter 4 and Chapter 5. The contributions in this research are:

I. Advanced unified ternary Markovian model of cyber-physical power system operation is achieved.

- The model demonstrates dynamic operation of subsystem layers' interactions from communication and coupling layer and decision-making layer to power layer.

- The model combines consequences of events from each of three main subsystem functional layers the communication and coupling layer, the decision-making layer and the power layer.
- The unified ternary Markovian model presents various states that a cyber-physical power system operation can exists.
- The model captures dynamics of the three subsystem layers' interactions for assessment of interdependency impacts.

II. An embedded innovative cyber-physical performance assessment algorithm that quantitatively assesses realistic impacts of subsystem layers' interactions on power system security is achieved.

Several scenarios were established to investigate the ternary Markovian model performance and to assess the interdependency in a cyber-physical power system operation in the event of the power system failure or cyber system failure: components failure, cyber-attacks, malicious attacks and false data-injection attacks.

Various failure rates of cyber-attacks are considered in the scenarios in order to explore any abnormal transitions within the cyber physical power system. Having such leverage can ensure extra planning in the events of unforeseen contingencies in the system and it is important to be aware of such transitions to mitigate unexpected contingencies. Thus, for every cyber physical power system failure caused by cyber-attacks many scenarios were considered.

- **Investigating impacts and sensitivities with possibilities of significant increase in failure rates of cyber-attacks on all generator substations and the generator associated transmission lines(scenario set A).**
    - The results suggest that increase in failure rates of cyber-attacks on the network impose same increased rate of system disturbance and system stress.

- The results suggest that increase in failure rates of cyber-attacks on the network impose various increase levels of load shed, however, rate of increase of the load shed is not consistent with the rate of increase of the cyber-attacks.
- This framework demonstrates nonlinearity behaviour of some power system components in response to system violations.

- **Investigating impacts and sensitivities with possibilities of significant increase in failure rates of cyber-attacks on all transformer substations and the transformer associated transmission lines(scenario set B).**
  - The results suggest that increase in failure rates of cyber-attacks on the network impose same increased rate of system disturbance and system stress.
  - The results suggest that increase in failure rates of cyber-attacks on the network impose various increase levels of load shed, however, rate of increase of the load shed is not consistent with the rate of increase of the cyber-attacks.
  - This framework demonstrates nonlinearity behaviour of some power system components in response to system violations.
  - The framework demonstrates various load shed increases regardless, of part or section of the network affected with cyber-attacks but rate of increase in different part of the network varies.

- **Investigating contrast between the ternary Markovian model base case security assessment and the traditional power system security assessment.**
  - The results suggest that there is a considerable increase in load shed as a result of interdependency operation in a CPPS operation due to subsystem layers' interactions and dynamics.

- This suggests CPPS operation is more unreliable than the traditional power system.

The presence of cyber-attacks in a cyber-physical power system components operation could lead to severe insecurities, however, value of impact varies with various power system components.

The TMM framework provides holistic assessment of interactions in the decision-making layer, information, communication and coupling layer and power system layer in a CPPS operation and offers innovative pathway to quantify the security impacts of interdependency of components in a CPPS effectively.

6.4 Future Work

Based on the research presented in the thesis, suggestion for future work is focused on the whole cyber physical power system operation assessment and impacts quantification to improve existing reliability evaluation models and methodologies.

The work in this thesis models a unified cyber-physical components interaction model of CPPS operation to analysis the three subsystem functional layers' interactions of the cyber-physical power system and to quantify impacts on physical power security.

- The area of analysis and quantification of the three subsystem functional layers' interactions can be further explore and developed to assess the whole system and quantify impacts on cyber part and physical power part.
- Both adequacy and security assessment can be explored for the cyber part and the physical part of the cyber physical power system.

Also, the work in this thesis established a comprehensive cyber-physical power test system by incorporating all generator buses of the conventional 24-Bus RTS (Reliability Test System) with ICT features, such as Merging Units, Ethernet Switches, and line protection panel.

- The 24-Bus reliability test system applied in this research can be further explored. Other equipment and devices of decision-making layer and communication and coupling layer can be further explored and incorporated.
- The 24-Bus RTS can be further explored and updated to incorporate cyber system reliability data to allow and support standardization of results.

Lastly, cyber-physical interactive operation and cyber physical system disturbances can be further explored to advance knowledge in operational grading of the smart grids.

- All hierarchical levels of cyber physical power system operation can be further research and developed. This will further advance a robust integration of cyber functionalities based models into cyber physical power system reliability studies.

References

[1] S. Sridhar, A. Hahn, and M. Govindarasu, “Cyber–physical system security for the electric power grid,” *Proc. IEEE*, vol. 100, no. 1, pp. 210–224, 2011.

[2] Z. Ullah *et al.*, “Smart Grid (SG) and Data Center (DC) Integration: A New Conceptual Framework,” in *2019 15th International Conference on Emerging Technologies (ICET)*, 2019, pp. 1–6.

[3] G. Simard, *IEEE Grid Vision 2050*. IEEE, 2013.

[4] X. Yu, C. Cecati, T. Dillon, and M. G. Simoes, “The new frontier of smart grids,” *IEEE Ind. Electron. Mag.*, vol. 5, no. 3, pp. 49–63, 2011.

[5] S. N. Kulkarni and P. Shingare, “A review on smart grid architecture and implementation challenges,” in *2016 International Conference on Electrical, Electronics, and Optimization Techniques (ICEEOT)*, 2016, pp. 3285–3290.

[6] B. K. Bose, “Artificial intelligence techniques in smart grid and renewable energy systems—Some example applications,” *Proc. IEEE*, vol. 105, no. 11, pp. 2262–2273, 2017.

[7] X. Yu and Y. Xue, “Smart grids: A cyber–physical systems perspective,” *Proc. IEEE*, vol. 104, no. 5, pp. 1058–1070, 2016.

[8] V. C. Gungor *et al.*, “Smart grid technologies: Communication technologies and standards,” *IEEE Trans. Ind. informatics*, vol. 7, no. 4, pp. 529–539, 2011.

[9] G. M. Shafiullah, A. M. T. Oo, A. B. M. S. Ali, and P. Wolfs, “Smart grid for a sustainable future,” *Smart Grid Renew. Energy*, vol. 4, no. 1, pp. 23–34, 2013.

[10] V. Gunes, S. Peter, T. Givargis, and F. Vahid, “A survey on concepts, applications, and challenges in cyber-physical systems.,” *KSII Trans. Internet Inf. Syst.*, vol. 8, no. 12, 2014.

[11] J. Dai *et al.*, “Cyber physical power system modeling and simulation based on graph

computing," in *2017 IEEE Conference on Energy Internet and Energy System Integration (EI2)*, 2017, pp. 1–6.

[12] J. Zhao, F. Wen, Y. Xue, X. Li, and Z. Dong, "Cyber physical power systems: architecture, implementation techniques and challenges," *Autom. Electr. Power Syst.*, vol. 34, no. 16, pp. 1–7, 2010.

[13] R. He, H. Xie, J. Deng, T. Feng, L. L. Lai, and M. Shahidehpour, "Reliability Modeling and Assessment of Cyber Space in Cyber-Physical Power Systems," *IEEE Trans. Smart Grid*, 2020.

[14] L. Sha, S. Gopalakrishnan, X. Liu, and Q. Wang, "Cyber-physical systems: A new frontier," in *2008 IEEE International Conference on Sensor Networks, Ubiquitous, and Trustworthy Computing (sutc 2008)*, 2008, pp. 1–9.

[15] A. Bose, "Smart transmission grid applications and their supporting infrastructure," *IEEE Trans. Smart Grid*, vol. 1, no. 1, pp. 11–19, 2010.

[16] A. Q. Huang, "Power semiconductor devices for smart grid and renewable energy systems," *Power Electron. Renew. Energy Syst. Smart Grid Technol. Appl.*, pp. 85–152, 2019.

[17] H. Abu-Rub, M. Malinowski, and K. Al-Haddad, *Power electronics for renewable energy systems, transportation and industrial applications*. John Wiley & Sons, 2014.

[18] S. R. Bull, "Renewable energy today and tomorrow," *Proc. IEEE*, vol. 89, no. 8, pp. 1216–1226, 2001.

[19] B. Wu, Y. Lang, N. Zargari, and S. Kouro, *Power conversion and control of wind energy systems*, vol. 76. John Wiley & Sons, 2011.

[20] R. Teodorescu, M. Liserre, and P. Rodriguez, *Grid converters for photovoltaic and wind power systems*, vol. 29. John Wiley & Sons, 2011.

[21] M. Z. Jacobson and M. A. Delucchi, "A path to sustainable energy by 2030," *Sci. Am.*,

vol. 301, no. 5, pp. 58–65, 2009.

[22] S.-T. E. O. J. USEIA, “US Energy Information Administration,” *Washington, DC. https//www.eia.gov/energyexplained/renewable-sources/*, 2018.

[23] D. Gielen, F. Boshell, D. Saygin, M. D. Bazilian, N. Wagner, and R. Gorini, “The role of renewable energy in the global energy transformation,” *Energy Strateg. Rev.*, vol. 24, pp. 38–50, 2019.

[24] B. B. Jensen, “Mission impossible? 100% renewable energy society: The European story—Denmark,” in *Proc. IEEE ECCE Conf.*, 2011.

[25] P. Fairley, “Customers seek 100-percent-renewable grids [News],” *IEEE Spectr.*, vol. 54, no. 9, pp. 12–13, 2017.

[26] C. Roselund and J. Bernhardt, “Lessons learned along europe’s road to renewables,” *IEEE Spectr.*, vol. 4, 2015.

[27] X. Liang and B. Bagen, “Probabilistic planning and risk analysis for renewable power generation system,” in *Proceedings of CIGRE Canada Conference, Winnipeg, Manitoba*, 2015, vol. 31.

[28] H. Akbari *et al.*, “Efficient energy storage technologies for photovoltaic systems,” *Sol. Energy*, vol. 192, pp. 144–168, 2019.

[29] I. Worighi, A. Maach, A. Hafid, O. Hegazy, and J. Van Mierlo, “Integrating renewable energy in smart grid system: Architecture, virtualization and analysis,” *Sustain. Energy, Grids Networks*, vol. 18, p. 100226, 2019.

[30] D. Kundur, X. Feng, S. Liu, T. Zourntos, and K. L. Butler-Purry, “Towards a framework for cyber attack impact analysis of the electric smart grid,” in *2010 First IEEE International Conference on Smart Grid Communications*, 2010, pp. 244–249.

[31] J. Wei and G. J. Mendis, “A deep learning-based cyber-physical strategy to mitigate false data injection attack in smart grids,” in *2016 Joint Workshop on Cyber-Physical*

Security and Resilience in Smart Grids (CPSR-SG), 2016, pp. 1–6.

[32] M. Panteli and D. S. Kirschen, "Assessing the effect of failures in the information and communication infrastructure on power system reliability," in *2011 IEEE/PES Power Systems Conference and Exposition*, 2011, pp. 1–7.

[33] M. N. Albasrawi, N. Jarus, K. A. Joshi, and S. S. Sarvestani, "Analysis of reliability and resilience for smart grids," in *2014 IEEE 38th Annual Computer Software and Applications Conference*, 2014, pp. 529–534.

[34] B. Falahati, A. Kargarian, and Y. Fu, "Impacts of information and communication failures on optimal power system operation," in *2013 IEEE PES Innovative Smart Grid Technologies Conference (ISGT)*, 2013, pp. 1–6.

[35] Y. Xue, M. Ni, J. Yu, J. Hu, and W. Yu, "Study of the impact of communication failures on power system," in *2015 IEEE Power & Energy Society General Meeting*, 2015, pp. 1–5.

[36] K. M. J. Rahman, M. M. Munnee, and S. Khan, "Largest blackouts around the world: Trends and data analyses," in *2016 IEEE International WIE Conference on Electrical and Computer Engineering (WIECON-ECE)*, 2016, pp. 155–159.

[37] A. Veremyev, A. Sorokin, V. Boginski, and E. L. Pasiliao, "Minimum vertex cover problem for coupled interdependent networks with cascading failures," *Eur. J. Oper. Res.*, vol. 232, no. 3, pp. 499–511, 2014.

[38] M. Čepin, *Assessment of power system reliability: methods and applications*. Springer Science & Business Media, 2011.

[39] M. Rahnamay-Naeini and M. M. Hayat, "Cascading failures in interdependent infrastructures: An interdependent Markov-chain approach," *IEEE Trans. Smart Grid*, vol. 7, no. 4, pp. 1997–2006, 2016.

[40] G. Andersson *et al.*, "Causes of the 2003 major grid blackouts in North America and

Europe, and recommended means to improve system dynamic performance," *IEEE Trans. Power Syst.*, vol. 20, no. 4, pp. 1922–1928, 2005.

[41] C. Singh and A. Sprintson, "Reliability assurance of cyber-physical power systems," in *IEEE PES General Meeting*, 2010, pp. 1–6.

[42] M. S. Mathavi, D. Vanitha, S. Jeyanthi, and P. Senthil, "The smart home: renewable energy management system for smart grid based on ISM band communications," *Int. J. Sci. Eng. Res.*, vol. 3, no. 3, pp. 1–8, 2012.

[43] F. Blaabjerg and J. M. Guerrero, "Smart grid and renewable energy systems," in *2011 International Conference on Electrical Machines and Systems*, 2011, pp. 1–10.

[44] D.-H. Yoon, H. Song, G. Jang, and S.-K. Joo, "Smart operation of HVDC systems for large penetration of wind energy resources," *IEEE Trans. Smart Grid*, vol. 4, no. 1, pp. 359–366, 2013.

[45] N. Jain, O. P. Yadav, A. P. S. Rathore, and R. Jain, "An approach for multi-state multi-component system reliability considering dependency behavior," in *2017 Annual Reliability and Maintainability Symposium (RAMS)*, 2017, pp. 1–6.

[46] J. E. Ramirez-Marquez, C. M. Rocco, B. A. Gebre, D. W. Coit, and M. Tortorella, "New insights on multi-state component criticality and importance," *Reliab. Eng. Syst. Saf.*, vol. 91, no. 8, pp. 894–904, 2006.

[47] J. E. Ramirez-Marquez and D. W. Coit, "A heuristic for solving the redundancy allocation problem for multi-state series-parallel systems," *Reliab. Eng. Syst. Saf.*, vol. 83, no. 3, pp. 341–349, 2004.

[48] R. Billinton and W. Zhang, "State extension for adequacy evaluation of composite power systems-applications," *IEEE Trans. Power Syst.*, vol. 15, no. 1, pp. 427–432, 2000.

[49] Z. Kovač, G. Knežević, and T. Danijel, "MODELING OF POWER SYSTEM

RELIABILITY ASSESSMENT," *Teh. Vjesn. Gaz.*, vol. 20, no. 1, p. 93, 2013.

[50] J. E. Ramirez-Marquez and D. W. Coit, "A Monte-Carlo simulation approach for approximating multi-state two-terminal reliability," *Reliab. Eng. Syst. Saf.*, vol. 87, no. 2, pp. 253–264, 2005.

[51] W.-C. Yeh, "A new method for verifying d-MC candidates," *Reliab. Eng. Syst. Saf.*, vol. 204, p. 107202, 2020.

[52] J. U. M. Smith, R. Billington, and R. N. Allan, *Reliability Evaluation of Engineering Systems.*, vol. 43, no. 4. Springer, 1994.

[53] M. Vujošević, D. Makajić-Nikolić, and P. Pavlović, "A new approach to determination of the most critical multi-state components in multi-state systems," *J. Appl. Eng. Sci.*, vol. 15, no. 4, pp. 401–405, 2017.

[54] M. Heidari-Kapourchali and V. Aravinthan, "Component reliability evaluation in the presence of smart monitoring," in *2013 North American Power Symposium (NAPS)*, 2013, pp. 1–6.

[55] J. Wäfler and P. E. Heegaard, "A combined structural and dynamic modelling approach for dependability analysis in smart grid," in *Proceedings of the 28th Annual ACM Symposium on Applied Computing*, 2013, pp. 660–665.

[56] B. Bousshoua and A. Elmaouhab, "Smart Grid Reliability Using Reliable Block Diagram Case Study: Adrar's Isolated Network of Algeria," in *2019 International Conference on Power Generation Systems and Renewable Energy Technologies (PGSRET)*, 2019, pp. 1–6.

[57] A.-M. Hariri, H. Hashemi-Dezaki, and M. A. Hejazi, "A novel generalized analytical reliability assessment method of smart grids including renewable and non-renewable distributed generations and plug-in hybrid electric vehicles," *Reliab. Eng. Syst. Saf.*, vol. 196, p. 106746, 2020.

[58] W. Zhu, M. Han, J. V Milanović, and P. Crossley, “Methodology for Reliability Assessment of Smart Grid Considering Risk of Failure of Communication Architecture,” *IEEE Trans. Smart Grid*, 2020.

[59] B. Li, R. Lu, K.-K. R. Choo, W. Wang, and S. Luo, “On reliability analysis of smart grids under topology attacks: A stochastic petri net approach,” *ACM Trans. Cyber-Physical Syst.*, vol. 3, no. 1, pp. 1–25, 2018.

[60] G. Celli, E. Ghiani, F. Pilo, and G. G. Soma, “Reliability assessment in smart distribution networks,” *Electr. Power Syst. Res.*, vol. 104, pp. 164–175, 2013.

[61] G. Song, H. Chen, and B. Guo, “A layered fault tree model for reliability evaluation of smart grids,” *Energies*, vol. 7, no. 8, pp. 4835–4857, 2014.

[62] B. Falahati and A. Kargarian, “Power system reliability enhancement considering smart monitoring,” in *2015 IEEE Power & Energy Society General Meeting*, 2015, pp. 1–5.

[63] K. Marashi and S. S. Sarvestani, “Towards comprehensive modeling of reliability for smart grids: Requirements and challenges,” in *2014 IEEE 15th International Symposium on High-Assurance Systems Engineering*, 2014, pp. 105–112.

[64] A. Mahmood, O. Hasan, H. R. Gillani, Y. Saleem, and S. R. Hasan, “Formal reliability analysis of protective systems in smart grids,” in *2016 IEEE Region 10 Symposium (TENSYMP)*, 2016, pp. 198–202.

[65] A. I. Sarwat, A. Domijan, M. H. Amini, A. Damnjanovic, and A. Moghadasi, “Smart Grid reliability assessment utilizing Boolean Driven Markov Process and variable weather conditions,” in *2015 North American Power Symposium (NAPS)*, 2015, pp. 1–6.

[66] V. Aravinthan *et al.*, “Reliability modeling considerations for emerging cyber-physical power systems,” in *2018 IEEE International Conference on Probabilistic Methods Applied to Power Systems (PMAPS)*, 2018, pp. 1–7.

[67] Y. Wang, Z. Lin, X. Liang, W. Xu, Q. Yang, and G. Yan, “On modeling of electrical cyber-physical systems considering cyber security,” *Front. Inf. Technol. Electron. Eng.*, vol. 17, no. 5, pp. 465–478, 2016.

[68] S. Xin, Q. Guo, H. Sun, B. Zhang, J. Wang, and C. Chen, “Cyber-physical modeling and cyber-contingency assessment of hierarchical control systems,” *IEEE Trans. Smart Grid*, vol. 6, no. 5, pp. 2375–2385, 2015.

[69] J. Wei, D. Kundur, T. Zourntos, and K. L. Butler-Purry, “A flocking-based paradigm for hierarchical cyber-physical smart grid modeling and control,” *IEEE Trans. Smart Grid*, vol. 5, no. 6, pp. 2687–2700, 2014.

[70] X. Shi, Y. Li, Y. Cao, Y. Tan, Z. Xu, and M. Wen, “Model predictive control considering cyber-physical system to dampen low frequency oscillation of interconnected power systems,” in *2015 IEEE PES Asia-Pacific Power and Energy Engineering Conference (APPEEC)*, 2015, pp. 1–5.

[71] S. Wang, Z. Wu, A. Su, S. Jin, Y. Xia, and D. Zhao, “Reliability Modeling and Simulation of Cyber-Physical Power Distribution System Considering the Impacts of Cyber Components and Transmission Quality,” in *2018 37th Chinese Control Conference (CCC)*, 2018, pp. 6166–6171.

[72] W. Liu, Q. Gong, H. Han, Z. Wang, and L. Wang, “Reliability modeling and evaluation of active cyber physical distribution system,” *IEEE Trans. Power Syst.*, vol. 33, no. 6, pp. 7096–7108, 2018.

[73] Y. Wang, W. Li, G. Yan, and S. Song, “Towards a framework for cyber attack impact analysis of electric cyber physical systems,” in *2017 IEEE International Conference on Industrial Technology (ICIT)*, 2017, pp. 638–643.

[74] H. Pan, H. Lian, C. Na, and X. Li, “Modeling and Vulnerability Analysis of Cyber-Physical Power Systems Based on Community Theory,” *IEEE Syst. J.*, 2020.

[75] M. Li, Y. Xue, M. Ni, and X. Li, “Modeling and Hybrid Calculation Architecture for Cyber Physical Power Systems,” *IEEE Access*, vol. 8, pp. 138251–138263, 2020.

[76] S. Xin, Q. Guo, H. Sun, C. Chen, J. Wang, and B. Zhang, “Information-energy flow computation and cyber-physical sensitivity analysis for power systems,” *IEEE J. Emerg. Sel. Top. Circuits Syst.*, vol. 7, no. 2, pp. 329–341, 2017.

[77] B. Moussa, P. Akaber, M. Debbabi, and C. Assi, “Critical Links Identification for Selective Outages in Interdependent Power-Communication Networks,” *IEEE Trans. Ind. Informatics*, vol. 14, no. 2, pp. 472–483, 2018.

[78] V. Aravinthan *et al.*, “Reliability Modeling Considerations for Emerging Cyber-Physical Power Systems,” no. i, pp. 1–7, 2018.

[79] B. Falahati and Y. Fu, “A study on interdependencies of cyber-power networks in smart grid applications,” in *2012 IEEE PES Innovative Smart Grid Technologies (ISGT)*, 2012, pp. 1–8.

[80] K. Marashi, S. S. Sarvestani, and A. R. Hurson, “Consideration of Cyber-Physical Interdependencies in Reliability Modeling of Smart Grids,” *IEEE Trans. Sustain. Comput.*, vol. 3, no. 2, pp. 73–83, 2018.

[81] A. H. Ahangar and H. A. Abyaneh, “Improvement of smart grid reliability considering various cyber network topologies and direct interdependency,” in *2016 IEEE PES Asia-Pacific Power and Energy Engineering Conference (APPEEC)*, 2016, pp. 267–272.

[82] M. Zeraati, Z. Aref, and M. A. Latify, “Vulnerability analysis of power systems under physical deliberate attacks considering geographic-cyber interdependence of the power system and communication network,” *IEEE Syst. J.*, vol. 12, no. 4, pp. 3181–3190, 2017.

[83] Z. Huang, C. Wang, M. Stojmenovic, and A. Nayak, “Characterization of cascading failures in interdependent cyber-physical systems,” *IEEE Trans. Comput.*, vol. 64, no. 8, pp. 2158–2168, 2014.

[84] K. Marashi, S. S. Sarvestani, and A. R. Hurson, “Quantification and analysis of interdependency in cyber-physical systems,” in *2016 46th Annual IEEE/IFIP International Conference on Dependable Systems and Networks Workshop (DSN-W)*, 2016, pp. 149–154.

[85] K. Hanada, T. Tsuchiya, and Y. Fujisaki, “Satisfiability-Based Analysis of Cascading Failures in Systems of Interdependent Networks,” in *2019 IEEE 24th Pacific Rim International Symposium on Dependable Computing (PRDC)*, 2019, pp. 105–1058.

[86] R. Peng, “Reliability of interdependent networks with cascading failures,” *Eksploat. i Niezawodn.*, vol. 20, 2018.

[87] Z. Chen, J. Wu, Y. Xia, and X. Zhang, “Robustness of interdependent power grids and communication networks: A complex network perspective,” *IEEE Trans. Circuits Syst. II Express Briefs*, vol. 65, no. 1, pp. 115–119, 2017.

[88] J. Fang, X. Zhang, J. Wu, and Z. Zheng, “Robustness Analysis of Power Grids Against Cascading Failures Based on a Multi-Objective Algorithm,” in *2019 IEEE International Symposium on Circuits and Systems (ISCAS)*, 2019, pp. 1–5.

[89] Y. Zhang, J. Wu, Z. Chen, Y. Huang, and Z. Zheng, “Sequential Node/Link Recovery Strategy of Power Grids Based on Q-Learning Approach,” in *2019 IEEE International Symposium on Circuits and Systems (ISCAS)*, 2019, pp. 1–5.

[90] B. Liu, Z. Li, X. Chen, Y. Huang, and X. Liu, “Recognition and vulnerability analysis of key nodes in power grid based on complex network centrality,” *IEEE Trans. Circuits Syst. II Express Briefs*, vol. 65, no. 3, pp. 346–350, 2017.

[91] Y. Chen *et al.*, “Cascading failure analysis of cyber physical power system with multiple interdependency and control threshold,” *IEEE Access*, vol. 6, pp. 39353–39362, 2018.

[92] W. Zhu and J. V Milanović, “Interdepedency modeling of cyber-physical systems using a weighted complex network approach,” in *2017 IEEE Manchester PowerTech*, 2017,

pp. 1–6.

[93] H. Lei, B. Chen, K. L. Butler-Purry, and C. Singh, “Security and reliability perspectives in cyber-physical smart grids,” in *2018 IEEE Innovative Smart Grid Technologies-Asia (ISGT Asia)*, 2018, pp. 42–47.

[94] B. Boussahoua and A. Elmaouhab, “Reliability Analysis of Electrical Power System Using Graph Theory and Reliability Block Diagram,” in *2019 Algerian Large Electrical Network Conference (CAGRE)*, 2019, pp. 1–6.

[95] R. N. Allan, *Reliability evaluation of power systems*. Springer Science & Business Media, 2013.

[96] M. Edimu, C. T. Gaunt, and R. Herman, “Using probability distribution functions in reliability analyses,” *Electr. Power Syst. Res.*, vol. 81, no. 4, pp. 915–921, 2011.

[97] W. Li, *Reliability assessment of electric power systems using Monte Carlo methods*. Springer Science & Business Media, 2013.

[98] A. K. Verma, S. Ajit, and D. R. Karanki, *Reliability and safety engineering*, vol. 43. Springer, 2010.

[99] M. P. Bhavaraju *et al.*, “IEEE tutorial on electric delivery system reliability evaluation,” in *IEEE Power Engineering Society General Meeting*, 2005.

[100] M. Xie, Y.-S. Dai, and K.-L. Poh, *Computing system reliability: models and analysis*. Springer Science & Business Media, 2004.

[101] M. Wadi, M. Baysal, A. Shobole, and M. R. Tur, “Reliability Evaluation in Smart Grids via Modified Monte Carlo Simulation Method,” in *2018 7th International Conference on Renewable Energy Research and Applications (ICRERA)*, 2018, pp. 841–845.

[102] L. N. Kishore and E. Fernandez, “Reliability well-being assessment of PV-wind hybrid system using Monte Carlo simulation,” in *2011 International Conference on Emerging Trends in Electrical and Computer Technology*, 2011, pp. 63–68.

[103] R. Billinton and W. Li, *Reliability Assessment of Electric Power Systems Using Monte Carlo Methods*. Springer Science & Business Media, 1994.

[104] P. A. Oyewole and D. Jayaweera, "RELIABILITY OF SMART GRIDS WITH SMART ASSETS AND LARGE WIND FARMS," *IET Conf. Proc. 10.1049/icp.2021.1405 IET Digit. Libr. https//digital-library.theiet.org/content/conferences/10.1049/icp.2021.1405*, pp. 59–64, 2021.

[105] J. F. Kitchin, "Practical Markov modeling for reliability analysis," in *1988. Proceedings., Annual Reliability and Maintainability Symposium,* 1988, pp. 290–296.

[106] T. K. Vrana and E. Johansson, "Overview of power system reliability assessment techniques," *CIGRE 2011*, pp. 51–62, 2011.

[107] G. Levitin, *Computational intelligence in reliability engineering: evolutionary techniques in reliability analysis and optimization*, vol. 39. Springer Science & Business Media, 2006.

[108] B. S. Dhillon, *Applied reliability and quality: fundamentals, methods and procedures*. Springer Science & Business Media, 2007.

[109] A. T. Johns, "Probability Concepts in Electric Power Systems," vol. 6, no. 1, p. 41, 1992.

[110] D. J. Smith, *Reliability, maintainability and risk: practical methods for engineers*. Butterworth-Heinemann, 2017.

[111] K. N. Smith, M. A. Taylor, A. A. Carroll, T. W. Manikas, and M. A. Thornton, "Automated Markov-chain based analysis for large state spaces," in *2017 Annual IEEE International Systems Conference (SysCon)*, 2017, pp. 1–8.

[112] C. Graham, *Markov chains: analytic and Monte Carlo computations*. John Wiley & Sons, 2014.

[113] N. B. Fuqua, "The Applicability of Markov Analysis Methods to Reliability, Maintainability and Safety," *Sel. Top. Assur. Relat. Technol.*, vol. 10, no. 2, p. 8, 2003.

[114] W. Li, *Risk assessment of power systems: models, methods, and applications*. John Wiley & Sons, 2014.

[115] J. Leithon, T. J. Lim, and S. Sun, "Renewable energy management in cellular networks: An online strategy based on ARIMA forecasting and a Markov chain model," in *2016 IEEE Wireless Communications and Networking Conference*, 2016, pp. 1–6.

[116] M. Ammar, K. A. Hoque, and O. A. Mohamed, "Formal analysis of fault tree using probabilistic model checking: A solar array case study," in *2016 Annual IEEE Systems Conference (SysCon)*, 2016, pp. 1–6.

[117] S. M. Verma, V. Reddy, K. Verma, and R. Kumar, "Markov models based short term forecasting of wind speed for estimating day-ahead wind power," in *2018 International Conference on Power, Energy, Control and Transmission Systems (ICPECTS)*, 2018, pp. 31–35.

[118] M. K. Ishak, G. Herrmann, and M. Pearson, "Performance evaluation using Markov model for a novel approach in Ethernet based embedded networked control communication," in *2016 Annual IEEE Systems Conference (SysCon)*, 2016, pp. 1–7.

[119] M. Takeshi, "A Monte Carlo simulation method for system reliability analysis," *Nucl. Saf. Simul*, vol. 4, pp. 44–52, 2013.

[120] J. Faulin, A. A. Juan, S. S. M. Alsina, and J. E. Ramirez-Marquez, *Simulation methods for reliability and availability of complex systems*. Springer Science & Business Media, 2010.

[121] C. Singh and J. Mitra, "Monte Carlo simulation for reliability analysis of emergency and standby power systems," in *IAS'95. Conference Record of the 1995 IEEE Industry Applications Conference Thirtieth IAS Annual Meeting*, 1995, vol. 3, pp. 2290–2295.

[122] P. A. Oyewole and D. Jayaweera, "Power System Security With Cyber-Physical Power System Operation," *IEEE Access*, vol. 8, pp. 179970–179982, 2020.

[123] E. Zaitseva, V. Levashenko, J. Kostolny, and M. Kvassay, “A multi-valued decision diagram for estimation of multi-state system,” in *Eurocon 2013*, 2013, pp. 645–650.

[124] Y.-K. Lin, “System reliability evaluation for a multistate supply chain network with failure nodes using minimal paths,” *IEEE Trans. Reliab.*, vol. 58, no. 1, pp. 34–40, 2009.

[125] Y.-K. Lin and P.-C. Chang, “Evaluate the system reliability for a manufacturing network with reworking actions,” *Reliab. Eng. Syst. Saf.*, vol. 106, pp. 127–137, 2012.

[126] J. E. Ramirez-Marquez and D. W. Coit, “Composite importance measures for multi-state systems with multi-state components,” *IEEE Trans. Reliab.*, vol. 54, no. 3, pp. 517–529, 2005.

[127] T. Liu, G. Bai, J. Tao, Y.-A. Zhang, and Y. Fang, “An improved bounding algorithm for approximating multistate network reliability based on state-space decomposition method,” *Reliab. Eng. Syst. Saf.*, vol. 210, p. 107500, 2021.

[128] R. Allan and R. Billinton, “Probabilistic assessment of power systems,” *Proc. IEEE*, vol. 88, no. 2, pp. 140–162, 2000.

[129] D. Jayaweera and S. Islam, “Security of energy supply with change in weather conditions and dynamic thermal limits,” *IEEE Trans. Smart Grid*, vol. 5, no. 5, pp. 2246–2254, 2014.

[130] K. K. Kariuki and R. N. Allan, “Evaluation of reliability worth and value of lost load,” *IEE Proc. - Gener. Transm. Distrib.*, vol. 143, no. 2, pp. 171–180, 1996.

[131] I. Staffell and S. Pfenninger, “Using bias-corrected reanalysis to simulate current and future wind power output,” *Energy*, vol. 114, pp. 1224–1239, 2016.

[132] C. Grigg *et al.*, “The IEEE reliability test system-1996. A report prepared by the reliability test system task force of the application of probability methods subcommittee,” *IEEE Trans. power Syst.*, vol. 14, no. 3, pp. 1010–1020, 1999.

[133] E. Santacana, G. Rackliffe, L. Tang, and X. Feng, “Getting smart,” *IEEE Power Energy*

Mag., vol. 8, no. 2, pp. 41–48, 2010.

[134] J. Hao, R. J. Piechocki, D. Kaleshi, W. H. Chin, and Z. Fan, "Sparse malicious false data injection attacks and defense mechanisms in smart grids," *IEEE Trans. Ind. Informatics*, vol. 11, no. 5, pp. 1–12, 2015.

[135] S. Mohebbi *et al.*, "Cyber-physical-social interdependencies and organizational resilience: A review of water, transportation, and cyber infrastructure systems and processes," *Sustain. Cities Soc.*, vol. 62, p. 102327, 2020.

[136] L. Galbusera, P. Trucco, and G. Giannopoulos, "Modeling interdependencies in multi-sectoral critical infrastructure systems: Evolving the DMCI approach," *Reliab. Eng. Syst. Saf.*, vol. 203, p. 107072, 2020.

[137] A. Sturaro, S. Silvestri, M. Conti, and S. K. Das, "A realistic model for failure propagation in interdependent cyber-physical systems," *IEEE Trans. Netw. Sci. Eng.*, vol. 7, no. 2, pp. 817–831, 2018.

[138] X. Wang, X. Luo, M. Zhang, Z. Jiang, and X. Guan, "Detection and isolation of false data injection attacks in smart grid via unknown input interval observer," *IEEE Internet Things J.*, vol. 7, no. 4, pp. 3214–3229, 2020.

[139] I. B. Gertsbakh, Y. Shpungin, and R. Vaisman, "D-spectra for networks with binary and ternary components," in *2016 Second International Symposium on Stochastic Models in Reliability Engineering, Life Science and Operations Management (SMRLO)*, 2016, pp. 217–220.

[140] I. B. Gertsbakh, Y. Shpungin, and R. Vaisman, "D-spectrum and reliability of a binary system with ternary components," *Probab. Eng. Informational Sci.*, vol. 30, no. 1, pp. 25–39, 2016.

[141] H. Lei and C. Singh, "Developing a benchmark test system for electric power grid cyber-physical reliability studies," in *2016 International Conference on Probabilistic Methods*

Applied to Power Systems (PMAPS), 2016, pp. 1–5.

[142] M. G. Kanabar and T. S. Sidhu, "Reliability and availability analysis of IEC 61850 based substation communication architectures," in *2009 IEEE Power & Energy Society General Meeting*, 2009, pp. 1–8.

[143] J. Guo, Y. Wang, C. Guo, S. Dong, and B. Wen, "Cyber-Physical Power System (CPPS) reliability assessment considering cyber attacks against monitoring functions," in *2016 IEEE Power and Energy Society General Meeting (PESGM)*, 2016, pp. 1–5.

Appendix

Appendix A: Reliability Test System

A.1 IEEE 24 Bus Reliability Test System

IEEE 24 Bus RTS (Reliability Test System) [132] as shown in Figure A.1, is used in the research presented in this thesis for different simulations conducted in Chapter 4 and Chapter 6. The bus data and transmission line data are given in Table A.1 and Table A.2, respectively.

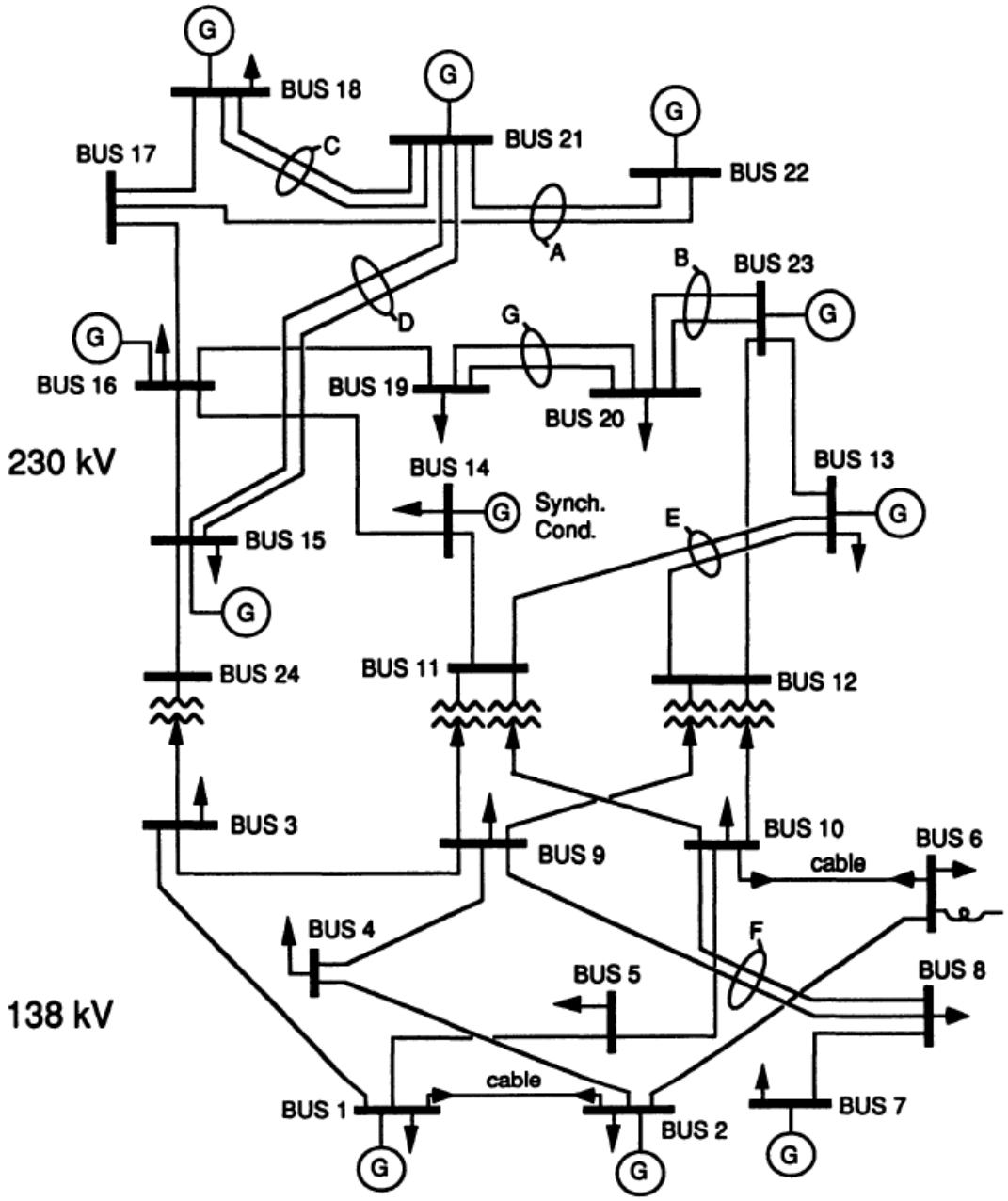

Figure A. 1. IEEE 24 Bus Reliability Test System [132]

Table A. 1 IEEE 24 Bus Reliability Test System Bus data(in p.u.) [132]

Bus No.	**Bus Type**	P_{G_i}	Q_{G_i}	P_{D_i}	$Q_{D,i}$	V_i	$V_{i\max}$	$V_{i\min}$	**Base KV**
1	2	1.72	0.282	1.08	0.22	1.035	1.05	0.95	138
2	2	1.72	0.14	0.97	0.2	1.035	1.05	0.95	138
3	1	0	0	1.8	0.37	0.9913	1.05	0.95	138
4	1	0	0	0.74	0.15	0.9982	1.05	0.95	138
5	1	0	0	0.71	0.14	1.0186	1.05	0.95	138
6	1	0	0	1.36	0.28	1.0126	1.05	0.95	138
7	2	2.4	0.516	1.25	0.25	1.025	1.05	0.95	138
8	1	0	0	1.71	0.35	0.9923	1.05	0.95	138
9	1	0	0	1.75	0.36	1.0022	1.05	0.95	138
10	1	0	0	1.95	0.4	1.0283	1.05	0.95	138
11	1	0	0	0	0	0.9892	1.05	0.95	230
12	1	0	0	0	0	1.0017	1.05	0.95	230
13	3	2.853	1.221	2.65	0.54	1.02	1.05	0.95	230
14	2	0	0	1.94	0.39	0.98	1.05	0.95	230
15	2	2.15	0.0005	3.17	0.64	1.014	1.05	0.95	230
16	2	1.55	0.2522	1	0.2	1.017	1.05	0.95	230
17	1	0	0	0	0	1.0392	1.05	0.95	230
18	2	4	1.374	3.33	0.68	1.05	1.05	0.95	230
19	1	0	0	1.81	0.37	1.0231	1.05	0.95	230
20	1	0	0	1.28	0.26	1.0382	1.05	0.95	230
21	2	4	1.082	0	0	1.05	1.05	0.95	230
22	2	3	-0.2976	0	0	1.05	1.05	0.95	230
23	2	6.6	1.3536	0	0	1.05	1.05	0.95	230
24	1	0	0	0	0	0.9818	1.05	0.95	230

Table A. 2 IEEE 24 Bus Transmission Line Data [132]

Line No	From Bus	To Bus	R(p.u)	X(p.u)	B(p.u)	CON (p.u)	LTE (MVA)	STE (MVA)	Tr (p.u.)	Failure Rate/yr λ	Repair Rate/yr μ
1	1	2	0.0026	0.0139	0.4611	1.75	193	200	0	0.24	547.5
2	1	3	0.0546	0.2112	0.0572	1.75	208	220	0	0.51	876
3	1	5	0.0218	0.0845	0.0229	1.75	208	220	0	0.33	876
4	2	4	0.0328	0.1267	0.0343	1.75	208	220	0	0.39	876
5	2	6	0.0497	0.192	0.052	1.75	208	220	0	0.48	876
6	3	9	0.0308	0.119	0.0322	1.75	208	220	0	0.38	876
7	3	24	0.0023	0.0839	0	4	510	600	1.02	0.02	11.4063
8	4	9	0.0268	0.1037	0.0281	1.75	208	220	0	0.36	876
9	5	10	0.0228	0.0883	0.0239	1.75	208	220	0	0.34	876
10	6	10	0.0139	0.0605	2.459	1.75	193	200	0	0.33	250.286
11	7	8	0.0159	0.0614	0.0166	1.75	208	220	0	0.3	876
12	8	9	0.0427	0.1651	0.0447	1.75	208	220	0	0.44	876
13	8	10	0.0427	0.1651	0.0447	1.75	208	220	0	0.44	876
14	9	11	0.0023	0.0839	0	4	510	600	1.03	0.02	11.4063
15	9	12	0.0023	0.0839	0	4	510	600	1.03	0.02	11.4063
16	10	11	0.0023	0.0839	0	4	510	600	1.02	0.02	11.4063
17	10	12	0.0023	0.0839	0	4	510	600	1.015	0.02	11.4063
18	11	13	0.0061	0.0476	0.0999	5	600	625	0	0.4	796.364
19	11	14	0.0054	0.0418	0.0879	5	600	625	0	0.39	796.364
20	12	13	0.0061	0.0476	0.0999	5	600	625	0	0.4	796.364
21	12	23	0.0124	0.0966	0.203	5	600	625	0	0.52	796.364
22	13	23	0.0111	0.0865	0.1818	5	600	625	0	0.49	796.364
23	14	16	0.005	0.0389	0.0818	5	600	625	0	0.38	796.364
24	15	16	0.0022	0.0173	0.0364	5	600	625	0	0.33	796.364
25	15	21	0.0063	0.049	0.103	5	600	625	0	0.41	796.364
26	15	21	0.0063	0.049	0.103	5	600	625	0	0.41	796.364
27	15	24	0.0067	0.0519	0.1091	5	600	625	0	0.41	796.364
28	16	17	0.0033	0.0259	0.0545	5	600	625	0	0.35	796.364
29	16	19	0.003	0.0231	0.0485	5	600	625	0	0.34	796.364
30	17	18	0.0018	0.0144	0.0303	5	600	625	0	0.32	796.364
31	17	22	0.0135	0.1053	0.2212	5	600	625	0	0.54	796.364
32	18	21	0.0033	0.0259	0.0545	5	600	625	0	0.35	796.364
33	18	21	0.0033	0.0259	0.0545	5	600	625	0	0.35	796.364
34	19	20	0.0051	0.0396	0.0833	5	600	625	0	0.38	796.364
35	19	20	0.0051	0.0396	0.0833	5	600	625	0	0.38	796.364
36	20	23	0.0028	0.0216	0.0455	5	600	625	0	0.34	796.364
37	20	23	0.0028	0.0216	0.0455	5	600	625	0	0.34	796.364
38	21	22	0.0087	0.0678	0.1424	5	600	625	0	0.45	796.364

Table A. 3 IEEE 24 Bus Generator Reliability Data [132]

Unit Group	Unit Size (MW)	Unit Type	Forced Outage Rate	MTTF (Hours)	MTTR (Hours)	Scheduled Maintenance
						Weeks per year
U12	12	Oil/Steam	0.02	2940	60	2
U20	20	Oil/CT	0.1	450	50	2
U50	50	Hydro	0.01	1980	20	2
U76	76	Coal/Steam	0.02	1960	40	3
U100	100	Oil/Steam	0.04	1200	50	3
U155	155	Coal/Steam	0.04	960	40	4
U197	197	Oil/Steam	0.05	950	50	4
U350	350	Coal/Steam	0.08	1150	100	5
U400	400	Nuclear	0.12	1100	150	6

P_D Load Real Power

Q_D Load Reactive Power

CON Continuous Rating in p.u

LTE Long-term Emergency Rating in MVA

STE Short -term Emergency Rating in MVA

Tr Transformer off-nominal tap ratio

Table A. 4 IEEE 24 Bus Generator Data at Each Bus [132]

Bus No	Unit Group	P_G (MW)	Q_G (MVAR)	$Q\_G\_^{max}$ (MVAR)	$Q\_G\_^{min}$ (MVAR)
1	U20	10	0	10	0
1	U20	10	0	10	0
1	U76	76	14.1	30	-25
1	U76	76	14.1	30	-25
2	U20	10	0	10	0
2	U20	10	0	10	0
2	U76	76	7	30	-25
2	U76	76	7	30	-25
7	U100	80	17.2	60	0
7	U100	80	17.2	60	0
7	U100	80	17.2	60	0
13	U197	95.1	40.7	80	0
13	U197	95.1	40.7	80	0
13	U197	95.1	40.7	80	0
15	U12	12	0	6	0
15	U12	12	0	6	0
15	U12	12	0	6	0
15	U12	12	0	6	0
15	U12	12	0	6	0
15	U155	155	0.05	80	-50
16	U155	155	25.22	80	-50
18	U400	400	137.4	200	-50
21	U400	400	108.2	200	-50
22	U50	50	-4.96	16	-10
22	U50	50	-4.96	16	-10
22	U50	50	-4.96	16	-10
22	U50	50	-4.96	16	-10
22	U50	50	-4.96	16	-10
22	U50	50	-4.96	16	-10
23	U155	155	31.79	80	-50
23	U155	155	31.79	80	-50
23	U350	350	71.78	150	-25

P_G Generating Unit's Real Power

Q_G Generating Unit's Reactive Power

$Q\_G\_^{max}$, $Q\_G\_^{min}$ Reactive Power Output Limits

Table A. 5 IEEE 24 Bus, Bus Load Data [132]

Bus Number	Bus Load	Load	
	% Of System Load	MW	Mvar
1	3.8	108	22
2	3.4	97	20
3	6.3	180	37
4	2.6	74	15
5	2.5	71	14
6	4.8	136	28
7	4.4	125	25
8	6	171	35
9	6.1	175	36
10	6.8	195	40
13	9.3	265	54
14	6.8	194	39
15	11.1	317	64
16	3.5	100	20
18	11.7	333	68
19	6.4	181	37
20	4.5	128	26
Total	100	2850	580

Table A. 6 IEEE 24 Bus Hourly Peak Load in Percentage of Daily Peak [132]

Hour	Winter Weeks		Summer Weeks		Spring/Fall Weeks	
	1 -8 & 44 - 52		18 -30		9-17 & 31 - 43	
	Weekday	Weekend	Weekday	Weekend	Weekday	Weekend
12-1 am	67	78	64	74	63	75
1-2am	63	72	60	70	62	73
2-3am	60	68	58	66	60	69
3-4am	59	66	56	65	58	66
4-5am	59	64	56	64	59	65
5-6am	60	65	58	62	65	65
6-7am	74	66	64	62	72	68
7-8am	86	70	76	66	85	74
8-9am	95	80	87	81	95	83
9-10am	96	88	95	86	99	89
10-11am	96	90	99	91	100	92
11-noon	95	91	100	93	99	94
noon-1pm	95	90	99	93	93	91
1-2pm	95	88	100	92	92	90
2-3pm	93	87	100	91	90	90
3-4pm	94	87	97	91	88	86
4-5pm	99	91	96	92	90	85
5-6pm	100	100	96	94	92	88
6-7pm	100	99	93	95	96	92
7-8pm	96	97	92	95	98	100
8-9pm	91	94	92	100	96	97
9-10pm	83	92	93	93	90	95
10-11pm	73	87	87	88	80	90
11-12pm	63	81	72	80	70	85

Appendix B: Matlab Codes

B.1 State Selection and State Probabilities Code

```
clear
clc
format long
Component_data=xlsread('myfileD.xlsx','sheet5','A2:B38');
%N=37 %component number
for J=1:1
    J;
        L=Component_data(:,1);
        U=Component_data(:,2);
    for T=1:1
        T;
        syms 's' 'l' 'u' 't' 'a'
        CompMat=[4*l -1*u -1*u -2*u;-2*l 2*l+1*u 0 0;-1*l -1*l
1*l+1*u -1*u;-1*l -1*l -1*l 3*u]
        diag_s=[s 0 0 0; 0 s 0 0; 0 0 s 0; 0 0 0 s];
        CompMat_2=diag_s+CompMat;
        D_CompMat_2=det(CompMat_2);
        F_D_CompMat_2 = factor(D_CompMat_2);
        P=inv(CompMat_2)*[1 0 0 0]'
        pretty(P)


        for i=1:4
            i;
             [n, d] = numden(P(i));
             F_n = factor(n);
            F_d=factor(d);
            syms s l u A B C D real
             T_deno=F_d';

            Final_P_3_S_L=ilaplace(P(i)) %finding inverse laplace of
each prop.
            pretty(Final_P_3_S_L) % to show


         end
     end
    ST_PR_4';
    ST_PR;
    PRO1=[ST_PR,ST_PR_4'];
    FOR_UP=PRO1(2)+PRO1(3)+PRO1(4)
    FOR_DETD=PRO1(2)+ PRO1(3)
    FOR_SMT=PRO1(2)
    U=rand
        if U>=PRO1(2)+PRO1(3)+PRO1(4)
```

```
                disp ('working state')
                elseif PRO1(2)+PRO1(3)<=U &&
U<PRO1(2)+PRO1(3)+PRO1(4)
                    disp ('failed')
                    elseif PRO1(2)<=U&&U<PRO1(2)+ PRO1(3)
                        disp ('derated')
                        elseif 0<=U&&U<PRO1(2)
                            disp ('intelligent')
        end


end
```

B.2 State Probabilities Code Solution

CompMat =

$$\begin{pmatrix} 4l & -u & -u & -2u \\ -2l & 2l+u & 0 & 0 \\ -l & -l & l+u & -u \\ -l & -l & -l & 3u \end{pmatrix}$$

P =

$$\begin{pmatrix} \frac{s^2+4su+ls+3u^2+2lu}{4l^2s+5ls^2+13lsu+s^3+\sigma_1+\sigma_2} \\ \frac{2\,(l^2s+2l^2u+ls^2+4lsu+3lu^2)}{8l^3s+14l^2s^2+30l^2su+7ls^3+26ls^2u+19lsu^2+s^4+5s^3u+7s^2u^2+3su^3} \\ \frac{ls+4lu}{2l^2s+3ls^2+7lsu+s^3+\sigma_1+\sigma_2} \\ \frac{l}{ls+3su+s^2} \end{pmatrix}$$

where

$$\sigma_1 = 4s^2u$$

$$\sigma_2 = 3su^2$$

```
/                                  2                        2
\
|                                 s  + 4 s u + l s + 3 u  + 2
l u                                 |
|                          ---------------------------------
--------                            |
|                             2           2                3
|
|                          4 l  s + 5 l s  + 13 l s u + s  +
#1 + #2                             |
```

```
|
|
|                                  2         2         2
2                                  |
|                               (l  s + 2 l  u + l s  + 4 l s u +
3 l u ) 2                                    |
| ------------------------------------------------------------
---------------------------------- |
|    3          2  2        2             3         2
2    4      3         2  2         3 |
| 8 l  s + 14 l  s  + 30 l  s u + 7 l s  + 26 l s  u + 19 l s
u  + s  + 5 s  u + 7 s  u  + 3 s u  |
|
|
|                                                 l s + 4 l u
|
|                                 ---------------------------------
--------                                 |
|                                    2          2              3
|
|                                 2 l  s + 3 l s  + 7 l s u + s  +
#1 + #2                                  |
|
|
|                                                       l
|
|                                              ----------------
|
|                                                             2
|
\                                              l s + 3 s u + s
/
```

where

$$\#1 == 4\,s^2\,u$$

$$\#2 == 3\,s\,u^2$$

Final_P_3_S_L =

$$\frac{3u^2+2lu}{(l+3u)(4l+u)} - \frac{e^{-t(4l+u)}(7lu-12l^2)}{(4l+u)\sigma_1} - \frac{lu\,e^{-t(l+3u)}}{(l+3u)\sigma_1}$$

where

$$\sigma_1 = 3l - 2u$$

```
      2                                                2
    3 u  + 2 l u       exp(-t (4 l + u)) (- 12 l  + u l 7)   l
u exp(-t (l + 3 u))
```

```
------------------ - ---------------------------------- - --
------------------
(l + 3 u) (4 l + u)                (4 l + u) #1
(l + 3 u) #1

where

   #1 == 3 l - 2 u
Final_P_3_S_L =
```

$$\frac{e^{-t\,(4l+u)}\,(7lu-12l^2)}{(4l+u)\,\sigma_1}-\frac{e^{-t\,(2l+u)}\,(3lu-2l^2)}{(l-2u)\,(2l+u)}+\frac{4l^2u+6lu^2}{(2l+u)\,(l+3u)\,(4l+u)}-\frac{2l^2u\,e^{-t\,(l+3u)}}{(l-2u)\,(l+3u)\,\sigma_1}$$

where

$$\sigma_1 = 3l-2u$$

```
                              2
2                           2           2
exp(-t (4 l + u)) (- 12 l  + u l 7)   exp(-t (2 l + u)) (- 2 l
+ u l 3)          4 l  u + 6 l u
---------------------------------- - ----------------------
---------- + ----------------------------
             (4 l + u) #1                       (l - 2 u) (2 l +
u)           (2 l + u) (l + 3 u) (4 l + u)

      2
     l  u exp(-t (l + 3 u)) 2
   - ------------------------
       (l - 2 u) (l + 3 u) #1

where

   #1 == 3 l - 2 u
Final_P_3_S_L =
```

$$\frac{e^{-t\,(2l+u)}\,(3lu-2l^2)}{(l-2u)\,(2l+u)}-\frac{e^{-t\,(l+3u)}\,(lu-l^2)}{(l-2u)\,(l+3u)}+\frac{4lu}{(2l+u)\,(l+3u)}$$

```
                                  2                              2
exp(-t (2 l + u)) (- 2 l  + u l 3)   exp(-t (l + 3 u)) (- l  +
u l)          4 l u
---------------------------------- - ------------------------
----- + -------------------
        (l - 2 u) (2 l + u)                (l - 2 u) (l + 3 u)
(2 l + u) (l + 3 u)
Final_P_3_S_L =
```

$$\frac{l}{l+3u}-\frac{l\,e^{-t\,(l+3u)}}{l+3u}$$

```
   l       l exp(-t (l + 3 u))
------- - -------------------

l + 3 u          l + 3 u
```

B.3 Newton-Raphson A/C power flow, Corrective Action and Wind Power Integration

```
clear
clc
tic
format short
T_ttt=[];


for ttt=1:100
    ttt;
    %intPV=intpv; %Calling hourly Intermittent penerationn.
    intWD=intwd; %Calling hourly Intermittent penerationn,Wind.
Component_data=probadata;
%xlsread('myfileD.xlsx','sheet28','A2:B71');
Bus_data1= otherbusinf;
%xlsread('myfileD.xlsx','sheet23','A2:B25');%Calling hourly bus load
data
d_a=[0.67 0.63 0.6 0.59 0.59 0.6 0.74 0.86 0.95 0.96 0.96 0.95 0.95
0.95 0.93 0.94 0.99 1 1 0.96 0.91 0.83 0.73 0.63];
 d_b=[0.78 0.72  0.68  0.66  0.64  0.65  0.66  0.7   0.8   0.88  0.9
     0.91  0.9   0.88  0.87  0.87  0.91  1     0.99  0.97  0.94  0.92
     0.87  0.81
];
  da1=[repmat(d_a,1,5),repmat(d_b,1,2)];%weekdays & weekend
(168hours)
  da2=repmat(da1,1,8);
d_c=[0.63  0.62  0.6   0.58  0.59  0.65  0.72  0.85  0.95  0.99  1
     0.99  0.93  0.92  0.9   0.88  0.9   0.92  0.96  0.98  0.96  0.9
     0.8   0.7];
d_d=[0.75  0.73  0.69  0.66  0.65  0.65  0.68  0.74  0.83  0.89  0.92
     0.94  0.91  0.9   0.9   0.86  0.85  0.88  0.92  1     0.97  0.95
     0.9   0.85];
  dd1= [repmat(d_c,1,5),repmat(d_d,1,2)];
  dd2=repmat(dd1,1,9);%wks9-17
  d_e=[0.64      0.6   0.58  0.56  0.56  0.58  0.64  0.76  0.87  0.95
     0.99  1     0.99  1     1     0.97  0.96  0.96  0.93  0.92  0.92
     0.93  0.87  0.72
];
de1=[0.74  0.7   0.66  0.65  0.64  0.62  0.62  0.66  0.81  0.86  0.91
     0.93  0.93  0.92  0.91  0.91  0.92  0.94  0.95  0.95  1     0.93
     0.88  0.8
];
de2= [repmat(d_e,1,5),repmat(de1,1,2)];%wks18
de3=repmat(de2,1,13);%wks18-30
df1=repmat(dd1,1,13);%wks31-43
dg1=repmat(da1,1,9);%wks44-52

 a3=[da2,dd2,de3,df1,dg1,d_a];
```

```
counter = 0;
counter_1 = 0;
counter_2= 0;
counter_3 = 0;
counter_4 = 1;
 counterV = 0;
 counterV1 = 0;
 counterV2 = 0;
 counterVLS=0;
 counterT = 0;
 T_dg3=[]; T_iter=[];
 T_dg=[];
 T_dg2=[];
 T_LS=[];
 T_Tap=[];
 T_ReLS=[];
T_Eld=[];
T_Re=[];
T_yes=[];
T_yesLS=[];
T_Re1=[];
T_LS1=[];
T_LS2=[];
   Tvals = 1:8760;%hourly iteration
a4vals =a3; %hourly load demand for (8760hours)
   wdPvals=intWD(:,1)'*1.425; %wind hourly Intermittent
peneration,active power, P  for (8760hours)
   wdQvals=intWD(:,2)'*0.29; %PV hourly Intermittent
peneration,active power, Q  for (8760hours)
for K=1 : length(Tvals)
        T = Tvals(K);
        a4= a4vals(K);
          wdP=wdPvals(K);
          wdQ=wdQvals(K);
     for J=1:70
           PROB=Component_data;

            U=rand;
                     if U>=PROB(J,2)+PROB(J,3)+PROB(J,4)
                            counter = counter + 1;
                             M_4=0;
                     elseif (PROB(J,2)+PROB(J,3)<=U) &&
(U<PROB(J,2)+PROB(J,3)+PROB(J,4))
                            counter_1 = counter_1 + 1;
                            C_4 = counter_4;
                            CC=counter_1;
                            Testdata= compntde;
%xlsread('myfileD.xlsx','sheet2','A2:E71');
```

```
                            Testdata(J,:)=zeros(1,10);% To identify
the failed component
                            %Bus_data3=Bus_data1.*a4vals(K);
                            %MMMM(1:70,(5*CC-4):5*CC)=Testdata
                            MMMMM(CC)=J; %failed Component
                            M_4(C_4)=J;
                            M_CC(CC)=T;   %time of failed Component
                        elseif (PROB(J,2)<=U)&&(U<PROB(J,2)+ PROB(J,3))
                            counter_2 = counter_2 + 1;
                            M_4=0;
                        elseif (0<=U)&&(U<PROB(J,2))
                            counter_3 = counter_3 + 1;
                            M_4=0;
                        end

            if (M_4 >=1)

                        Bus_data3=Bus_data1.*a4vals(K);
                        Bustok=Bus_data3;
                        HPD=sum(Bus_data3(:,1));
                        Line_INF=Testdata(33:end,:);
                        Line_INF(:,6:10)=[];
                        Bus_INF=Testdata(1:32,:);
                        Bus_INF2=Bus_INF(:,6:10);
                        Bus_INF1=[Bus_INF(:,1),Bus_INF2];
                       %Bus_INF1(~any(Bus_INF1,2),:) = [];
                         Bus_INF(:,6:10)=[];
                       % To get the Line data
                        %Line_data1=
xlsread('myfileD.xlsx','sheet24','A2:A39');
                        Line_data=otherlineinf;
%xlsread('myfileD.xlsx','sheet20','A2:B39');%Calling other Line data
                        Flinedata=[Line_INF,Line_data];
%Horizontally Concatenating the matrix
                        Flinedata(:,1)=1:38; %Replacing the column 1
with 1-38
    %Deleting any line that is not available
    indices = Flinedata(:,2)==0; %To check for any column with zeros
    Flinedata(indices,:) = [];          %To remove any row(s)with
zeros
    %T_Line = array2table(Flinedata, 'VariableNames', {'Line_No',
'From_Bus', 'To_Bus','R_pu', 'X_pu','B_pu','Xmer_Tap'});
    Line_No = Flinedata(:,1);
    From_Bus = Flinedata(:,2);
    To_Bus = Flinedata(:,3);
    R = Flinedata(:,4); %Resistance between buses (transmission
lines or power transformers)
    X = Flinedata(:,5); %Reactance between buses (transmission lines
or power transformers)
```

```
    B_TL = Flinedata(:,6);     %Susceptance of transmission lines
    a = Flinedata(:,7);          %Xmer_Tap
    ConR= Flinedata(:,8);
    Z = R + 1i*X;
    y = 1./Z; %%To calculate inverse of each element
    size(y);
    y_2 = 1i*B_TL;
    Bus_number = max(max(From_Bus),max(To_Bus)); %Maximum number of
buses
    Branch_num = length(From_Bus); %Number of Branches
    Y = zeros(Bus_number, Bus_number); %Creation of an empty
admittance matrix

            %Off-diagonal elements of the admittance matrix
formation
                for i=1:Branch_num

                    Y(From_Bus(i),To_Bus(i)) =
Y(From_Bus(i),To_Bus(i)) -y(i)/a(i);
                    Y(To_Bus(i),From_Bus(i)) =
Y(From_Bus(i),To_Bus(i));
                end

            %Diagonal elements of the admittance matrix formation


      for m=1:Bus_number
          for n=1:Branch_num
              if From_Bus(n)==m
                 Y(m,m) = Y(m,m) + y(n)/(a(n)^2) + y_2(n);
              elseif To_Bus(n)==m
                     Y(m,m) = Y(m,m) + y(n) + y_2(n);
             end
          end
      end

      Bus_data2=otherbusinf2;
%xlsread('myfileD.xlsx','sheet23','C2:E25');%Calling other hourly
bus data
      Bus_data=[Bus_data3,Bus_data2];
      % To get the total generation at each bus
      [U11,~,idx] = unique(Bus_INF(:,1 ));
      A1 = accumarray(idx,Bus_INF(:,2 ));
      B11 = accumarray(idx,Bus_INF(:,3 ));
      C_11 = accumarray(idx,Bus_INF(:,4 ));
      F_11 = accumarray(idx,Bus_INF(:,5 ));
      H=[U11,A1,B11,C_11,F_11];
      %Removing zero element rows in the matrix, if any
```

```
      H(~any(H,2),:) = []; %The 2 means to work across the second
dimension, which is across rows in MATLAB,
      %the first dimension is columns and is the default direction
for the majority of MATLAB operations.


      % Get size of A.
      [rows, columns] = size(H);
      % Extract just the first column.
      column1 = H(:, 1)';
      % Find out what numbers SHOULD be in the first column.
      allNumbers = H(1,1) : 1 : H(end, 1);
      % Initialize an output array.
      H_out = zeros(length(allNumbers), columns);
      % Assign existing numbers to the rows where they belong.
      H_out(column1,:) = H;
      %Vertically Concatenating the matrix
      bb=[24 0 0 0 0];
      y_1=[H_out;bb];
      y_1(:,1)=1:24; %Replacing the column 1 with 1-24
      y_1(14,:)=[14 0 13.7 200 -50 ];
      Fbusdata=[y_1,Bus_data];%Horizontally Concatenating the
matrix.
      %To make Slack bus first on the bus numbering.
      Fbrow1= Fbusdata(1,:);
      Fbusdata(1,:)=Fbusdata(13,:);
      Fbusdata(13,:)=Fbrow1;
      %T_Bus = array2table(Fbusdata, 'VariableNames', {'Bus', 'Pgi',
'QGi','Qmax', 'Qmin','Pdi', 'Qdi','Bus_Type','V_B','The_B'});
      %MMCC(CC)=T_Bus
      %h=varfun(@sum, T_Bus, 'GroupingVariables', 'Bus');

      BMva=100;
      mIter=100; %maximum iteration
      Bus_numbering1=Fbusdata(:,1);
      Bus_numbering2=Fbusdata(:,1);
      Bus_numbering=1:24;
      Bus_numbering=Bus_numbering';
      Bus_Type = Fbusdata(:,8);
      V_B = Fbusdata(:,9);
      The_B = Fbusdata(:,10);
      P_Ga = Fbusdata(:,2)/BMva;
      P_G2n=P_Ga(2:24)-(0.05*P_Ga(2:24));
      P_G=[P_Ga(1);P_G2n];
      P_G(3,1)=wdPvals(K);
      Q_G11 = Fbusdata(:,3)/BMva;
      Q_G2n=Q_G11(2:24)-(0.05*Q_G11(2:24));
      Q_G=[Q_G11(1);Q_G2n];
      Q_G(3,1)=wdQvals(K);
```

```
      Q_G1 =Q_G;%Fbusdata(:,3)/BMva;
      Q_max = Fbusdata(:,4)/BMva;      % Minimum Reactive Power
Limit..
      Q_min = Fbusdata(:,5)/BMva;     % Maximum Reactive Power
Limit..
      P_D = Fbusdata(:,6)/BMva;
      P_D1 = Fbusdata(:,6)/BMva;
      Q_D = Fbusdata(:,7)/BMva;
      Q_D1 = Fbusdata(:,7)/BMva;
      Qsht=Fbusdata(:,11)/BMva;       % Injected Shunt Compensation
      P_inj=P_G-P_D;                 %Specified Power injections
      Q_inj=Q_G-Q_D+Qsht;          %Specified Power injections
      %1 = Slack BUS; 2 = PV BUS; 3 = PQ BUS
      pv = find(Bus_Type == 2);% PV Buses..
      pq = find(Bus_Type == 3);%PQ Buses..
      n_pv = length(pv);       % No. of PV buses..
      n_pq = length(pq);       % No. of PQ buses..
      G = real(Y);              %Conductance of the admittance
matrix.
      B = imag(Y);              %Susceptance of the admittance
matrix.


 Tol = 1;
Iter = 1;
 while (Tol > 0.000001)  %Start Iteration
        P = zeros(Bus_number,1);
        Q = zeros(Bus_number,1);
        %Calculate P and Q
            for i = 1:Bus_number
                for k = 1:Bus_number
                    P(i) = P(i) + V_B(i)*
V_B(k)*(G(i,k)*cos(The_B(i)-The_B(k)) + B(i,k)*sin(The_B(i)-
The_B(k)));
                    Q(i) = Q(i) + V_B(i)*
V_B(k)*(G(i,k)*sin(The_B(i)-The_B(k)) - B(i,k)*cos(The_B(i)-
The_B(k)));
                end
            end


     if Iter <= 7 && Iter > 2    % Only checked up to 7th
iterations..
        for n = 2:Bus_number
            if Bus_Type(n) == 2
                QG = Q(n)+Q_D(n);
                if QG < Q_min(n)
                    V_B(n) = V_B(n) + 0.01;
                elseif QG > Q_max(n)
```

```
                    V_B(n) = V_B(n) - 0.01;
                end
            end
        end
    end
    delta_P = P_inj-P;          %Calculate change using specified
values
    delta_Q = Q_inj-Q;
    k = 1;
     dQ = zeros(n_pq,1);
            for i = 1:Bus_number
                if Bus_Type(i) == 3
                    dQ(k,1) = delta_Q(i);
                    k = k+1;
                end
            end
            k = 1;
    dbus = zeros(n_pq,1);
    for i = 1:Bus_number
        if Bus_Type(i) == 3
            dbus(k,1) = Bus_numbering(i);
            k = k+1;
        end
    end
            dP = delta_P(2:Bus_number);
            M_Vctr = [dP; dQ];                  %Mismatch Vector

            dPn = delta_P(1:Bus_number);
            dQbus=[dQ,dbus];
             dPbus=Bus_numbering(1:Bus_number);
             DPbus=[dPn,dPbus];
             M_Vctrdg = [DPbus; dQbus];

                    %Jacobian Matrix formation
        %Jacobian matrix formation
             %J1 - Derivative of Real Power Injections with angles
    J1 = zeros(Bus_number-1,Bus_number-1);
            for i = 1:(Bus_number-1)
                m = i+1;
                for k = 1:(Bus_number-1)
                    n = k+1;
                    if n == m
                        for n = 1:Bus_number
                            J1(i,k) = J1(i,k) + V_B(m)* V_B(n)*(-
G(m,n)*sin(The_B(m)-The_B(n)) + B(m,n)*cos(The_B(m)-The_B(n)));
                        end
                        J1(i,k) = J1(i,k) - V_B(m)^2*B(m,m);
                        else
```

```
                J1(i,k) = V_B(m)* V_B(n)*(G(m,n)*sin(The_B(m)-
The_B(n)) - B(m,n)*cos(The_B(m)-The_B(n)));
                    end
                end
            end
        % J2 - Derivative of Real Power Injections with Voltage
    J2 = zeros(Bus_number-1,n_pq);
    for i = 1:(Bus_number-1)
        m = i+1;
        for k = 1:n_pq
            n = pq(k);
            if n == m
                for n = 1:Bus_number
                    J2(i,k) = J2(i,k) + V_B(n)*(G(m,n)*cos(The_B(m)-
The_B(n)) + B(m,n)*sin(The_B(m)-The_B(n)));
                end
                J2(i,k) = J2(i,k) + V_B(m)*G(m,m);
            else
                J2(i,k) = V_B(m)*(G(m,n)*cos(The_B(m)-The_B(n)) +
B(m,n)*sin(The_B(m)-The_B(n)));
            end
        end
    end

    % J3 - Derivative of Reactive Power Injections with Angles
    J3 = zeros(n_pq,Bus_number-1);
    for i = 1:n_pq
        m = pq(i);
        for k = 1:(Bus_number-1)
            n = k+1;
            if n == m
                for n = 1:Bus_number
                    J3(i,k) = J3(i,k) + V_B(m)*
V_B(n)*(G(m,n)*cos(The_B(m)-The_B(n)) + B(m,n)*sin(The_B(m)-
The_B(n)));
                end
                J3(i,k) = J3(i,k) - V_B(m)^2*G(m,m);
            else
                J3(i,k) = V_B(m)* V_B(n)*(-G(m,n)*cos(The_B(m)-
The_B(n)) - B(m,n)*sin(The_B(m)-The_B(n)));
            end
        end
    end

    % J4 - Derivative of Reactive Power Injections with Voltage
    J4 = zeros(n_pq,n_pq);
    for i = 1:n_pq
        m = pq(i);
        for k = 1:n_pq
```

```
            n = pq(k);
            if n == m
                for n = 1:Bus_number
                    J4(i,k) = J4(i,k) + V_B(n)*(G(m,n)*sin(The_B(m)-
The_B(n)) - B(m,n)*cos(The_B(m)-The_B(n)));
                end
                J4(i,k) = J4(i,k) - V_B(m)*B(m,m);
            else
                J4(i,k) = V_B(m)*(G(m,n)*sin(The_B(m)-The_B(n)) -
B(m,n)*cos(The_B(m)-The_B(n)));
            end
        end
    end

        J_M = [J1 J2; J3 J4];                %Jacobian Matrix

         C_Vctr = inv(J_M)*M_Vctr;               %Correction Vector

        dThe = C_Vctr(1:Bus_number-1);                %Change in
Voltage Angle
         dV = C_Vctr(Bus_number:end);                  %Change in
Voltage Magnitude

            %Updating State Vectors

    The_B(2:Bus_number) = dThe + The_B(2:Bus_number);
%Voltage Angle
    The_B_deg = rad2deg(The_B(2:Bus_number));

    k = 1;
            for i = 2:Bus_number
                if Bus_Type(i) == 3
                    V_B(i) = dV(k) + V_B(i);
%Voltage Magnitude
                    k = k+1;
                end
            end

       Iter = Iter + 1;
%        flagdg2 = Iter + 1;
%        flagdg3=flagdg2+1
       Tol = max(abs(M_Vctr));
       if Iter>mIter
        break
       end
 end
 T_iter =[T_iter; T Iter];
 if Iter<mIter
     Vtap=V_B;
```

```
     for k=1:Bus_number
      V_B(k);
      if V_B(k)<0.95  || V_B(k)>1.05
         V_MT(k)=1;
      else
        V_MT(k)=0;

      end
     end
      V_MT;
    sV_MT=sum(V_MT);
 elseif Iter>=mIter
     for dd= 0.05:0.05:1
     M_Vctrdg(1,:)=[];
     MLSmx=max(M_Vctrdg(:,1));
     [rw,col]= find(M_Vctrdg==MLSmx);
     busid=M_Vctrdg(rw,2);
     CorL=Fbusdata(busid,6)*dd;
     Pln=P_D1(busid,1)-CorL/BMva;
     P_D1(busid,1)=Pln;
     Iterdg=1;
     Toldg=1;

 while (Toldg > 0.000001)   % Iteration starting..

    Pdg = zeros(Bus_number,1);
    Qdg = zeros(Bus_number,1);
    % Calculate P and Q
    for i = 1:Bus_number
        for k = 1:Bus_number
            Pdg(i) = Pdg(i) + V_B(i)* V_B(k)*(G(i,k)*cos(The_B(i)-
The_B(k)) + B(i,k)*sin(The_B(i)-The_B(k)));
            Qdg(i) = Qdg(i) + V_B(i)* V_B(k)*(G(i,k)*sin(The_B(i)-
The_B(k)) - B(i,k)*cos(The_B(i)-The_B(k)));
        end
    end


    % Checking Q-limit violations..
    if Iter <= 7 && Iter > 2    % Only checked up to 7th
iterations..
        for n = 2:Bus_number
            if Bus_Type(n) == 2
                QG = Qdg(n)+Q_D(n);
                if QG < Q_min(n)
                    V_B(n) = V_B(n) + 0.01;
                elseif QG > Q_max(n)
                    V_B(n) = V_B(n) - 0.01;
                end
```

```
            end
         end
    end

    % Calculate change from specified value
    Pspdg = P_G - P_D1;                % Pi = PGi - PLi..
    Qspdg = Q_G - Q_D+Qsht;                % Qi = QGi - QLi..
    dPadg = Pspdg-Pdg;
    dQadg = Qspdg-Qdg;

    k = 1;
    dQdg = zeros(n_pq,1);
    for i = 1:Bus_number
        if Bus_Type(i) == 3
            dQdg(k,1) = dQadg(i);
            k = k+1;
        end
    end
     k = 1;

    dbus = zeros(n_pq,1);
    for i = 1:Bus_number
        if Bus_Type(i) == 3
            dbus(k,1) = Bus_numbering(i);
            k = k+1;
        end
    end
    dPdg = dPadg(2:Bus_number);
    Mdg = [dPdg; dQdg];       % Mismatch Vector


    % Jacobian
    % J1 - Derivative of Real Power Injections with Angles..
    J1 = zeros(Bus_number-1,Bus_number-1);
    for i = 1:(Bus_number-1)
        m = i+1;
        for k = 1:(Bus_number-1)
            n = k+1;
            if n == m
                for n = 1:Bus_number
                    J1(i,k) = J1(i,k) + V_B(m)* V_B(n)*(-
G(m,n)*sin(The_B(m)-The_B(n)) + B(m,n)*cos(The_B(m)-The_B(n)));
                end
                J1(i,k) = J1(i,k) - V_B(m)^2*B(m,m);
            else
                J1(i,k) = V_B(m)* V_B(n)*(G(m,n)*sin(The_B(m)-
The_B(n)) - B(m,n)*cos(The_B(m)-The_B(n)));
            end
        end
```

```
    end

    % J2 - Derivative of Real Power Injections with V..
    J2 = zeros(Bus_number-1,n_pq);
    for i = 1:(Bus_number-1)
        m = i+1;
        for k = 1:n_pq
            n = pq(k);
            if n == m
                for n = 1:Bus_number
                    J2(i,k) = J2(i,k) + V_B(n)*(G(m,n)*cos(The_B(m)-
The_B(n)) + B(m,n)*sin(The_B(m)-The_B(n)));
                end
                J2(i,k) = J2(i,k) + V_B(m)*G(m,m);
            else
                J2(i,k) = V_B(m)*(G(m,n)*cos(The_B(m)-The_B(n)) +
B(m,n)*sin(The_B(m)-The_B(n)));
            end
        end
    end

    % J3 - Derivative of Reactive Power Injections with Angles..
    J3 = zeros(n_pq,Bus_number-1);
    for i = 1:n_pq
        m = pq(i);
        for k = 1:(Bus_number-1)
            n = k+1;
            if n == m
                for n = 1:Bus_number
                    J3(i,k) = J3(i,k) + V_B(m)*
V_B(n)*(G(m,n)*cos(The_B(m)-The_B(n)) + B(m,n)*sin(The_B(m)-
The_B(n)));
                end
                J3(i,k) = J3(i,k) - V_B(m)^2*G(m,m);
            else
                J3(i,k) = V_B(m)* V_B(n)*(-G(m,n)*cos(The_B(m)-
The_B(n)) - B(m,n)*sin(The_B(m)-The_B(n)));
            end
        end
    end

    % J4 - Derivative of Reactive Power Injections with V..
    J4 = zeros(n_pq,n_pq);
    for i = 1:n_pq
        m = pq(i);
        for k = 1:n_pq
            n = pq(k);
            if n == m
                for n = 1:Bus_number
```

```
                    J4(i,k) = J4(i,k) + V_B(n)*(G(m,n)*sin(The_B(m)-
The_B(n)) - B(m,n)*cos(The_B(m)-The_B(n)));
                end
                J4(i,k) = J4(i,k) - V_B(m)*B(m,m);
            else
                J4(i,k) = V_B(m)*(G(m,n)*sin(The_B(m)-The_B(n)) -
B(m,n)*cos(The_B(m)-The_B(n)));
            end
        end
    end

    JAC = [J1 J2; J3 J4];     % Jacobian Matrix..

    Xdg = inv(JAC)*Mdg;           % Correction Vector
    dThdg = Xdg(1:Bus_number-1);      % Change in Voltage Angle..
    dVdg = Xdg(Bus_number:end);       % Change in Voltage
Magnitude..

    % Updating State Vectors..
    The_B(2:Bus_number) = dThdg + The_B(2:Bus_number);    % Voltage
Angle..
    k = 1;
    for i = 2:Bus_number
        if Bus_Type(i) == 3
            V_B(i) = dVdg(k) + V_B(i);        % Voltage Magnitude..
            k = k+1;
        end
    end

    Iterdg = Iterdg + 1;
    flagdg=Iterdg;
    flagdg2=flagdg+1;
    Toldg = max(abs(Mdg));                  % Tolerance..
    if Iterdg>mIter
        break
    end

 end
   if flagdg<=mIter
        break
    end
    end
     Vtap=V_B;
     for k=1:Bus_number
      V_B(k);
      if V_B(k)<0.95  || V_B(k)>1.05
         V_MT(k)=1;
      else
        V_MT(k)=0;
```

```
      end
     end
      V_MT;
    sV_MT=sum(V_MT);
 elseif flagdg2>mIter
     Iterdg2=1;
     Toldg2=1;
 while (Toldg2 > 0.000001)   % Iteration starting..

    Pdg = zeros(Bus_number,1);
    Qdg = zeros(Bus_number,1);
    % Calculate P and Q
    for i = 1:Bus_number
        for k = 1:Bus_number
            Pdg(i) = Pdg(i) + V_B(i)* V_B(k)*(G(i,k)*cos(The_B(i)-
The_B(k)) + B(i,k)*sin(The_B(i)-The_B(k)));
            Qdg(i) = Qdg(i) + V_B(i)* V_B(k)*(G(i,k)*sin(The_B(i)-
The_B(k)) - B(i,k)*cos(The_B(i)-The_B(k)));
        end
    end


    % Checking Q-limit violations..
    if Iter <= 7 && Iter > 2    % Only checked up to 7th
iterations..
        for n = 2:Bus_number
            if Bus_Type(n) == 2
                QG = Qdg(n)+Q_D(n);
                if QG < Q_min(n)
                    V_B(n) = V_B(n) + 0.01;
                elseif QG > Q_max(n)
                    V_B(n) = V_B(n) - 0.01;
                end
            end
         end
    end

    % Calculate change from specified value
    Pspdg2 = P_G - (P_D*0.5);                % Pi = PGi - PLi..
    Qspdg2 = Q_G - Q_D+Qsht;                % Qi = QGi - QLi..
    dPadg = Pspdg2-Pdg;
    dQadg = Qspdg2-Qdg;

    k = 1;
    dQdg = zeros(n_pq,1);
    for i = 1:Bus_number
        if Bus_Type(i) == 3
            dQdg(k,1) = dQadg(i);
```

```
            k = k+1;
        end
    end
     k = 1;
    dbus = zeros(n_pq,1);
    for i = 1:Bus_number
        if Bus_Type(i) == 3
            dbus(k,1) = Bus_numbering(i);
            k = k+1;
        end
    end
    dPdg = dPadg(2:Bus_number);
    Mdg1 = [dPdg; dQdg];       % Mismatch Vector


    % Jacobian
    % J1 - Derivative of Real Power Injections with Angles..
    J1 = zeros(Bus_number-1,Bus_number-1);
    for i = 1:(Bus_number-1)
        m = i+1;
        for k = 1:(Bus_number-1)
            n = k+1;
            if n == m
                for n = 1:Bus_number
                    J1(i,k) = J1(i,k) + V_B(m)* V_B(n)*(-
G(m,n)*sin(The_B(m)-The_B(n)) + B(m,n)*cos(The_B(m)-The_B(n)));
                end
                J1(i,k) = J1(i,k) - V_B(m)^2*B(m,m);
            else
                J1(i,k) = V_B(m)* V_B(n)*(G(m,n)*sin(The_B(m)-
The_B(n)) - B(m,n)*cos(The_B(m)-The_B(n)));
            end
        end
    end

    % J2 - Derivative of Real Power Injections with V..
    J2 = zeros(Bus_number-1,n_pq);
    for i = 1:(Bus_number-1)
        m = i+1;
        for k = 1:n_pq
            n = pq(k);
            if n == m
                for n = 1:Bus_number
                    J2(i,k) = J2(i,k) + V_B(n)*(G(m,n)*cos(The_B(m)-
The_B(n)) + B(m,n)*sin(The_B(m)-The_B(n)));
                end
                J2(i,k) = J2(i,k) + V_B(m)*G(m,m);
            else
```

```
                J2(i,k) = V_B(m)*(G(m,n)*cos(The_B(m)-The_B(n)) +
B(m,n)*sin(The_B(m)-The_B(n)));
            end
        end
    end

    % J3 - Derivative of Reactive Power Injections with Angles..
    J3 = zeros(n_pq,Bus_number-1);
    for i = 1:n_pq
        m = pq(i);
        for k = 1:(Bus_number-1)
            n = k+1;
            if n == m
                for n = 1:Bus_number
                    J3(i,k) = J3(i,k) + V_B(m)*
V_B(n)*(G(m,n)*cos(The_B(m)-The_B(n)) + B(m,n)*sin(The_B(m)-
The_B(n)));
                end
                J3(i,k) = J3(i,k) - V_B(m)^2*G(m,m);
            else
                J3(i,k) = V_B(m)* V_B(n)*(-G(m,n)*cos(The_B(m)-
The_B(n)) - B(m,n)*sin(The_B(m)-The_B(n)));
            end
        end
    end

    % J4 - Derivative of Reactive Power Injections with V..
    J4 = zeros(n_pq,n_pq);
    for i = 1:n_pq
        m = pq(i);
        for k = 1:n_pq
            n = pq(k);
            if n == m
                for n = 1:Bus_number
                    J4(i,k) = J4(i,k) + V_B(n)*(G(m,n)*sin(The_B(m)-
The_B(n)) - B(m,n)*cos(The_B(m)-The_B(n)));
                end
                J4(i,k) = J4(i,k) - V_B(m)*B(m,m);
            else
                J4(i,k) = V_B(m)*(G(m,n)*sin(The_B(m)-The_B(n)) -
B(m,n)*cos(The_B(m)-The_B(n)));
            end
        end
    end

    Jac2 = [J1 J2; J3 J4];     % Jacobian Matrix..

    Xdg = inv(Jac2)*Mdg1;           % Correction Vector
    dThdg = Xdg(1:Bus_number-1);      % Change in Voltage Angle..
```

```
    dVdg = Xdg(Bus_number:end);       % Change in Voltage
Magnitude..

    % Updating State Vectors..
    The_B(2:Bus_number) = dThdg + The_B(2:Bus_number);    % Voltage
Angle..
    k = 1;
    for i = 2:Bus_number
        if Bus_Type(i) == 3
            V_B(i) = dVdg(k) + V_B(i);        % Voltage Magnitude..
            k = k+1;
        end
    end

    Iterdg2 = Iterdg2 + 1;
    flagdg3 = Iterdg2 + 2;
    Toldg2 = max(abs(Mdg1));                  % Tolerance..
    if Iterdg2>mIter
        break
    end

 end
       Vtap=V_B;
     for k=1:Bus_number
      V_B(k);
      if V_B(k)<0.95  || V_B(k)>1.05
         V_MT(k)=1;
      else
        V_MT(k)=0;

      end
     end
      V_MT;
    sV_MT=sum(V_MT);
 elseif flagdg3>mIter
        sV_MT=-1
        sPldg=HPD
        T_dg =[T_dg; T J sPldg];
 end
  if sV_MT > 0
     counterT = counterT + 1;
     T_Tap=[T_Tap; T J sV_MT];
     Bus_Type;
        Bus_Type(24,1)= 2;
        type1=Bus_Type';
        %LTCVM is the Target volatge magnitude at LTC bus
  R_LTCVM = 0.95 + (1.015-0.95).*rand(10,1); % random number between
0.95 and 1.015 to determine LTCVM.
  rLTCVM=sum(R_LTCVM)/10;
```

```
  NLTC=1;
  LTCsend(1) = 24; LTCrec(1) = 3;
  Tap(1) = 1.015 ; TapHi(1) = 1.05 ; TapLo(1) = 0.5 ; Bus(1) = 24 ;
LTCVM(1) = rLTCVM ;
    if ((type1(LTCsend(1)) == 2) && (Bus(1) == LTCsend(1)))
    V_B(LTCsend(1)) = LTCVM(1);
    %Tap(1) = Tap(1) + (X(2*LTCsend(1))*Tap(1));
    elseif ( (type1(LTCrec(1)) == 3) & (Bus(1) == LTCrec(1)) )
         Tap(1) = Tap(1) + X(2*LTCrec(1))*Tap(1);
            V_B(LTCrec(1)) = LTCVM(1);
    end
    V_Btap1=V_B;
      Bus_Type=type1';
      Bus_TypeT=Bus_Type;
      TolT = 1;
      IterT = 1;
 while (TolT > 0.000001)  %Start Iteration
       P = zeros(Bus_number,1);
       Q = zeros(Bus_number,1);
       %Calculate P and Q
           for i = 1:Bus_number
               for k = 1:Bus_number
                   P(i) = P(i) + V_B(i)*
V_B(k)*(G(i,k)*cos(The_B(i)-The_B(k)) + B(i,k)*sin(The_B(i)-
The_B(k)));
                   Q(i) = Q(i) + V_B(i)*
V_B(k)*(G(i,k)*sin(The_B(i)-The_B(k)) - B(i,k)*cos(The_B(i)-
The_B(k)));
               end
           end


     if Iter <= 7 && Iter > 2    % Only checked up to 7th
iterations..
        for n = 2:Bus_number
           if Bus_Type(n) == 2
               QG = Q(n)+Q_D(n);
               if QG < Q_min(n)
                   V_B(n) = V_B(n) + 0.01;
               elseif QG > Q_max(n)
                   V_B(n) = V_B(n) - 0.01;
               end
           end
         end
    end
    delta_P = P_inj-P;          %Calculate change using specified
values
    delta_Q = Q_inj-Q;
    k = 1;
```

```
     dQ = zeros(n_pq,1);
            for i = 1:Bus_number
                if Bus_Type(i) == 3
                    dQ(k,1) = delta_Q(i);
                    k = k+1;
                end
            end
            dP = delta_P(2:Bus_number);
            M_Vctr = [dP; dQ];                  %Mismatch Vector

                    %Jacobian Matrix formation
        %Jacobian matrix formation
             %J1 - Derivative of Real Power Injections with angles
    J1 = zeros(Bus_number-1,Bus_number-1);
            for i = 1:(Bus_number-1)
                m = i+1;
                for k = 1:(Bus_number-1)
                    n = k+1;
                    if n == m
                        for n = 1:Bus_number
                            J1(i,k) = J1(i,k) + V_B(m)* V_B(n)*(-
G(m,n)*sin(The_B(m)-The_B(n)) + B(m,n)*cos(The_B(m)-The_B(n)));
                        end
                        J1(i,k) = J1(i,k) - V_B(m)^2*B(m,m);
                    else
                       J1(i,k) = V_B(m)*
V_B(n)*(G(m,n)*sin(The_B(m)-The_B(n)) - B(m,n)*cos(The_B(m)-
The_B(n)));
                    end
                end
            end
        % J2 - Derivative of Real Power Injections with Voltage
    J2 = zeros(Bus_number-1,n_pq);
    for i = 1:(Bus_number-1)
        m = i+1;
        for k = 1:n_pq
            n = pq(k);
            if n == m
                for n = 1:Bus_number
                    J2(i,k) = J2(i,k) + V_B(n)*(G(m,n)*cos(The_B(m)-
The_B(n)) + B(m,n)*sin(The_B(m)-The_B(n)));
                end
                J2(i,k) = J2(i,k) + V_B(m)*G(m,m);
            else
                J2(i,k) = V_B(m)*(G(m,n)*cos(The_B(m)-The_B(n)) +
B(m,n)*sin(The_B(m)-The_B(n)));
            end
        end
    end
```

```
    % J3 - Derivative of Reactive Power Injections with Angles
    J3 = zeros(n_pq,Bus_number-1);
    for i = 1:n_pq
        m = pq(i);
        for k = 1:(Bus_number-1)
            n = k+1;
            if n == m
                for n = 1:Bus_number
                    J3(i,k) = J3(i,k) + V_B(m)*
V_B(n)*(G(m,n)*cos(The_B(m)-The_B(n)) + B(m,n)*sin(The_B(m)-
The_B(n)));
                end
                J3(i,k) = J3(i,k) - V_B(m)^2*G(m,m);
            else
                J3(i,k) = V_B(m)* V_B(n)*(-G(m,n)*cos(The_B(m)-
The_B(n)) - B(m,n)*sin(The_B(m)-The_B(n)));
            end
        end
    end

    % J4 - Derivative of Reactive Power Injections with Voltage
    J4 = zeros(n_pq,n_pq);
    for i = 1:n_pq
        m = pq(i);
        for k = 1:n_pq
            n = pq(k);
            if n == m
                for n = 1:Bus_number
                    J4(i,k) = J4(i,k) + V_B(n)*(G(m,n)*sin(The_B(m)-
The_B(n)) - B(m,n)*cos(The_B(m)-The_B(n)));
                end
                J4(i,k) = J4(i,k) - V_B(m)*B(m,m);
            else
                J4(i,k) = V_B(m)*(G(m,n)*sin(The_B(m)-The_B(n)) -
B(m,n)*cos(The_B(m)-The_B(n)));
            end
        end
    end

        J_M1 = [J1 J2; J3 J4];                %Jacobian Matrix

         C_Vctr = inv(J_M1)*M_Vctr;               %Correction Vector

         dThe = C_Vctr(1:Bus_number-1);                %Change in
Voltage Angle
         dV = C_Vctr(Bus_number:end);                  %Change in
Voltage Magnitude
```

```
            %Updating State Vectors

    The_B(2:Bus_number) = dThe + The_B(2:Bus_number);
%Voltage Angle
    The_B_deg = rad2deg(The_B(2:Bus_number));

    k = 1;
            for i = 2:Bus_number
                if Bus_Type(i) == 3
                    V_B(i) = dV(k) + V_B(i);
%Voltage Magnitude
                    k = k+1;
                end
            end

       IterT = IterT + 1;
       TolT = max(abs(M_Vctr));
       if IterT>100
        break
       end


 end
V_Btap=V_B;


%lineflow deviations


V_B_re = V_B.*cos(The_B) + 1i*V_B.*sin(The_B);        %Converting
Polar to Rectangular(Bus Voltages).
  The_B_Degr = 180/pi*The_B;                           %Bus Voltage
Angles in Degree.

Iij = zeros(Bus_number,Bus_number);
%Initializing Matrices.
Sij = zeros(Bus_number,Bus_number);
%Lloss = zeros(Branch_num,1);
Sinjt = zeros(Bus_number,1);


                    %Line Current Flows.
for m = 1:Branch_num
    p = From_Bus(m); q = To_Bus(m);
    Iij(p,q) = -(V_B_re(p) - V_B_re(q))*Y(p,q);           %Y(m,n) =
-y(m,n).
    Iij(q,p) = -Iij(p,q);
end
   %Iij = sparse(Iij);     % Commented out..
   Iijm = abs(Iij);
```

```
   Iija = angle(Iij);
                    %Line Power Flows.
    for m = 1:Bus_number
        for n = 1:Bus_number
            if m ~= n
            Sij(m,n) = V_B_re(m)*conj(Iij(m,n))*BMva;
            end
        end
    end
%Sij = sparse(Sij);     % Commented out..
[theta, rho] = cart2pol(real(Sij), imag(Sij));
rhoij=rho;
thetaij=theta;
T_1=[];
 for m = 1:Branch_num
      p = From_Bus(m);
      q = To_Bus(m);
      rhoij(p,q);
      thetaij(p,q);
      rhoij(q,p);
      thetaij(q,p);
       T_1 = [T_1; p q rhoij(p,q)];

 end
  T_1;


%          %%%%Thermal limit Violation........
T2=[T_1,ConR];  %Horizontally Concatenating line matrix with
Continuos rating to check themal limit of the line
 T_LP=[];
  for j=1:size(T2,1)
         p1 = T2(j,3);
         q1= T2(j,4);
         if p1>q1
             V_M2=p1;
          else
             V_M2=0;
         end
       T_LP=[T_LP;T2(j,1),T2(j,2),p1,q1];
   end
V_M2;
 for k=1:Bus_number
      V_B(k);
      if V_B(k)<0.95  || V_B(k)>1.05
         V_M(k)=1;
      else
        V_M(k)=0;
```

```
      end
 end
V_M;
sTL=sum(V_M2);
sVL=sum(V_M);
V_M1=sTL+sVL;


       if  V_M1 > 0
           disp ('yes')
            V_M3=V_M1;
            counterV = counterV + 1;
            V_MC=counterV; % To get number of component for Load
Curtailments
            T_yes =[T_yes; T J V_M3 sTL sVL];
           Bus_INF11=Bus_INF1;
           Bus_INF11(~any(Bus_INF11,2),:) = [];
           DEld=HPD;
           b_Eld=Bus_INF11(:,5);
           c_Eld=Bus_INF11(:,4);
           Pl=Bus_INF11(:,3);
           Ph=Bus_INF11(:,2);
           dP_Eld=DEld;
           x_Eld=max(b_Eld); % assume lambda
           iter_eld=0;
           while abs(dP_Eld)>0.001
               PEld=(x_Eld-b_Eld)./c_Eld/2;
               PEld=min(PEld,Ph);
               PEld=max(PEld,Pl);
               sPEld=sum(PEld);
               dP_Eld=DEld-sum(PEld);
               x_Eld=x_Eld+dP_Eld*2/(sum(1./c_Eld));
               iter_eld=iter_eld+1;
           end
           PEld; sP=sum(PEld); PEld=PEld/BMva;
           Unum=Bus_INF(:,1);
           Unum(~any(Unum,2),:) = [];
           PEld_U=[Unum,PEld];
           [U22,~,idx] = unique(PEld_U(:,1 ));
           A22 = accumarray(idx,PEld_U(:,2 ));
           PEld_UH=[U22,A22];
           HB=[U22,A22];
           [rows1, columns1] = size(PEld_UH);
           column11 = PEld_UH(:, 1)';
           allNumbers1 = PEld_UH(1,1) : 1 : PEld_UH(end, 1);
           PEld_out = zeros(length(allNumbers1), columns1);
           PEld_out(column11,:) = PEld_UH;
            yy1=[24 0];
            PEld_out=[PEld_out;yy1];
```

```
            PEld_out(:,1)=1:24;
            P_G=PEld_out(:,2);

       %end
            PGN=PEld_out(:,2);
            %V_B = Fbusdata(:,9);
            %The_B = Fbusdata(:,10);
           %P_D = Fbusdata(:,6)/BMva;
           Bus_Type(24,1)= 3;
             Psp=PGN-P_D;              %Specified Power injections
            Qsp=Q_G1-Q_D+Qsht;             %Specified Power
injections
           Tolld = 1;
           Iterld = 1;

         %while (V_M11~=0 )%|| Iter2 <= 20)


           while (Tolld > 0.000001)  %Start Iteration
               P1 = zeros(Bus_number,1);
               Q1 = zeros(Bus_number,1);
               %Calculate P and Q
               for i = 1:Bus_number
                   for k = 1:Bus_number
                       P1(i) = P1(i) + V_B(i)*
V_B(k)*(G(i,k)*cos(The_B(i)-The_B(k)) + B(i,k)*sin(The_B(i)-
The_B(k)));
                       Q1(i) = Q1(i) + V_B(i)*
V_B(k)*(G(i,k)*sin(The_B(i)-The_B(k)) - B(i,k)*cos(The_B(i)-
The_B(k)));
                   end
               end


               if Iter <= 7 && Iter > 2    % Only checked up to 7th
iterations..
                   for n = 2:Bus_number
                       if Bus_Type(n) == 2
                           QG = Q1(n)+Q_D(n);
                           if QG < Q_min(n)
                               V_B(n) = V_B(n) + 0.01;
                           elseif QG > Q_max(n)
                               V_B(n) = V_B(n) - 0.01;
                           end
                       end
                   end
               end
%                Psp=PGN-P_D;                   %Specified Power
injections
```

```
%                 Qsp=Q_G1-Q_D+Qsht;              %Specified Power
injections

                delta_P1 = Psp-P1;          %Calculate change using
specified values
                delta_Q1 = Qsp-Q1;
                k = 1;
                dQ = zeros(n_pq,1);
                for i = 1:Bus_number
                    if Bus_Type(i) == 3
                        dQ(k,1) = delta_Q1(i);
                        k = k+1;
                    end
                end
                dP = delta_P1(2:Bus_number);
                M_Vctr1 = [dP; dQ];                   %Mismatch Vector

                %Jacobian Matrix formation
                %Jacobian matrix formation
                %J1 - Derivative of Real Power Injections with angles
                J1 = zeros(Bus_number-1,Bus_number-1);
                for i = 1:(Bus_number-1)
                    m = i+1;
                    for k = 1:(Bus_number-1)
                        n = k+1;
                        if n == m
                            for n = 1:Bus_number
                                J1(i,k) = J1(i,k) + V_B(m)* V_B(n)*(-
G(m,n)*sin(The_B(m)-The_B(n)) + B(m,n)*cos(The_B(m)-The_B(n)));
                            end
                            J1(i,k) = J1(i,k) - V_B(m)^2*B(m,m);
                        else
                            J1(i,k) = V_B(m)*
V_B(n)*(G(m,n)*sin(The_B(m)-The_B(n)) - B(m,n)*cos(The_B(m)-
The_B(n)));
                        end
                    end
                end
                % J2 - Derivative of Real Power Injections with
Voltage
                J2 = zeros(Bus_number-1,n_pq);
                for i = 1:(Bus_number-1)
                    m = i+1;
                    for k = 1:n_pq
                        n = pq(k);
                        if n == m
                            for n = 1:Bus_number
```

```
                                J2(i,k) = J2(i,k) +
V_B(n)*(G(m,n)*cos(The_B(m)-The_B(n)) + B(m,n)*sin(The_B(m)-
The_B(n)));
                            end
                            J2(i,k) = J2(i,k) + V_B(m)*G(m,m);
                        else
                            J2(i,k) = V_B(m)*(G(m,n)*cos(The_B(m)-
The_B(n)) + B(m,n)*sin(The_B(m)-The_B(n)));
                        end
                    end
                end

                % J3 - Derivative of Reactive Power Injections with
Angles
                J3 = zeros(n_pq,Bus_number-1);
                for i = 1:n_pq
                    m = pq(i);
                    for k = 1:(Bus_number-1)
                        n = k+1;
                        if n == m
                            for n = 1:Bus_number
                                J3(i,k) = J3(i,k) + V_B(m)*
V_B(n)*(G(m,n)*cos(The_B(m)-The_B(n)) + B(m,n)*sin(The_B(m)-
The_B(n)));
                            end
                            J3(i,k) = J3(i,k) - V_B(m)^2*G(m,m);
                        else
                            J3(i,k) = V_B(m)* V_B(n)*(-
G(m,n)*cos(The_B(m)-The_B(n)) - B(m,n)*sin(The_B(m)-The_B(n)));
                        end
                    end
                end

                % J4 - Derivative of Reactive Power Injections with
Voltage
                J4 = zeros(n_pq,n_pq);
                for i = 1:n_pq
                    m = pq(i);
                    for k = 1:n_pq
                        n = pq(k);
                        if n == m
                            for n = 1:Bus_number
                                J4(i,k) = J4(i,k) +
V_B(n)*(G(m,n)*sin(The_B(m)-The_B(n)) - B(m,n)*cos(The_B(m)-
The_B(n)));
                            end
                            J4(i,k) = J4(i,k) - V_B(m)*B(m,m);
                        else
```

```
                            J4(i,k) = V_B(m)*(G(m,n)*sin(The_B(m)-
The_B(n)) - B(m,n)*cos(The_B(m)-The_B(n)));
                        end
                    end
                end

                J_M2 = [J1 J2; J3 J4];                %Jacobian
Matrix

                C_Vctr = J_M2\M_Vctr1;               %Correction
Vector

                dThe = C_Vctr(1:Bus_number-1);
%Change in Voltage Angle
                dV = C_Vctr(Bus_number:end);
%Change in Voltage Magnitude

                %Updating State Vectors

                The_B(2:Bus_number) = dThe + The_B(2:Bus_number);
%Voltage Angle
                The_B_deg = rad2deg(The_B(2:Bus_number));

                k = 1;
                for i = 2:Bus_number
                    if Bus_Type(i) == 3
                        V_B(i) = dV(k) + V_B(i);
%Voltage Magnitude
                        k = k+1;
                    end
                end

                Iterld = Iterld + 1;
                Tolld = max(abs(M_Vctr1));
                if Iterld>100
                break
               end

            end
          V_BEld=V_B;
          %lineflow deviations
V_B_re = V_B.*cos(The_B) + 1i*V_B.*sin(The_B);        %Converting
Polar to Rectangular(Bus Voltages).
  The_B_Degr = 180/pi*The_B;                           %Bus Voltage
Angles in Degree.

Iij = zeros(Bus_number,Bus_number);
%Initializing Matrices.
Sij = zeros(Bus_number,Bus_number);
```

```
%Lloss = zeros(Branch_num,1);
Sinjt = zeros(Bus_number,1);


                    %Line Current Flows.
for m = 1:Branch_num
    p = From_Bus(m); q = To_Bus(m);
    Iij(p,q) = -(V_B_re(p) - V_B_re(q))*Y(p,q);           %Y(m,n) =
-y(m,n).
    Iij(q,p) = -Iij(p,q);
end
   %Iij = sparse(Iij);     % Commented out..
   Iijm = abs(Iij);
   Iija = angle(Iij);
                    %Line Power Flows.
    for m = 1:Bus_number
        for n = 1:Bus_number
            if m ~= n
            Sij(m,n) = V_B_re(m)*conj(Iij(m,n))*BMva;
            end
        end
    end
%Sij = sparse(Sij);     % Commented out..
[theta, rho] = cart2pol(real(Sij), imag(Sij));
rhoij=rho;
thetaij=theta;
T_1=[];
 for m = 1:Branch_num
      p = From_Bus(m);
      q = To_Bus(m);
      rhoij(p,q);
      thetaij(p,q);
      rhoij(q,p);
      thetaij(q,p);
       T_1 = [T_1; p q rhoij(p,q)];

 end
  T_1;


T2=[T_1,ConR];  %Horizontally Concatenating line matrix with
Continuos rating to check themal limit of the line
           T_LP=[];
           for j=1:size(T2,1)
               p1 = T2(j,3);
               q1= T2(j,4);
               if p1>q1
                   V_M21=p1;
               else
```

```
                    V_M21=0;
                end
                T_LP=[T_LP;T2(j,1),T2(j,2),p1,q1];
            end
            V_M21;
            for k=1:Bus_number
                V_B(k);
                if V_B(k)<0.95  || V_B(k)>1.05
                    V_ME(k)=1;
                else
                    V_ME(k)=0;
                end
            end
            V_BNC=V_B;
            sTLEld=sum(V_M21);
            sVLEld=sum(V_ME);
            V_M11=sTLEld+sVLEld;
            T_Eld=[T_Eld; T J sVLEld sTLEld];
            sV_Mls=1;sVMl=0;
            Itls=1;
        while (sV_Mls>=1)%|| Itls <= 20)
        if V_M11>0
              V_M3LS=V_M11;
             counterVLS = counterVLS + 1;
             V_BNC=V_B;
             V_MCLS=counterVLS; % To get number of component for Load
Curtailments
             T_yesLS=[T_yesLS; T J V_M3LS V_MCLS sVLEld];

beta=[0.2;0.2;0.5;0.2;0.2;0.3;0.3;0.3;0.3;0.3;0;0;0.5;0.5;0.5;0.2;0;
0.5;0.5;0.5;0;0;0;0];%weighing factors for the load
             Bus_dataB3=Bus_data3;
             UL=Bus_dataB3(:,1);%.*Alp;
             %ULQ=Bus_dataB3(:,2).*beta;%.*Alp;
             UL(~any(UL,2),:) = [];
             LB=zeros(1,17);
             UB=UL';
          %pso parameters values
             m=17; % number of variables
             n=50; % population size
             wmax=0.9; % inertia weight
             wmin=0.4; % inertia weight
             c1=2; % acceleration factor
             c2=2; % acceleration factor
             % pso main program-----------------------------------
--------------start
             maxite=1000; % set maximum number of iteration
             maxrun=10; % set maximum number of runs need to be
```

```
            for run=1:maxrun
                run;
                % pso initialization-----------------------------------
--------------start
                for i=1:n
                    for j=1:m
                        x0(i,j)=round(LB(j)+rand()*(UB(j)-LB(j)));
                    end
                end
                x=x0; % initial population
                v=0.1*x0; % initial velocity
                for i=1:n
                    f0(i,1)=ofua(x0(i,:));
                end
                [fmin0,index0]=min(f0);
                pbest=x0; % initial pbest
                gbest=x0(index0,:); % initial gbest
                % pso initialization-----------------------------------
----------------end
                % pso algorithm----------------------------------------
--------------start
                ite=1;
                tolerance=1;
                while ite<=maxite && tolerance>10^-12
                    w=wmax-(wmax-wmin)*ite/maxite; % update inertial
weight
                    % pso velocity updates
                    for i=1:n
                        for j=1:m
                            v(i,j)=w*v(i,j)+c1*rand()*(pbest(i,j)-
x(i,j))...
                                +c2*rand()*(gbest(1,j)-x(i,j));
                        end
                    end
                    % pso position update
                    for i=1:n
                        for j=1:m
                            x(i,j)=x(i,j)+v(i,j);
                        end
                    end
                    % handling boundary violations
                    for i=1:n
                        for j=1:m
                            if x(i,j)<LB(j)
                                x(i,j)=LB(j);
                            elseif x(i,j)>UB(j)
                                x(i,j)=UB(j);
                            end
                        end
```

```
                    end
                    % evaluating fitness
                    for i=1:n
                        f(i,1)=ofua(x(i,:));
                    end
                    % updating pbest and fitness
                    for i=1:n
                        if f(i,1)<f0(i,1)
                            pbest(i,:)=x(i,:);
                            f0(i,1)=f(i,1);
                        end
                    end
                    [fmin,index]=min(f0); % finding out the best
particle
                    ffmin(ite,run)=fmin; % storing best fitness
                    ffite(run)=ite; % storing iteration count
                    % updating gbest and best fitness
                    if fmin<fmin0
                        gbest=pbest(index,:);
                        fmin0=fmin;
                    end
                    % calculating tolerance
                    if ite>100
                        tolerance=abs(ffmin(ite-100,run)-fmin0);
                    end
                    % displaying iterative results
                    if ite==1
                        fprintf('Iteration Best particle Objective
fun\n');
                    end
                    fprintf('%8g %8g %8.4f\n',ite,index,fmin0);
                    ite=ite+1;
                end
                % pso algorithm-------------------------------------
----------------end
                gbest;

fvalue=gbest(1)+gbest(2)+gbest(3)+gbest(4)+gbest(5)+gbest(6)+gbest(7
)....

+gbest(8)+gbest(9)+gbest(10)+gbest(11)+gbest(12)+gbest(13)+gbest(14)
+gbest(15)+gbest(16)+gbest(17);

%fvalue=0.2*(gbest(1)+gbest(2)+gbest(3)+gbest(4)+gbest(5))+0.3*(gbes
t(6)+gbest(7)+gbest(8)+gbest(9)+gbest(10))+0.5*(gbest(11)+gbest(12)+
gbest(13)+gbest(14)+gbest(15)+gbest(16)+gbest(17));

%fvalue=0.2*gbest(1)+0.2*gbest(2)+0.5*gbest(3)+0.2*gbest(4)....
```

```
%
+0.2*gbest(5)+0.3*gbest(6)+0.3*gbest(7)+0.3*gbest(8)+0.3*gbest(9)...
.
%
+0.3*gbest(10)+0.5*gbest(11)+0.5*gbest(12)+0.5*gbest(13)+0.2*gbest(1
4)....
%                    +0.5*gbest(15)+0.5*gbest(16)+0.5*gbest(17);
                fff(run)=fvalue;
                rgbest(run,:)=gbest;
                fprintf('--------------------------------------\n');
            end
            % pso main program-----------------------------------
----------------end
            % disp(sprintf('\n'));
            %
disp(sprintf('**************************************************
***'));
            % disp(sprintf('Final Results--------------------------
--'));

            [bestfun,bestrun]=min(fff(fff>0));
            %rgbest(~any(rgbest,2),:) = [];
            best_variables=rgbest(bestrun,:);
            if isempty(best_variables)
                best_variables=zeros(1,17);
            end
            DN1=best_variables';
            SDN1=sum(DN1);
            DNb=[0 0]';
            DNa=0;
            DNc=[0 0 0 0]';
            DN2=DN1(1:10,:);
            DN2a=[DN2;DNb];
            DN3=DN1(11:14,:);
            DN3a=[DN3;DNa];
            DN4=DN1(15:end,:);
            DN4a=[DN4;DNc];
            LC=[DN2a;DN3a;DN4a];
            LCbe=LC;%.*beta;
            %[rId,cId,val] = find(LCbe);
%             eqULQ=ULQ(rId,cId);
%             eqZ=zeros(24,1);
%             eqZ(rId,cId)=eqULQ;
%             BPQ=[LCbe,ULQ];
            LC_S=sum(LCbe);
            if LC_S<=300 % incorporate time resroration
               restT=(1/10*LC_S)/60; % restoration time in hour.
               LCSrT=restT*LC_S;
            elseif LC_S>300 && LC_S<=999
```

```
                restT=(30+(1/33.3*(LC_S-300)))/60;
                LCSrT=restT*LC_S;
            elseif LC_S>999 && LC_S<=1998
                restT=(30+30+(1/66.6*(LC_S-1299)))/60;
                LCSrT=restT*LC_S;
            elseif LC_S>1998
                restT=(30+30+30+(1/83.3*(LC_S-1998)))/60;
                LCSrT=restT*LC_S;
            end
            LCSrT; %load curtained in MWh
            PDopf=P_D1-LCbe/BMva;
            %QDopf=Q_D1-eqZ/BMva;
            Plopf2=PDopf;
            %Qlopf2=QDopf;
            sPlopf=sum(Plopf2);
            TLC=sum(LC_S);
            T_Re=[T_Re; T J TLC LC_S LCSrT sum(PDopf)];
            ST_Re=sum(T_Re(:,3:5));
            P_D=PDopf;
            %Q_D=QDopf;
            PspLS=PGN-P_D;              %Specified Power injections
            QspLS=Q_G1-Q_D+Qsht;             %Specified Power
injections
           TolLS = 1;
           IterLS = 1;
   while (TolLS > 0.000001)  %Start Iteration
        PLS = zeros(Bus_number,1);
        QLS = zeros(Bus_number,1);
        %Calculate P and Q
            for i = 1:Bus_number
                for k = 1:Bus_number
                    PLS(i) = PLS(i) + V_B(i)*
V_B(k)*(G(i,k)*cos(The_B(i)-The_B(k)) + B(i,k)*sin(The_B(i)-
The_B(k)));
                    QLS(i) = QLS(i) + V_B(i)*
V_B(k)*(G(i,k)*sin(The_B(i)-The_B(k)) - B(i,k)*cos(The_B(i)-
The_B(k)));
                end
            end


     if Iter <= 7 && Iter > 2    % Only checked up to 7th
iterations..
        for n = 2:Bus_number
            if Bus_Type(n) == 2
                QG = QLS(n)+Q_D(n);
                if QG < Q_min(n)
                    V_B(n) = V_B(n) + 0.01;
                elseif QG > Q_max(n)
```

```
                    V_B(n) = V_B(n) - 0.01;
                end
            end
         end
    end
    delta_P = PspLS-PLS;          %Calculate change using specified
values
    delta_Q = QspLS-QLS;
    k = 1;
     dQ = zeros(n_pq,1);
            for i = 1:Bus_number
                if Bus_Type(i) == 3
                    dQ(k,1) = delta_Q(i);
                    k = k+1;
                end
            end
            dP = delta_P(2:Bus_number);
            M_Vctr = [dP; dQ];                  %Mismatch Vector
            k = 1;
    dbusLS = zeros(n_pq,1);
    for i = 1:Bus_number
        if Bus_Type(i) == 3
            dbusLS(k,1) = Bus_numbering(i);
            k = k+1;
        end
    end

    dPnLS = delta_P(1:Bus_number);
            dQbusLS=[dQ,dbusLS];
            dPbusLS=Bus_numbering(1:Bus_number);
            DPbusLS=[dPnLS,dPbusLS];
            M_VctrdgLS = [DPbusLS; dQbusLS];



                    %Jacobian Matrix formation
        %Jacobian matrix formation
             %J1 - Derivative of Real Power Injections with angles
    J1 = zeros(Bus_number-1,Bus_number-1);
            for i = 1:(Bus_number-1)
                m = i+1;
                for k = 1:(Bus_number-1)
                    n = k+1;
                    if n == m
                        for n = 1:Bus_number
                            J1(i,k) = J1(i,k) + V_B(m)* V_B(n)*(-
G(m,n)*sin(The_B(m)-The_B(n)) + B(m,n)*cos(The_B(m)-The_B(n)));
                        end
                        J1(i,k) = J1(i,k) - V_B(m)^2*B(m,m);
```

```
                        else
                J1(i,k) = V_B(m)* V_B(n)*(G(m,n)*sin(The_B(m)-
The_B(n)) - B(m,n)*cos(The_B(m)-The_B(n)));
                    end
                end
            end
        % J2 - Derivative of Real Power Injections with Voltage
    J2 = zeros(Bus_number-1,n_pq);
    for i = 1:(Bus_number-1)
        m = i+1;
        for k = 1:n_pq
            n = pq(k);
            if n == m
                for n = 1:Bus_number
                    J2(i,k) = J2(i,k) + V_B(n)*(G(m,n)*cos(The_B(m)-
The_B(n)) + B(m,n)*sin(The_B(m)-The_B(n)));
                end
                J2(i,k) = J2(i,k) + V_B(m)*G(m,m);
            else
                J2(i,k) = V_B(m)*(G(m,n)*cos(The_B(m)-The_B(n)) +
B(m,n)*sin(The_B(m)-The_B(n)));
            end
        end
    end

    % J3 - Derivative of Reactive Power Injections with Angles
    J3 = zeros(n_pq,Bus_number-1);
    for i = 1:n_pq
        m = pq(i);
        for k = 1:(Bus_number-1)
            n = k+1;
            if n == m
                for n = 1:Bus_number
                    J3(i,k) = J3(i,k) + V_B(m)*
V_B(n)*(G(m,n)*cos(The_B(m)-The_B(n)) + B(m,n)*sin(The_B(m)-
The_B(n)));
                end
                J3(i,k) = J3(i,k) - V_B(m)^2*G(m,m);
            else
                J3(i,k) = V_B(m)* V_B(n)*(-G(m,n)*cos(The_B(m)-
The_B(n)) - B(m,n)*sin(The_B(m)-The_B(n)));
            end
        end
    end

    % J4 - Derivative of Reactive Power Injections with Voltage
    J4 = zeros(n_pq,n_pq);
    for i = 1:n_pq
        m = pq(i);
```

```
        for k = 1:n_pq
            n = pq(k);
            if n == m
                for n = 1:Bus_number
                    J4(i,k) = J4(i,k) + V_B(n)*(G(m,n)*sin(The_B(m)-
The_B(n)) - B(m,n)*cos(The_B(m)-The_B(n)));
                end
                J4(i,k) = J4(i,k) - V_B(m)*B(m,m);
            else
                J4(i,k) = V_B(m)*(G(m,n)*sin(The_B(m)-The_B(n)) -
B(m,n)*cos(The_B(m)-The_B(n)));
            end
        end
    end

        J_M = [J1 J2; J3 J4];                %Jacobian Matrix

         C_Vctr = J_M\M_Vctr;               %Correction Vector

         dThe = C_Vctr(1:Bus_number-1);                %Change in
Voltage Angle
         dV = C_Vctr(Bus_number:end);                  %Change in
Voltage Magnitude

            %Updating State Vectors

    The_B(2:Bus_number) = dThe + The_B(2:Bus_number);
%Voltage Angle
    The_B_deg = rad2deg(The_B(2:Bus_number));

    k = 1;
            for i = 2:Bus_number
                if Bus_Type(i) == 3
                    V_B(i) = dV(k) + V_B(i);
%Voltage Magnitude
                    k = k+1;
                end
            end

       IterLS = IterLS + 1;
       TolLS = max(abs(M_Vctr));
       if IterLS>100
        break
        end

   end

   V_B_re = V_B.*cos(The_B) + 1i*V_B.*sin(The_B);        %Converting
Polar to Rectangular(Bus Voltages).
```

```
  The_B_Degr = 180/pi*The_B;                                  %Bus Voltage
Angles in Degree.

Iij = zeros(Bus_number,Bus_number);
%Initializing Matrices.
Sij = zeros(Bus_number,Bus_number);
%Lloss = zeros(Branch_num,1);
Sinjt = zeros(Bus_number,1);
                    %Line Current Flows.
for m = 1:Branch_num
    p = From_Bus(m); q = To_Bus(m);
    Iij(p,q) = -(V_B_re(p) - V_B_re(q))*Y(p,q);           %Y(m,n) =
-y(m,n).
    Iij(q,p) = -Iij(p,q);
end
   %Iij = sparse(Iij);     % Commented out..
   Iijm = abs(Iij);
   Iija = angle(Iij);
                    %Line Power Flows.
    for m = 1:Bus_number
        for n = 1:Bus_number
            if m ~= n
            Sij(m,n) = V_B_re(m)*conj(Iij(m,n))*BMva;
            end
        end
    end
%Sij = sparse(Sij);     % Commented out..
[theta, rho] = cart2pol(real(Sij), imag(Sij));
rhoij=rho;
thetaij=theta;
T_1ls=[];
 for m = 1:Branch_num
      p = From_Bus(m);
      q = To_Bus(m);
      rhoij(p,q);
      thetaij(p,q);
      thetaij(q,p);
       T_1ls = [T_1ls; p q rhoij(p,q)];

 end
  T_1ls;
  T2ls=[T_1ls,ConR];  %Horizontally Concatenating line matrix with
Continuos rating to check themal limit of the line
 T_LPls=[];
  for j=1:size(T2ls,1)
         p1 = T2ls(j,3);
         q1= T2ls(j,4);
         if p1>q1
             V_M2ls=p1;
```

```
          else
             V_M2ls=0;
          end
       T_LPls=[T_LPls;T2ls(j,1),T2ls(j,2),p1,q1];
   end
V_M2ls;
   for k=1:Bus_number
      V_B(k);
      if V_B(k)<0.95  || V_B(k)>1.05
         V_Mls(k)=1;
      else
        V_Mls(k)=0;

      end
 end
V_Mls;
VLls=sum(V_Mls);
TLls=sum(V_M2ls);
V_Mls_V_B=V_B;
sV_Mls=sum(V_Mls)+sum(V_M2ls);
sVMl=VLls+TLls;
SUL=sum(UL);
 if SUL<=300 % incorporate time resroration
               restT1=(1/10*SUL)/60; % restoration time in hour.
               LCSrT1=restT1*SUL;
            elseif SUL>300 && SUL<=999
                restT1=(30+(1/33.3*(SUL-300)))/60;
                LCSrT1=restT1*SUL;
            elseif SUL>999 && SUL<=1998
                restT1=(30+30+(1/66.6*(SUL-1299)))/60;
                LCSrT1=restT1*SUL;
            elseif SUL>1998
                restT1=(30+30+30+(1/83.3*(SUL-1998)))/60;
                LCSrT1=restT1*SUL;
  end
T_Re1=[T_Re1; T J LCSrT LC_S sV_Mls LCSrT1 VLls TLls];
       end
      Itls = Itls + 1;

      if Itls > 100

        break
      end

       end

       if sVMl>0 && Itls>100

 rr=Fbusdata(:,6)/BMva;
```

```
for jj=1:size(rr,1)
    pp=rr;
for ddls=0.05:0.05:1
    aa=rr(jj,1)*ddls;
    pp(jj,1)=pp(jj,1)-aa;
           retT=(1/10*aa1)/60; % restoration time in hour.
               LCretT=retT*aa1;
              Iterls1=1;
              Tolls1=1;

 while (Tolls1 > 0.000001)   % Iteration starting..

    Pls1 = zeros(Bus_number,1);
    Qls1 = zeros(Bus_number,1);
    % Calculate P and Q
    for i = 1:Bus_number
        for k = 1:Bus_number
            Pls1(i) = Pls1(i) + V_B(i)* V_B(k)*(G(i,k)*cos(The_B(i)-
The_B(k)) + B(i,k)*sin(The_B(i)-The_B(k)));
            Qls1(i) = Qls1(i) + V_B(i)* V_B(k)*(G(i,k)*sin(The_B(i)-
The_B(k)) - B(i,k)*cos(The_B(i)-The_B(k)));
        end
    end
    % Checking Q-limit violations..
    if Iter <= 7 && Iter > 2    % Only checked up to 7th
iterations..
        for n = 2:Bus_number
            if Bus_Type(n) == 2
                QG = Qls1(n)+Q_D(n);
                if QG < Q_min(n)
                    V_B(n) = V_B(n) + 0.01;
                elseif QG > Q_max(n)
                    V_B(n) = V_B(n) - 0.01;
                end
            end
         end
    end

    % Calculate change from specified value
    Pspls1 = P_G - pp;                % Pi = PGi - PLi..
    Qspls1 = Q_G - Q_D+Qsht;                % Qi = QGi - QLi..
    dPals1 = Pspls1-Pls1;
    dQals1 = Qspls1-Qls1;

    k = 1;
    dQls1 = zeros(n_pq,1);
    for i = 1:Bus_number
        if Bus_Type(i) == 3
            dQls1(k,1) = dQals1(i);
```

```
            k = k+1;
        end
    end
     k = 1;

    dbusLS = zeros(n_pq,1);
    for i = 1:Bus_number
        if Bus_Type(i) == 3
            dbusLS(k,1) = Bus_numbering(i);
            k = k+1;
        end
    end
    dPls = dPals1(2:Bus_number);
    Mls1 = [dPls; dQls1];       % Mismatch Vector


    % Jacobian
    % J1 - Derivative of Real Power Injections with Angles..
    J1 = zeros(Bus_number-1,Bus_number-1);
    for i = 1:(Bus_number-1)
        m = i+1;
        for k = 1:(Bus_number-1)
            n = k+1;
            if n == m
                for n = 1:Bus_number
                    J1(i,k) = J1(i,k) + V_B(m)* V_B(n)*(-
G(m,n)*sin(The_B(m)-The_B(n)) + B(m,n)*cos(The_B(m)-The_B(n)));
                end
                J1(i,k) = J1(i,k) - V_B(m)^2*B(m,m);
            else
                J1(i,k) = V_B(m)* V_B(n)*(G(m,n)*sin(The_B(m)-
The_B(n)) - B(m,n)*cos(The_B(m)-The_B(n)));
            end
        end
    end

    % J2 - Derivative of Real Power Injections with V..
    J2 = zeros(Bus_number-1,n_pq);
    for i = 1:(Bus_number-1)
        m = i+1;
        for k = 1:n_pq
            n = pq(k);
            if n == m
                for n = 1:Bus_number
                    J2(i,k) = J2(i,k) + V_B(n)*(G(m,n)*cos(The_B(m)-
The_B(n)) + B(m,n)*sin(The_B(m)-The_B(n)));
                end
                J2(i,k) = J2(i,k) + V_B(m)*G(m,m);
            else
```

```
                J2(i,k) = V_B(m)*(G(m,n)*cos(The_B(m)-The_B(n)) +
B(m,n)*sin(The_B(m)-The_B(n)));
            end
        end
    end

    % J3 - Derivative of Reactive Power Injections with Angles..
    J3 = zeros(n_pq,Bus_number-1);
    for i = 1:n_pq
        m = pq(i);
        for k = 1:(Bus_number-1)
            n = k+1;
            if n == m
                for n = 1:Bus_number
                    J3(i,k) = J3(i,k) + V_B(m)*
V_B(n)*(G(m,n)*cos(The_B(m)-The_B(n)) + B(m,n)*sin(The_B(m)-
The_B(n)));
                end
                J3(i,k) = J3(i,k) - V_B(m)^2*G(m,m);
            else
                J3(i,k) = V_B(m)* V_B(n)*(-G(m,n)*cos(The_B(m)-
The_B(n)) - B(m,n)*sin(The_B(m)-The_B(n)));
            end
        end
    end

    % J4 - Derivative of Reactive Power Injections with V..
    J4 = zeros(n_pq,n_pq);
    for i = 1:n_pq
        m = pq(i);
        for k = 1:n_pq
            n = pq(k);
            if n == m
                for n = 1:Bus_number
                    J4(i,k) = J4(i,k) + V_B(n)*(G(m,n)*sin(The_B(m)-
The_B(n)) - B(m,n)*cos(The_B(m)-The_B(n)));
                end
                J4(i,k) = J4(i,k) - V_B(m)*B(m,m);
            else
                J4(i,k) = V_B(m)*(G(m,n)*sin(The_B(m)-The_B(n)) -
B(m,n)*cos(The_B(m)-The_B(n)));
            end
        end
    end

    JACls = [J1 J2; J3 J4];     % Jacobian Matrix..

    Xls1 = inv(JACls)*Mls1;           % Correction Vector
    dThls1 = Xls1(1:Bus_number-1);      % Change in Voltage Angle..
```

```
    dVsl = Xls1(Bus_number:end);       % Change in Voltage
Magnitude..

    % Updating State Vectors..
    The_B(2:Bus_number) = dThls1 + The_B(2:Bus_number);    % Voltage
Angle..
    k = 1;
    for i = 2:Bus_number
        if Bus_Type(i) == 3
            V_B(i) = dVsl(k) + V_B(i);        % Voltage Magnitude..
            k = k+1;
        end
    end

    Iterls1 = Iterls1 + 1;
    flagls1=Iterls1;
    %flagdg2=flagls1+1;
    Tolls1 = max(abs(Mls1));                  % Tolerance..
    if Iterls1>mIter
        break
    end

 end
 V_ls=V_B;
     for k=1:Bus_number
      V_B(k);
      if V_B(k)<0.95  || V_B(k)>1.05
         V_Mls1(k)=1;
      else
        V_Mls1(k)=0;

      end
     end
      V_Mls1;
    sV_Mls1=sum(V_Mls1);
    T_LS=[T_LS; T J LCretT jj sV_Mls1 VLls TLls ddls];

   if sV_Mls1==0
       T_LS1=[T_LS1; T J LCretT jj sV_Mls1 VLls TLls ddls];
        break
   end

end
 T_LS2=[T_LS2; T J LCretT jj sV_Mls1 VLls TLls ddls];
end
       end

       end
```

```
   elseif sV_MT<0
          sPldg=HPD
          T_dg2 =[T_dg2; T J sPldg];
 end


        end

     end


end
 tre3= T_LS2;
 tre2= T_LS1;
 gg= T_LS;
 tre1= T_Re1;
 ff=T_Re1;
 if  ~isempty(ff)% if ff is not an empty matrix
 ff1=ff;
 ff1=ff1(ff1(:,5)==0, :); % to identify any zero in column 5
 ff1(:,6)=0; % to make the whole of column 6 zero
 %This removes any rows where the value in the first column has
already been used.
 [~,idx] = unique(ff(:,1));   %which rows have a unique first value?
  ff = ff(idx,:);                %only use those
  ff(:,3:4)=0;
[y,x] = ismember(ff1(:,1),ff(:,1));  % find where the indexes match
in the 1st column
x = x(y);  % save only the row numbers where the indexes match
ff(x,:) = ff1(y,:);  % replace the rows where the indexes match
if  ~isempty(gg)% if ff is not an empty matrix
 tr22=gg;
 tr22=tr22(tr22(:,5)==0, :);
 if  ~isempty(tr22)% if tr22 is not an empty matrix
 tr22(:,6)=0;
 [y1,x1] = ismember(tr22(:,1),ff(:,1));  % find where the indexes
match in the 1st column
 x1 = x1(y1);
 ff(x1,:) = tr22(y1,:);
 end
end
Sls=sum(ff(:,3));
Sls2=sum(ff(:,6));
Total_LS=Sls2+Sls;
T_ttt=[T_ttt; ttt Total_LS];
 end
end
MT_ttt = mean(T_ttt);
toc
```

B.4 Ternary Markovian Model System State Selection Code

```
TC2=[];
TC1=[];
% counterU=0;
% counterD=0;
% counterE=0;up=0;
%counterR=0;
TC=[];
%R = rand(10,1)1
for J= 1:7
PROB=prodatS; % assumed probability data,
%TC=[];
counterU=0;
counterD=0;
counter8=0;up=0;counter7=0;counter6=0;counter5=0;counter4=0;counter3
=0;
counter9=0;counter10=0;counter11=0;counter12=0;counter13=0;counter14
=0;
counter15=0;counter16=0;counter17=0;counter18=0;
for V=1:10000
    U=rand;U1=rand;U3=rand;

if
U>=PROB(J,3)+PROB(J,4)+PROB(J,5)+PROB(J,6)+PROB(J,7)+PROB(J,8)+...
        PROB(J,9)+PROB(J,10)+PROB(J,11)+PROB(J,12)+PROB(J,13)+...

PROB(J,14)+PROB(J,15)+PROB(J,16)+PROB(J,17)+PROB(J,18)+PROB(J,2)
         counterU = counterU + 1;
         counterS=1;

elseif
PROB(J,3)+PROB(J,4)+PROB(J,5)+PROB(J,6)+PROB(J,7)+PROB(J,8)+...
        PROB(J,9)+PROB(J,10)+PROB(J,11)+PROB(J,12)+PROB(J,13)+...
        PROB(J,14)+PROB(J,15)+PROB(J,16)+PROB(J,17)+PROB(J,18)<=U &&
U<PROB(J,3)+...

PROB(J,4)+PROB(J,5)+PROB(J,6)+PROB(J,7)+PROB(J,8)+PROB(J,9)+PROB(J,1
0)+PROB(J,11)+...

PROB(J,12)+PROB(J,13)+PROB(J,14)+PROB(J,15)+PROB(J,16)+PROB(J,17)+PR
OB(J,18)+PROB(J,2)
        counterD = counterD + 1;
        counterS=0;

elseif
PROB(J,3)+PROB(J,4)+PROB(J,5)+PROB(J,6)+PROB(J,7)+PROB(J,8)+PROB(J,9
)+PROB(J,10)+PROB(J,11)+...
```

```
PROB(J,12)+PROB(J,13)+PROB(J,14)+PROB(J,15)+PROB(J,16)+PROB(J,17)<=U
&& U<PROB(J,3)+PROB(J,4)+...

PROB(J,5)+PROB(J,6)+PROB(J,7)+PROB(J,8)+PROB(J,9)+PROB(J,10)+PROB(J,
11)+PROB(J,12)+PROB(J,13)+...
        PROB(J,14)+PROB(J,15)+PROB(J,16)+PROB(J,17)+PROB(J,18)
        counter18 = counter18 + 1;
        counterS=18;
 elseif
PROB(J,3)+PROB(J,4)+PROB(J,5)+PROB(J,6)+PROB(J,7)+PROB(J,8)+PROB(J,9
)+PROB(J,10)+PROB(J,11)+...
        PROB(J,12)+PROB(J,13)+PROB(J,14)+PROB(J,15)+PROB(J,16)<=U &&
U<PROB(J,3)+PROB(J,4)+...

PROB(J,5)+PROB(J,6)+PROB(J,7)+PROB(J,8)+PROB(J,9)+PROB(J,10)+PROB(J,
11)+PROB(J,12)+PROB(J,13)+...
        PROB(J,14)+PROB(J,15)+PROB(J,16)+PROB(J,17)
        counter17 = counter17 + 1;
        counterS=17;
elseif
PROB(J,3)+PROB(J,4)+PROB(J,5)+PROB(J,6)+PROB(J,7)+PROB(J,8)+PROB(J,9
)+PROB(J,10)+PROB(J,11)+...
        PROB(J,12)+PROB(J,13)+PROB(J,14)+PROB(J,15)<=U &&
U<PROB(J,3)+PROB(J,4)+PROB(J,5)+PROB(J,6)+...

PROB(J,7)+PROB(J,8)+PROB(J,9)+PROB(J,10)+PROB(J,11)+PROB(J,12)+PROB(
J,13)+...
        PROB(J,14)+PROB(J,15)+PROB(J,16)
        counter16 = counter16 + 1;
        counterS=16;
elseif
PROB(J,3)+PROB(J,4)+PROB(J,5)+PROB(J,6)+PROB(J,7)+PROB(J,8)+PROB(J,9
)+PROB(J,10)+PROB(J,11)+...
        PROB(J,12)+PROB(J,13)+PROB(J,14)<=U &&
U<PROB(J,3)+PROB(J,4)+PROB(J,5)+PROB(J,6)+...

PROB(J,7)+PROB(J,8)+PROB(J,9)+PROB(J,10)+PROB(J,11)+PROB(J,12)+PROB(
J,13)+...
        PROB(J,14)+PROB(J,15)
        counter15 = counter15 + 1;
        counterS=15;
elseif
PROB(J,3)+PROB(J,4)+PROB(J,5)+PROB(J,6)+PROB(J,7)+PROB(J,8)+PROB(J,9
)+PROB(J,10)+PROB(J,11)+...
        PROB(J,12)+PROB(J,13)<=U &&
U<PROB(J,3)+PROB(J,4)+PROB(J,5)+PROB(J,6)+...
```

```
PROB(J,7)+PROB(J,8)+PROB(J,9)+PROB(J,10)+PROB(J,11)+PROB(J,12)+PROB(
J,13)+PROB(J,14)
        counter14 = counter14 + 1;
        counterS=14;
elseif
PROB(J,3)+PROB(J,4)+PROB(J,5)+PROB(J,6)+PROB(J,7)+PROB(J,8)+PROB(J,9
)+PROB(J,10)+PROB(J,11)+...
        PROB(J,12)<=U &&
U<PROB(J,3)+PROB(J,4)+PROB(J,5)+PROB(J,6)+PROB(J,7)+PROB(J,8)+PROB(J
,9)+...
        PROB(J,10)+PROB(J,11)+PROB(J,12)+PROB(J,13)
        counter13 = counter13 + 1;
        counterS=13;
elseif
PROB(J,3)+PROB(J,4)+PROB(J,5)+PROB(J,6)+PROB(J,7)+PROB(J,8)+PROB(J,9
)+PROB(J,10)+...
        PROB(J,11)<=U &&
U<PROB(J,3)+PROB(J,4)+PROB(J,5)+PROB(J,6)+PROB(J,7)+PROB(J,8)+PROB(J
,9)+...
        PROB(J,10)+PROB(J,11)+PROB(J,12)
        counter12 = counter12 + 1;
        counterS=12;
elseif
PROB(J,3)+PROB(J,4)+PROB(J,5)+PROB(J,6)+PROB(J,7)+PROB(J,8)+PROB(J,9
)+PROB(J,10)...
        <=U &&
U<PROB(J,3)+PROB(J,4)+PROB(J,5)+PROB(J,6)+PROB(J,7)+PROB(J,8)+PROB(J
,9)+...
        PROB(J,10)+PROB(J,11)
        counter11 = counter11 + 1;
        counterS=11;
elseif
PROB(J,3)+PROB(J,4)+PROB(J,5)+PROB(J,6)+PROB(J,7)+PROB(J,8)+PROB(J,9
)<=U && U<PROB(J,3)+...

PROB(J,4)+PROB(J,5)+PROB(J,6)+PROB(J,7)+PROB(J,8)+PROB(J,9)+PROB(J,1
0)
        counter10 = counter10 + 1;
        counterS=10;
elseif
PROB(J,3)+PROB(J,4)+PROB(J,5)+PROB(J,6)+PROB(J,7)+PROB(J,8)<=U &&
U<PROB(J,3)+...
        PROB(J,4)+PROB(J,5)+PROB(J,6)+PROB(J,7)+PROB(J,8)+PROB(J,9)
        counter9 = counter9 + 1;
        counterS=9;
elseif PROB(J,3)+PROB(J,4)+PROB(J,5)+PROB(J,6)+PROB(J,7)<=U &&
U<PROB(J,3)+...
        PROB(J,4)+PROB(J,5)+PROB(J,6)+PROB(J,7)+PROB(J,8)
```

```
        counter8 = counter8 + 1;
        counterS=8;
elseif PROB(J,3)+PROB(J,4)+PROB(J,5)+PROB(J,6)<=U && U<PROB(J,3)+...
        PROB(J,4)+PROB(J,5)+PROB(J,6)+PROB(J,7)
        counter7 = counter7 + 1;
        counterS=7;
elseif PROB(J,3)+PROB(J,4)+PROB(J,5)<=U &&
U<PROB(J,3)+PROB(J,4)+PROB(J,5)+PROB(J,6)
        counter6 = counter6 + 1;
        counterS=6;
elseif PROB(J,3)+PROB(J,4)<=U && U<PROB(J,3)+PROB(J,4)+PROB(J,5)
        counter5 = counter5 + 1;
        counterS=5;
elseif PROB(J,3)<=U && U<PROB(J,3)+PROB(J,4)
        counter4 = counter4 + 1;
        counterS=4;
elseif 0<=U&&U<PROB(J,3)
    counter3 = counter3 + 1;
    counterS=3;
end


  TC=[TC; V U counterS counterU counterD counter3 counter4 counter5
counter6 counter7 counter8...
      counter9 counter10 counter11 counter12 counter13 counter14
counter15 counter16 counter17 counter18];



end
  TC1=[TC1; J counterU counterD counter3 counter4 counter5 counter6
counter7 counter8...
      counter9 counter10 counter11 counter12 counter13 counter14
counter15 counter16 counter17 counter18];% Frequency of occurrance
in a state.

   sTC=TC1(:,2)+ TC1(:,3)+ TC1(:,4)+TC1(:,5)+ TC1(:,6)+ TC1(:,7)+
TC1(:,8)+TC1(:,9)+TC1(:,17)+ TC1(:,18)+...
       TC1(:,10)+ TC1(:,11)+ TC1(:,12)+TC1(:,13)+ TC1(:,14)+
TC1(:,15)+ TC1(:,16)+TC1(:,19);
   PTCU=(TC1(:,2)/sTC(1,:))*100;
   PTCD=(TC1(:,3)/sTC(1,:))*100;
   PTC3=(TC1(:,4)/sTC(1,:))*100;
   PTC4=(TC1(:,5)/sTC(1,:))*100;
   PTC5=(TC1(:,6)/sTC(1,:))*100;
   PTC6=(TC1(:,7)/sTC(1,:))*100;
   PTC7=(TC1(:,8)/sTC(1,:))*100;
   PTC8=(TC1(:,9)/sTC(1,:))*100;
   PTC9=(TC1(:,10)/sTC(1,:))*100;
```

```
   PTC10=(TC1(:,11)/sTC(1,:))*100;
   PTC11=(TC1(:,12)/sTC(1,:))*100;
   PTC12=(TC1(:,13)/sTC(1,:))*100;
   PTC13=(TC1(:,14)/sTC(1,:))*100;
   PTC14=(TC1(:,15)/sTC(1,:))*100;
   PTC15=(TC1(:,16)/sTC(1,:))*100;
   PTC16=(TC1(:,17)/sTC(1,:))*100;
   PTC17=(TC1(:,18)/sTC(1,:))*100;
   PTC18=(TC1(:,19)/sTC(1,:))*100;
   TC2= [PTCU,PTCD,PTC3,PTC4,PTC5,PTC6,PTC7,PTC8,PTC9,PTC10,...
       PTC11,PTC12,PTC13,PTC14,PTC15,PTC16,PTC17,PTC18]; %percentage
of reciding in a stste.
end
```